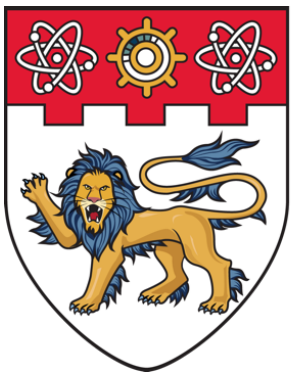

NANYANG TECHNOLOGICAL UNIVERSITY
SINGAPORE

BIOABSORBABLE RADIOPAQUE WATER RESPONSIVE SHAPE MEMORY POLYMER-HYDROGEL COMPOSITE DEVICE FOR TEMPORARY VASCULAR OCCLUSION IN LIVER CANCER TREATMENT

ABHIJIT VIJAY SALVEKAR

Interdisciplinary Graduate School
NTU Institute for Health Technologies

2018

BIOABSORBABLE RADIOPAQUE WATER RESPONSIVE SHAPE MEMORY POLYMER-HYDROGEL COMPOSITE DEVICE FOR TEMPORARY VASCULAR OCCLUSION IN LIVER CANCER TREATMENT

ABHIJIT VIJAY SALVEKAR

Interdisciplinary Graduate School

NTU Institute for Health Technologies

A thesis submitted to the Nanyang Technological University in partial fulfilment of the requirement for the degree of Doctor of Philosophy

2018

Abstract

Hepatocellular carcinoma (HCC) is the second most reason of cancer related death worldwide (approximately 800,000 deaths globally per annum). Whilst the surgery is the only curative way, only 10% of primary and metastatic liver cancer patients are eligible for resection while the remaining patients can only opt for palliative treatments such as transarterial chemo embolization (TACE). TACE treatment requires temporary embolization/blocking of hepatic artery, which accounts for 90% blood supply of tumor. Repeat sessions at six- to twelve-weeks intervals of the treatment are recommended, so patency of the hepatic artery needs to be restored before next treatment. Use of biodegradable embolic agent holds great promise for this application.

Most of the embolic device available in the market are metallic. In this regard, Gelfoam is the most widely used biodegradable embolic agent for intravascular embolization, but their use is associated with some problems such as unpredictable occlusion level, non-target embolization and inaccurate placement, uncontrolled degradation, permanent occlusion (at times) etc. We have proposed biodegradable shape memory polymer-hydrogel composite as an embolic agent which will prevail over above-mentioned limitations of Gelfoam.

The proposed embolic device consists of biodegradable Poly(DL-Lactide-co-Glcolide) (PLGA) filament coated with Polyethylene Glycol (PEG) hydrogel. The main objective of this research work is to understand the water induced buckling mechanism of the PEG hydrogel and to use it for making a shape memory embolic device which can be activated on contact with body fluid at body temperature to facilitate occlusion of a blood vessel. To do so, in this work shape memory characteristics of individual components poly(dl-lactide-co-glcolide) and polyethylene glycol hydrogel were investigated. PLGA evinces thermo responsive shape memory around body temperature. Different PLGA compositions with the varying amount of plasticizer and radiopaque fillers were extruded in filament form with the objective of having a filament with shape memory effect and radiopacity at body temperature. Theses compositions were characterized for thermal, mechanical, shape memory, and radiopacity in order to find the optimized composition. From the studies, it was found

that the PLGA formulation with 2% plasticizer and 50% bismuth oxychloride exhibited the optimal properties.

Mechanical and swelling characteristics of different hydrogel formulations were studied to investigate the effect of different parameters such as PEG concentration, initiator concentration, and crosslinking time. Shape memory effect and shape change effect in dry PEG hydrogel were studied individually. Buckling mechanism of the PEG hydrogel filament, synthesized using photo-crosslinking method was explored and correlated to several factors, including extent of strain, deformation temperature, and diameter of the sample. Parameters to control buckling of the PEG hydrogel were identified and validated using theoretical modelling and experimental results. It was found that the original diameter and amount of pre-stretching are identified as two influential parameters to tailor the buckling time as confirmed by both experiments and simulation.

The polymer-hydrogel composite was then fabricated using optimized formulation and conditions derived from the individual characterization results of the PLGA and PEG hydrogel. Fabricated device samples programmed for water induced shape memory using melting transition temperature of the PEG. *In-vitro* performance of the device was investigated using simulated flow model, with 100% occlusion being achieved within 2-3 minutes of deployment. Performance characteristics of the device such as stability in flow, degradation, cytotoxicity, hemocompatibility and shelf life were investigated. The cytotoxicity and hemocompatibility studies indicated good biocompatibility and non-hemolytic properties of the embolic plug. The shelf life studies confirmed the mechanical integrity of the device as well as no loss of shape memory properties over a period of six months.

Finally, a feasibility study was conducted *in- vivo* in a rabbit model to investigate the ease of device deployment, device migration and extent of vessel occlusion. *In-vivo* studies in rabbit model evinced successful deployment of the new embolic plug using existing method and complete occlusion at targeted location of the vessel was achieved in less than two minutes.

Acknowledgements

Firstly, I sincerely would like to thank Prof Huang Weimin and Prof Subbu S. Venkatraman, for initiating me into experimental research and giving me opportunity to work under their guidance on this exciting project.

I would like to take this opportunity to express my sincere gratitude towards my supervisor Prof Huang Weimin, for extending me all the supports and freedom to carry out my research. I thank him for all the valuable suggestions which has shaped my research in the most efficient way. It has been very enlightening and enjoyable experience under his supervision. He has also been very patients hearing my concerns and rectifying it in a very humble way. Every discussion with him was new insight into shape memory materials.

I also wish to express my gratitude Prof Subbu S Venkatraman for guiding me and giving me valuable suggestion on my research. I am highly thankful to him for giving me access to all facilities of material science and engineering school. His continuous encouragement and motivation was driving force for my research work.

I wish to thank and extend my appreciation to my guide Dr. Wong Yee Shan. My research would not have been completed without the help and support from her. Her valuable suggestions and comments are the basic pillar of my research. I am especially grateful for her consistent and sure support and her considerate attitude.

I wish to express my sincere gratitude to Dr. Tay Kiang Hiong (SGH), for the time he took out in spite of his busy schedule. His inputs and suggestions were invaluable. I am also thankful to him for facilitating the testing of prototypes at SGH facilities.

I would like to thank Prof Bo Liedberg (IGS) for providing a great support and motivation throughout the PhD duration.

Last but not the least, I would like to thank Wie Shan, Jing Ni, Hui Yee, Gordon, Pei Qi, Cao Ye and the laboratory executives at the B2 laboratory, Mr. Wilson, Mr. Patrick and Mr. Zi Li, for assisting me in the experiments. I would like thank Ms. Fiona (MSE) Ms. Suriani (IGS-NITHM), Ms. Ellen (IGS) for taking care of the administrative work and helping me out from time to time. I also would like to thank all Bio-group members for supporting me some or the other way.

Table of Contents

List of Tables

List of Figures

Abbreviations

AVM	: Arteriovenous Malformations
BiOCl	: Bismuth Oxychloride
BO	: Bismuth Oxychloride
BS	: Barium Sulfate
DI	: Deionized
DSC	: Differential Scanning Calorimetry
ETO	: Ethylene Oxide
FBGC	: Foreign Body Giant Cells
FDA	: Food and Drug Administration
GDA	: Gastroduodenal Artery
HCC	: Hepatocellular carcinoma
ID	: Internal Diameter
PEG	: Polyethylene Glycol
PEGDA	: Polyethylene Glycol Diacrylate
PEGTMO	: Poly (ethylene glycol-b-tetramethylene oxide)
PI	: Photoinitiator
PLGA	: Poly(DL-lactide-co-glycolide) / Poly (lactic-co-glycolic acid)
PMMA	: Poly(methyl methacrylate)
PPP	: Platelet-poor Plasma
PRP	: Platelet-rich Plasma
PRT	: Plasma Recalcification Times
RBC	: Red Blood Cells
RH	: Relative Humidity
ROI	: Reactive Oxygen Intermediates
SCE	: Shape Change Effect
SD	: Standard Deviation
SEM	: Scanning Electron Microscope
SIRT	: Selective Internal Radiation Therapy
SME	: Shape Memory Effect
SMP	: Shape Memory Polymer
TACE	: Transarterial Chemoembolization

TAE : Transarterial embolization

TGA : Thermogravimetric Analysis

TT : Tantalum

UV : Ultraviolet

Chapter 1 Introduction

1.1 Liver cancer and need of embolization

This research work was proposed to address the necessity of a fully biodegradable polymeric device for temporary endovascular embolization in interventional radiology for liver cancer treatment. Embolization is a minimally invasive procedure to selectively occlude blood vessels by intentionally introducing embolic agents into the vessels[1]. The embolization procedure is carried out by percutaneous insertion of a catheter into the desired artery or vein under X-ray fluoroscopy guidance. Once in place, an embolic agent is then deployed to stop blood flow by either direct occlusion of the vessel and/or induction of local thrombosis. Embolization can be used as independent procedure or can be used as adjunct to surgery. It has been applied to treat various conditions whereby occlusion of blood vessels is beneficial, e.g. traumatic hemorrhage, bleeding from gastrointestinal or respiratory tracts, arteriovenous malformations (AVMs), aneurysm, uterine fibroids, transcatheter arterial chemo-embolization (TACE) and selective internal radiation therapy (SIRT) for unresectable liver tumors[2]. Liver cancer (Hepatocellular Carcinoma) is fifth-most common type of cancer and the second most reason for cancer-related death worldwide and is highly prevalent in Asia[3]. Whilst the surgery is the only curative way only 10% of primary and metastatic liver cancer patients are eligible for resection while the remaining patients can only opt for palliative treatments such as TACE and SIRT[4, 5]

In TACE chemotherapy drug is injected into the hepatic artery that supplies the liver tumor, and an embolic agent is introduced to block (embolize) the small sub-branches of the hepatic artery. The physiological basis for Transarterial therapy is the dual blood supply of liver from portal vein and hepatic artery (Figure 1.1). Normal liver parenchyma is supplied by portal vein while hepatic artery is primary blood supply (more than 90%) for liver tumors[6, 7]. Making use of this fact chemotherapy agents are infused particularly through the hepatic artery directly to the HCC tumor. This technique is advantageous in a way that it delivers higher concentrations of the chemotherapy agents to the tumors without subjecting the patients to the systemic toxicity of the agents.

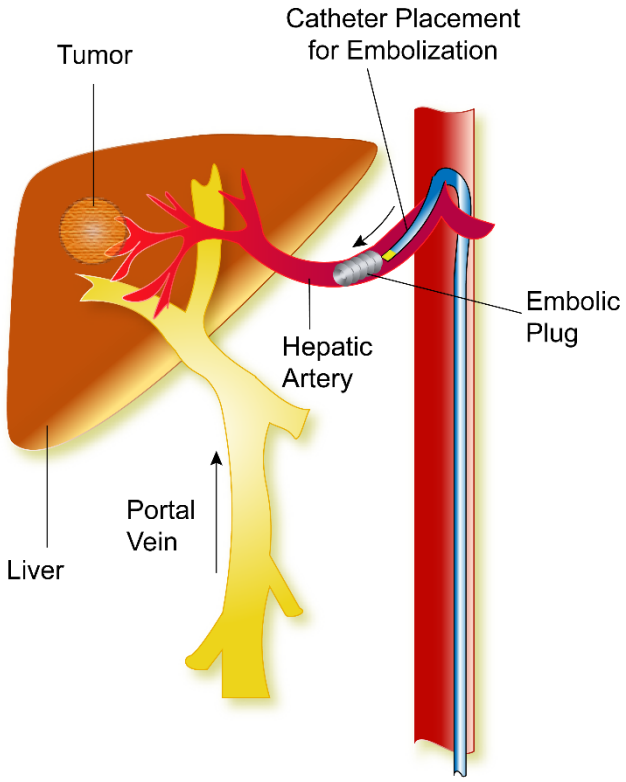

Figure 1.1 Dual blood supply of liver

This procedure is done under the guidance of X-ray fluoroscopy imaging. A catheter is introduced in the femoral artery in the groin and is then, threaded into the aorta. From the aorta, the catheter is pushed further into the hepatic artery. The branches of the hepatic artery supplying the liver cancer are identified and then chemotherapy agent is delivered. Then comes the additional step of embolizing (blocking) the small blood vessels with different embolic agents. Thus, TACE therapy has advantages of exposing the tumor to higher concentrations of chemotherapy agents and restricting the agents locally since they are not washed away by the blood stream. At the same time, this technique suspends the blood supply to tumor, which can result in the damage or death of the tumor cells by ischemia. Some patients may undergo repeat sessions at six- to twelve-weeks intervals so patency of the hepatic arteries needs to be restored before the next TACE can be performed. Therefore, temporary occlusion of the hepatic artery using a biodegradable agent is desirable. In this regard, Gelfoam, a biodegradable gelatin sponge, is typically used. It is usually cut into small pledgets (1mm or larger) and delivered as a particulate embolic agent[8].

In other instances, occlusion of vessels is required to divert blood flow or to protect the vascular territory from reflux of toxic materials. For example, in SIRT of liver cancers, radio-active particles are delivered into the hepatic artery and the gastroduodenal artery (GDA) is often prophylactically embolized to prevent reflux of the radioactive particles into the stomach and small intestines as the radioactive particles can cause radiation ulcers which often lead to devastating gastrointestinal hemorrhages. Currently, solid embolic device in the form of coil are used. They are usually made of metals (stainless steel, platinum or nitinol alloys) and are therefore non-biodegradable. As the reflux prophylaxis is only relevant during delivery of the radioactive particles, permanent occlusion of the GDA is unnecessary and a biodegradable embolic would be ideal in this situation.

1.2 Motivation

Currently, there are limited numbers of biodegradable embolic devices available. In this regard, Gelfoam is considered the most widely used biodegradable embolic agent for intravascular embolization. It can be typically resorbed in days to weeks depending on the amount of use, degree of fluid saturation and the site of use. Nevertheless, permanent occlusion can occur by residual organized thrombi or fibrotic change of the vessel. In addition, the occlusion level is unpredictable because of their irregular shape and variability in size. In general, they tend to aggregate in vessels more proximally than intended, but their tiny fragments can migrate into the capillary beds. Therefore, it is difficult to perform controlled target embolization using these agents. Occlusin^{TM} 500 Artificial Embolic Device (OCL500, IM Biotechnologies Ltd., Edmonton,AB) is another biodegradable embolic agent recently approved by FDA for highly vascularized tumors. The agent consists of biodegradable poly(lactic-co-glycolic acid) microspheres coated with type I bovine collagen. Though OCL 500 is manufactured in multiple size ranges, there is a risk of migration of microspheres during the administration process. For biodegradable liquid embolic agent, fibrin glue is the only one in the market but despite its good biocompatibility, the use of fibrin glue is hindered by its fast degradation and need for double-lumen catheterization[9]. So with existing embolic devices the major problems are unpredictable occlusion level, uncontrollable target embolization and uncontrollable degradation rate.

Accordingly, there is a need in providing a biodegradable solid embolic device, i.e. biodegradable embolic foam or plug, which can precisely occlude the blood vessel and degrade at a predictable rate. It would facilitate recanalization of the vessels and allow embolization procedures to be repeated especially in liver cancer treatment.

Shape Memory Polymer (SMP) is good material of choice for making embolic device. These materials can change their shape from temporary shape to predefined permanent shape when external stimulus is applied. External stimulus can be temperature, water or moisture, magnetic or electric field, pH change or solvent and light[10]. In biomedical applications especially in minimally invasive procedures SMP have leading edge over traditional polymeric material as these materials can be deployed with low profile (lower dimensions or compact shapes) temporary shape and then allowed to expand to a desired permanent shape at the target site[11]. So in such application temporary shape provides ease of deployment and permanent shape caters better functionality to the device.

1.3 Requirements for Embolic Device

Figure 1.2 outlines the main features/requirements of the embolic device for liver cancer treatment. The device needs to be biodegradable with control rate of degradation in order to facilitate temporary embolization. Actuation of the device should take place using body temperature or body fluid as source of activation. Radiopacity is another essential requirement for the device for proper delivery and placement of device in blood vessel using fluoroscopy. Following factors have to be considered while designing the embolic device.

- Limitations on the dimension of device and the dimensions of the target blood vessel.
- Easy delivery and deployment.
- Maximum occlusion in less time.
- Stability or anchoring of device at different flow rates and pressures.

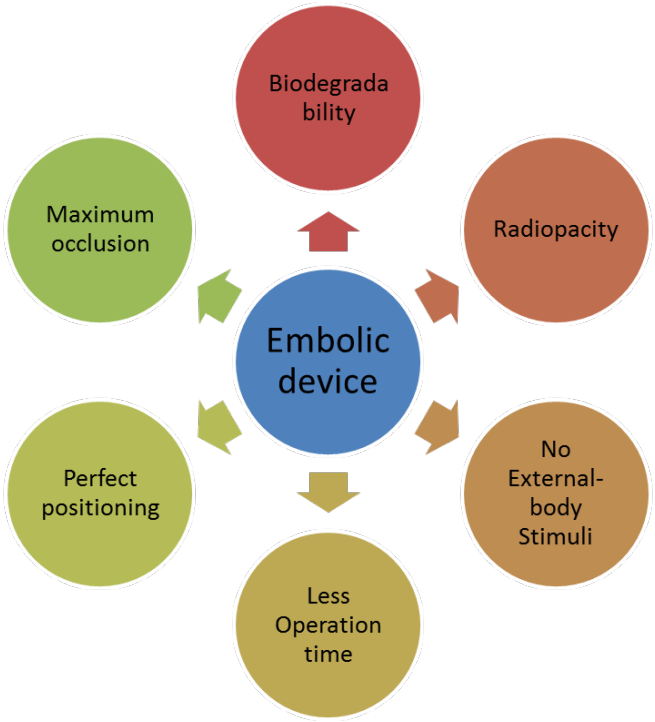

Figure 1.2 Features/requirements of embolic device.

1.4 Proposed Solution

Biodegradable shape-memory polymer hydrogel composite was proposed for making biodegradable embolic device (Figure 1.3). It is composed of a radiopaque PLGA core coated with PEG hydrogel. The PLGA filament coated with hydrogel can be thermally programmed into temporary shape using melt transition and crystallinity of the crosslinked hydrogel. A polymer-hydrogel composite filament in its temporary shape will be introduced through catheter and shape recovery of embolic device will be actuated on contact with body fluid i.e. blood at body temperature by water responsive shape recovery induced buckling mechanism of hydrogel followed by complete mechanical occlusion by hydrogel swelling.

In this approach the primary source for device actuation is water induced shape memory effect of hydrogel and the thermal shape memory effect of polymer filament at body temperature is secondary for device actuation which may assist the recovery. In this system biodegradable shape memory polymer core plays two roles: one as carrier for hydrogel and another is to provide radiopacity for visualization of device under X-Ray. Hydrogel provides the driving force for actuation of device and then mechanically

block the blood vessel. So it is important to study different formulations of these two materials for swelling, shape memory, radiopacity, thermal and mechanical properties, etc.

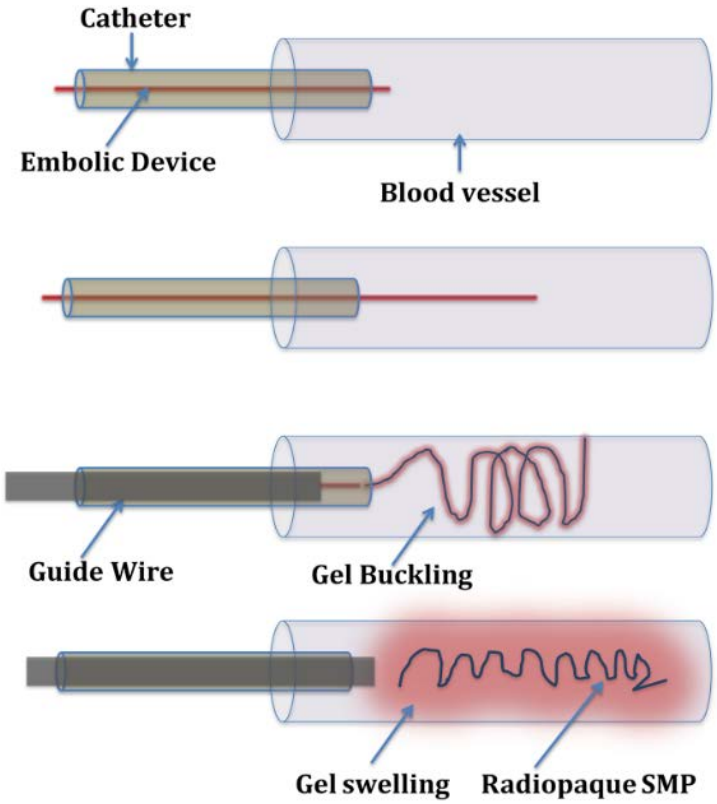

Figure 1.3 Proposed mechanism of working for water activated biodegradable polymer-hydrogel composite device for embolization of blood vessel

NOVELTY

Novelty of this work resides in the use of water responsive shape recovery induced buckling phenomena of PEG hydrogel for actuation of the embolic device without using any body-external source for activation. Use of hydrogel coating on metal coil for embolic device have been reported in some of the commercial products but it solely serves the purpose of maximizing occlusion volume by water induced swelling i.e shape change effect (SCE). In this work the water induced buckling due to contact with blood at body temperature is the driving force for shape recovery of the device followed by swelling to achieve complete occlusion. So, this work presents a fully biodegradable embolic device to provide temporary occlusion with precise control of the target location in a blood vessel without any body-external source for activation.

1.5 Objectives and Scope of the Research

The overall aim of this research work is to develop a novel embolic device for liver cancer treatment using a biodegradable shape memory polymer which gets activated when it comes in contact with blood at body temperature.

The objectives of this thesis work are:

I. To explore the shape memory properties of the PLGA, PEG hydrogel and PLGA-PEG composites.
II. To investigate the water induced buckling and swelling of PEG hydrogel and PLGA-hydrogel composites and to discern the underlying mechanisms and factors.
III. To study the deployment and performance of the prototypical PLGA-PEG composite embolic device in *in-vitro* flow system and *in-vivo* and to assess the feasibility and safety of the device.

To achieve these objectives, the work of this thesis is divided into three sections.

The first section involved the primary characterizations of individual materials (PLGA and PEG hydrogel). The PLGA materials with radiopaque fillers to impart radiopacity and plasticizers to tune the transition temperature near to body temperature were prepared at various levels of parameters and investigated for thermal, mechanical, radioopacity and shape memory properties. PEG hydrogel formulation was optimized based on hydrogel characterizations (Swelling, Gel Content, and Rheology). The optimized formulations were used to the construction of the PLGA-PEG hydrogel composite by coating PEG hydrogel onto the PLGA filament by photo-crosslinking. The device and method of making were improvised by conducting mechanical, shape memory characterization on the device. Underlying molecular mechanism of working of the device was elucidated.

In the second part solvent/water induced buckling mechanism of the PEG hydrogel, governing the recovery of the device in water at near body temperature (37°C) was explored. Shape change effect (SCE) in hydrogel and thermos-responsive shape

memory effect in dry state of hydrogel were combined to generate water responsive shape recovery induced buckling in dry PEG filament. The effects of various parameters controlling/affecting the recovery process were elucidated by studying the mechanical, shape-memory, thermal and swelling properties of PEG hydrogel. The parameters studied were deformation strain, dimensions and deformation temperature. Existing model for solvent induced buckling of pre-deformed polymers was modified to accommodate for the high swelling, and the theoretical result were generated for the buckling time and verified it with experimental results.

In the third part of the research work, the embolic device recovery in constrained setting was examined using *in-vitro* flow model at different flow rates and different sizes of the tubing's diameter's equivalent to those in actual human vascular system. The prototypical embolic devices were fabricated using the suitable material and processing methods selected on the basis of outcomes of the work in part one and two. Ease of delivery, stability of the device, extent of occlusion, occlusion timings were the factors observed in *in-vitro* flow system. The feasibility and safety studies such as in-flow stability, cytotoxicity, hemocompatibility, *in-vitro* degradability and shelf life, were carried out for the device prototype.
On account of performance of embolic device in *in-vitro* model, modifications were implemented and *in-vivo* studies in rabbit model were performed.

References

[1] Wen Guang Y. Advanced Shape Memory Technology to Reshape Product Design, Manufacturing and Recycling. Polymers. 2014;6:2287.
[2] Catheter Embolization. Radiological Society of North America, Inc; 2014.
[3] Jemal A, Bray F, Center MM, Ferlay J, Ward E, Forman D. Global cancer statistics. CA: A Cancer Journal for Clinicians. 2011;61:69-90.
[4] El-Serag HB, Mason AC, Key C. Trends in survival of patients with hepatocellular carcinoma between 1977 and 1996 in the United States. Hepatology. 2001;33:62-5.
[5] Llovet J. Treatment of hepatocellular carcinoma. Curr Treat Options Gastro. 2004;7:431-41.

[6] Breedis C, Young G. The blood supply of neoplasms in the liver. The American journal of pathology. 1954;30:969.

[7] Healey Jr J, Sheena K. VASCULAR PATTERNS IN METASTATIC LIVER TUMORS. Surgical forum1963. p. 121.

[8] Liapi E, Geschwind J-F. Transcatheter Arterial Chemoembolization for Liver Cancer: Is It Time to Distinguish Conventional from Drug-Eluting Chemoembolization? Cardiovasc Intervent Radiol. 2011;34:37-49.

[9] Kessel D, Robertson I. Interventional Radiology: A Survival Guide: Elsevier Health Sciences UK; 2011.

[10] Sun L, Huang WM, Ding Z, Zhao Y, Wang CC, Purnawali H, et al. Stimulus-responsive shape memory materials: A review. Mater Des. 2012;33:577-640.

[11] Wong YS, Xiong Y, Venkatraman SS, Boey FYC. Shape memory in un-cross-linked biodegradable polymers. Journal of Biomaterials Science, Polymer Edition. 2008;19:175-91.

Chapter 2 Literature review

2.1 Transarterial chemoembolization (TACE) and embolic agents

Transarterial chemoembolization (TACE) is an effective minimally invasive palliative treatment for patients with intermediate-stage hepatocellular carcinoma (HCC) and relatively preserved liver function. Repeated TACE are found to be effective with the repetition frequency of two to three months[1]. TACE treatment has shown to improve median survival from 16 to 20 months[2]. TACE has several benefits over surgical resection including the anticipated reduction in morbidity and mortality, minimal trauma and pain, short hospital stay and recovery, low cost, suitability for real-time image guidance, and cosmesis[3]. Rationale for the use of transarterial therapies like TACE and TAE lies in the extensive dependence of the tumor on hepatic artery for the blood supply. The TACE procedure briefly involves intra-arterial injection of a viscous emulsion, made by a chemotherapeutic drug such as doxorubicin or cisplatin mixed with iodized oil, followed by embolization of the blood vessel with embolic agents by catheterization[4]. Beneficial effect of TACE are derived by two methods. Since the hepatic artery supplies most of the tumors, arterial embolization suspends their blood supply and delays their growth until replaced by neovascularity. Secondly, targeted administration of chemotherapy allows a higher dose to the tissue while simultaneously reducing systemic exposure, which is typically the dose-limiting factor. With high concentration of drugs in the tumor area, the cytotoxic effect on the tumor cells is enhanced and side effects of the chemotherapy drugs are reduced. This effect is enhanced by the fact that the chemotherapeutic drug is not washed out from the tumor bed after embolization[5]. Transcatheter arterial embolization (TAE), known as bland embolization, is another treatment which differs from TACE in a way that it involves the embolization of the hepatic artery without use of any chemotherapeutic agents[6]. Several studies suggested that embolization alone gives the same survival advantage as TACE. Nevertheless, in recent years, TACE has replaced TAE as the most extensively used and investigated palliative modality for unresectable HCC[7].

2.1.1 Clinical procedure of TACE or TAE

The procedure for transarterial embolization (TAE) starts with accessing the arterial system via the femoral artery, using Seldinger technique[8]. Once stable access is attained, a guidewire and catheter system are advanced to the target location under angiographic guidance. The vascular supply to the tumor is identified along with any potential anatomic variants by performing a diagnostic angiogram. After which, a vessel or a branch of a vessel to be embolized is identified. The catheter is used to access the target vessel, and location is confirmed by injection of contrast. The catheter is then used to deliver the selected embolic agent. The primary procedural endpoint is angiographic evidence of stasis. The selection of embolic agents depends on desired outcome of the treatment. For a temporary occlusion, gelatin sponge is used whereas, for permanent occlusion poly(vinyl alcohol) or trisacryl gelatin particles are used. An additional step, in case of TACE, is the localized delivery of chemotherapeutics via the same catheter prior to the delivery of embolic agent.

2.1.2 An overview of embolic agents

Embolization is a common procedure performed by interventional radiologist, with the intention of endovascular occlusion of an artery or vein to derive therapeutic benefits. A wide variety of embolic agents are available for the multimodality treatment paradigms in trauma, oncology, and endovascular therapy of vascular malformations and aneurysms. The embolic agents can be classified on the basis of their form (solid or liquid), shape (foam, coil or plug), function (temporary, permanent or drug eluting)[9, 10]. Following Table 2.1 gives overview of widely used embolic agents and their characteristics and drawbacks.

Table 2.1 Overview of embolic agents and their characteristics and drawbacks[8-10].

Nature	Type	Material	Size	Drawbacks
Permanent	Embolization Coil	Platinum, Steel	Length: 1-300 mm Dia.: 1-27 mm	Less occlusion volume, permanent, multiple deployments, costly, limitation on MRI and CT scan
		Hydrogel coated platinum	-	Permanent
	Polymer Particles	PVA	100-1100 µm	Non-target embolization, inflammatory response, thrombosis
		Tris-acryl gelatin	40-1200 µm	Allergic potential, non-target embolization
Temporary	Mechanical	Gelfoam	1000-2000 µm	Infection, non-target embolization, thrombus formation, uncontrolled degradation
	Particulate	PLGA microspheres	150-300 µm	Migration during administration, full recanalization period 1 year.
	Liquid embolic	Fibrin glue	-	Faster degradation, need of double lumen catheter

For temporary embolization gelfoam is the most widely accepted embolic agent. Gelatin foam is a water-insoluble hemostatic agent made from purified porcine skin gelatin. It is available in sterile foam sheets and as a powder comprised of 40 to 60 µm particles. For TACE, gelfoam sheet is cut into the pledgets and thoroughly mixed with saline and contrast agents such as omnipaque or lipidol-oil and injected through the catheter. Once injected gelatine foam causes mechanical obstruction, slowing down the blood flow and facilitating the thrombus formation. The advantages of gelfoam include low cost, versatility of use, and temporary nature. The degradation of gelfoam is enzymatic, so the degradation timeframe varies giving unpredictable recanalization or permanent embolization[8]. It has also been reported that gelfoam can be associated

with infection due to trapped air bubbles and animal source of gelatine[11]. Further, gelatin foam powder can potentially cause ischemia due to the small size (especially at sizes < 70 μm) of the particles, allowing distal embolization making it difficult to obtain precise target embolization. These all drawbacks of gelfoam present the unmet need of better embolic agent for temporary embolization.

2.2 Shape memory polymers

The shape memory is not an inherent property of polymeric materials. Rather it is understood as the functionalization of polymer since it is the result of combination of specific processing of polymer and polymers morphology. Any variation in these two factors will change the shape memory effect of the polymer. Primarily any shape memory polymer will exhibit two shapes- permanent and temporary. Net-points are responsible for holding the permanent shape of the polymer. Net-point can be covalent bonds between molecules (chemical) or intermolecular interactions (physical). Some examples of net-points can be crystalline phase, chemical crosslinks, molecular entanglement (in case of high molecular weight polymer), hard segments (in case of block copolymers) etc.[12, 13]. The temporary shape of shape memory polymers is held by reversible switch points. Switch points accomplish this by reversibly preventing deformed chain segments, which are under external stress, from recoiling. Switching points can be reversible crosslinks, molecular interactions, crystalline phase or a particular molecular state which can be activated by use of external stimulus such as temperature, light, solvent or pH etc. Upon activation it results in the entropic elastic behavior of the polymer network thus returning to the permanent shape of the network [12-15].

In thermal shape memory polymers, either glass transition-Tg or melting temperature-Tm is used as an activation temperature for shape memory effect. The typical thermal responsive shape memory mechanism can be described as follows. The polymer is heated to highest transition temperature, T_{perm} where the molecular mobility is highest and then can be formed into the desired permanent shape followed by cooling down to below transition temperature or room temperature whichever is low. This is the step where permanent net-points formation takes place. Then in the next step to fix

temporary shape the polymer is heated to second highest transition temperature T_{trans} which is lower than the T_{perm}. At T_{trans} molecules gain limited mobility but still keep permanent shape intact unless acted upon by an external stress. The polymer is then deformed at T_{trans}, and without removing the stress it is cooled down to below T_{trans}. In this step the temporary shape is formed with locked-in stresses held by reversible switch points.

When the polymer is heated again above T_{trasn}, this locked in stress are released and molecules are recovered back to high entropy configuration (random coil) i.e. Permanent Shape. Following Figure 2.1 shows the mechanism of thermal shape memory effect.

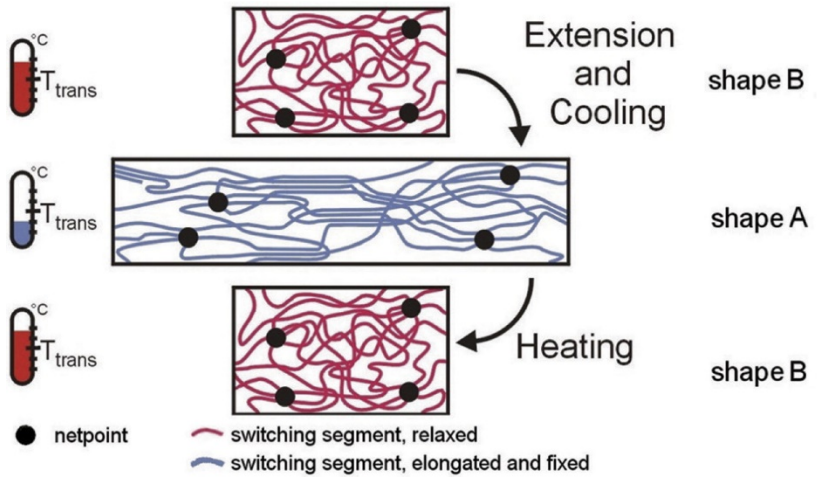

Figure 2.1 Mechanism of Thermo-responsive shape memory effect [13]

2.3 Polyethylene glycol hydrogel

Hydrogels are of great interest as a choice biomaterial for various medical applications such as tissue engineering, drug delivery, coatings on medical devices, wound treatment etc. owing to their biocompatibility and hydrophilic character[16, 17]. In recent years one of the promising areas of hydrogel application is in the embolic devices for cancer treatment or for brain aneurysm as it provides maximum occlusion volume upon swelling on contact with aqueous media (blood).

Polyethylene Glycol is hydrophilic semicrystalline polymer that upon crosslinking into 3-D network structure can absorb large amount of water or biological fluids. PEG is approved by FDA (Food and Drugs Association, USA) for clinical application because it does not elicit toxicity or immune response[18].

2.3.1 Synthesis and chemistry

Polyethylene Glycol hydrogels are typically synthesized by covalent crosslinking of modified PEG macromeres having reactive chain ends such as acrylate, methacrylate, allyl ether, maleimide, vinyl sulfone, NHS ester, vinyl ether (Figure 2.2).

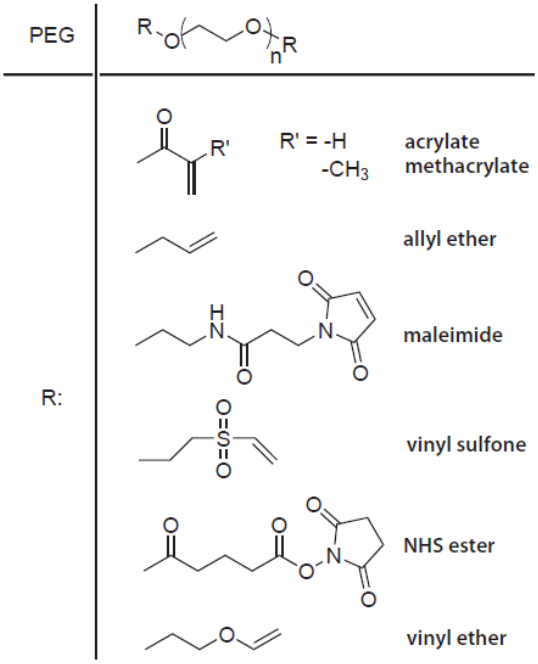

Figure 2.2 Functional groups for end modification PEG macromers[19]

Polyethylene Glycol Diacrylate (PEGDA) undergoes chain polymerization with Photoinitiator- Irgacure® 2959 under UV light (λ=365 nm) (Figure 2.3). Network defects can occur when crosslinking takes place because of loop formation, dangling/unreacted chain ends or permanent entanglements. Dangling bonds limit the deformation strain and may acts as weak point or starting point for breaking of gel.

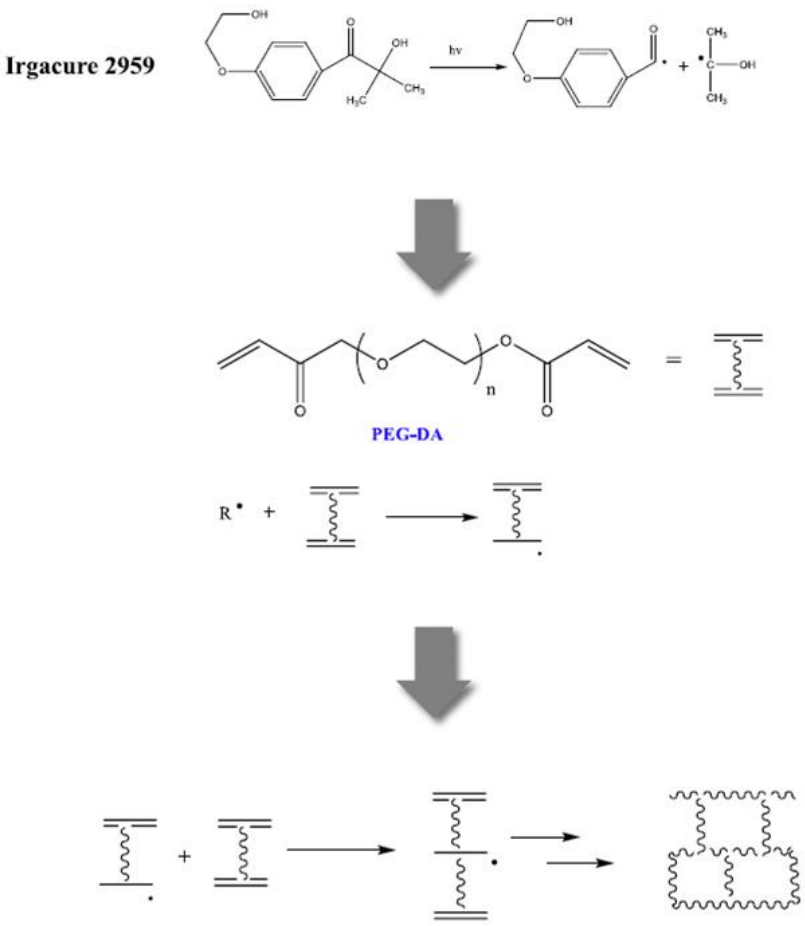

Figure 2.3 Free radical photo-polymerization of PEGDA hydrogel [20]

Limited studies have been published on degradation of photocrosslinked PEGDA hydrogel. Browning, et al; have reported in vivo degradation period for PEGDA (10kDa, 10%) to be 12 weeks[21]. Another report by Lynn, et al; has mentioned degradation rate to be 4 weeks for PEGDA (3 kDa, 20%)[22]. PEGDA degradation is facilitated by the hydrolysis of the end group esters while the main chain ethers are resistant to oxidation. Rate of degradation depends on the molecular weight of the macromers, concentration of macromers, crosslinking density (i.e. initiator amount and crosslinking time).

2.3.2 Shape memory and buckling/recovery of PEG hydrogel

For any material to have shape memory effect the basic requirements are to have permanent net-points, which defines the permanent shape for the material, and switching segments which are responsible for holding the temporary shape[14, 15].

In PEG hydrogel shape memory effect (SME) as well as shape change effect (SCE) are observed. For shape memory effect in PEG hydrogel, acrylate crosslinks acts as the permanent net-points and crystallites formed from solution or melt acts as the switching segments, which gets activated either by temperature or solvent (water). Hence PEG shows thermo-responsive as well as water induced shape memory effect. When water is used as source of actuation shape memory effect is combined with shape change effect i.e. swelling. Depending on the amount of deformation strain used for fixing temporary shape the recovery will be either normal or will proceed via buckling. The advantage of PEG hydrogel is that any one of the three ways of shape memory programming and recovery can be utilized according to application. The three methods of shape memory programing and recovery are :

- Thermal – heating PEG hydrogel above transition temperature (55-60°C)
- Water – using water to hydrate switching segment
- Humidity- saturating sample with high humidity

For biomedical applications water induced recovery using body fluid or blood as source for activation can be utilized. Whereas for programming the temporary shape, a thermal method found to be more advantageous because high deformation strain and good shape fixity is possible with easy and swift implementation.

Crystallization and dissolution transition of PEG chains induced by dehydration and hydration respectively, impart it with water responsive shape-memory properties. For both water-responsive and thermo-responsive shape recovery processes, the shape recovery speed is substantially dependent on the dimension /size of the sample. The thinner hydrogel samples give faster recovery, which can be tuned according to different applications. Besides, combination of water and thermo-responsiveness, i.e.

water induced recovery at elevated temperature can be used to achieve faster shape-recovery speeds[23].

Hydrogel swelling proceeds via three steps as follows:

1. Diffusion/penetration of water molecules
2. Hydration and relaxation of polymer molecules
3. Expansion of the polymeric network

The relaxation process is the primary determining step when diffusion rate is much faster than the dissolution/relaxation rate. Continuous formation of renewable interface between the swollen (soft) hydrogel region and the non-hydrated internal polymer network (glassy core) takes place (Figure 2.4). With time the gel absorbs more water and this interface moves continuously from the external boundary to the internal core until fully swollen hydrogel is formed [24]

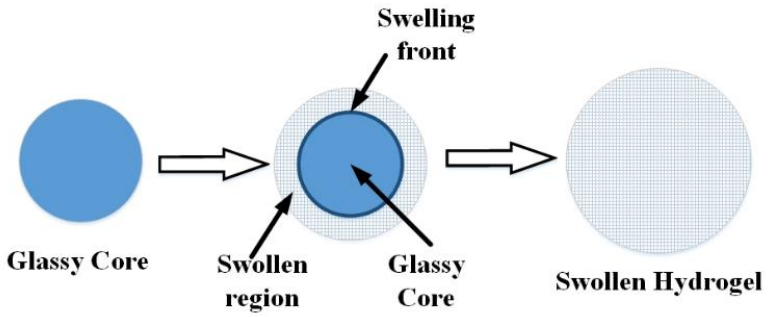

Figure 2.4 Process of hydrogel swelling

2.3.3 Degradation of PEG hydrogel

Poly(ethylene glycol) (PEG) is nontoxic and has been approved by the Food and Drug Administration (FDA) for internal consumption. [25-27]. Use of PEG in blood interfacing applications is promising due to its reduced thrombin adsorption, intrinsic resistance to protein adsorption and cell adhesion [28-30]. Acrylate end modified PEG (PEGDA) is commonly used in the development of PEG hydrogels due to its ease of

fabrication and degradibility [21]. PEG based hydrogels are used in various biomedical applications such as tissues engineering, drug delivery and other therapeutics[21, 31].

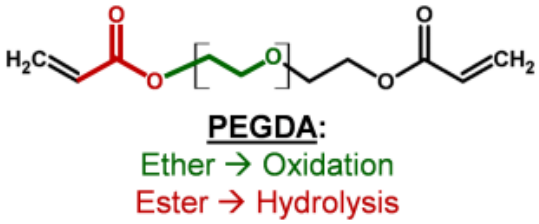

Figure 2.5 Structures of PEG diacrylate (PEGDA). The ether backbone of both PEGDA is susceptible to oxidation. The endgroup esters of PEGDA are hydrolytically labile. (reproduced from *[21]* with permission)

PEGDA hydrogel degrades primarily due to hydrolysis of the endgroup acrylate esters. Studies on *in-vivo* response and degradation of PEGDA hydrogel have been reported [21, 22, 32]. On the basis of this studies it appears that in vivo degradation of PEGDA hydrogels could be result of hydrolysis, oxidation or combination of two. PEG hydrogels are typically characterized as bioinert, however PEG-based devices can promote a degree of nonspecific protein adsorption and/or complement activation in vivo, which can result in macrophage recruitment, attachment and activation at the implantation site generating a privileged microenvironment between the cell membrane and the material surface. Upon activation, macrophages and foreign body giant cells (FBGCs) secrete degradative agents including acids, reactive oxygen intermediates (ROIs), and enzymes into this microenvironment, which promote hydrolysis of the endgroup esters as well as ROIs mediated oxidation of ether backbone of PEG. However, the response subsides once the material is completely degraded.

PEG with molar mass between 400 Da and 40-60 kDa are mentioned to be used to eliminate problem associated with low molecular weight toxicity and high molecular weight liver accumulation. Studies on free PEG intravenous administration to humans shows that PEG with molar mass 20 kDa readily excreted through the kidney, while higher molar mass PEG is eliminated rather slowly[31, 33]. In clinical study, 6 men were injected intravenously with PEG 6000. Approximately 63% of the dose was recovered in urine after 1 hour and 96% was recovered after 12 hours[31, 34].

2.4 Theory of buckling

Multilayer structures, used in many applications, can often results in to development of stresses due to mismatch in swelling by solvents, shrinking, pre-strain or thermal expansion. This stresses in combination with inherently slender aspect ratios can make structures vulnerable to buckling in out of plane such as folding, wrinkling, creasing and delamination. Although mechanical stabilities causing buckling have considered to downgrade the performance of the material or even cause for mechanical failure, these effects can be controlled and tailored to develop next generation devices with added values[35].

Huang WM et al., (2011) have reported the solvent and heat induced buckling of PMMA during shape recovery. Buckling is generic phenomena applicable to all materials during solvent- or thermo-responsive shape recovery if they meet certain conditions.

Figure 2.6 delineates the mechanism of solvent induced buckling of pre-stretched PMMA. In pre-stretched temporary shape of PMMA elastic energy generated due to rearrangement of molecules to state of lower entropy, is stored locally in entanglements and molecules. When it is immersed in ethanol, it absorbs ethanol and softens. Initially the outer surface softens and then with time swelling/softening front continues to travel inside towards the hard core till complete solvation takes place. During this solvation process elastic energy stored locally get released in the form of recoiling of molecules to higher state of entropy, which develop compressive stresses in the solvated or softened part of the sample. Depending on the magnitude of developed stresses, deformation strain and the dimension of the sample, the sample can either break by delamination or can buckle[36].

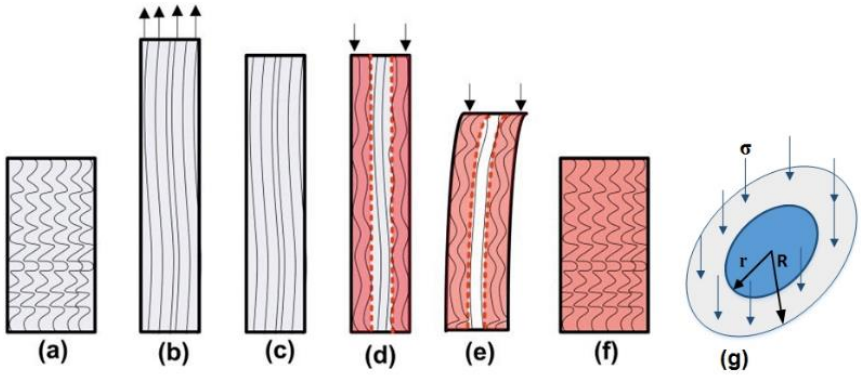

Figure 2.6 Illustration of mechanism of buckling. (a) amorphous PMMA before stretching; (b) high temperature stretching of PMMA; (c) cooling and unloading; (d) penetration of ethanol and outer layer softening; (e) critical penetration depth is reached and sample is buckled; and (f) recover shape after complete softening; (g) cross-section of "figure (d)". Shaded area represents area softened by ethanol. (Reprinted from Appl. Phys. Lett. 99, 131911 (2011))

The critical value r^c, of radius r of hard core for buckling condition can be calculated from following equation:

$$\boldsymbol{r^c = \frac{2\sqrt{2}L}{\pi\sqrt{E_r}}\left[\sqrt{\sigma^2 + \frac{\pi^2}{4L^2}E_r R^2\sigma} - \sigma\right]^{1/2}} . \qquad 2.1$$

where R is the radius of the sample after pres-stretching;

r is the radius of inner hard core

L is the length of the sample

E_r is the Young's modulus of inner hard core

σ is the compressive force acting on the softened part

Assuming $\sigma=\alpha E_r$ and $L=\beta R$

When v_p is constant; R- $r^c=v_p t^c$

Equation (2.1) can be modified to

$$\boldsymbol{\frac{V_p t^c}{R} = 1 - \frac{2\sqrt{2}}{R}\left[\sqrt{\beta^2\alpha^2 + \frac{\pi^2\alpha}{4}} - \beta\alpha\right]^{1/2}} \qquad 2.2$$

where α is measure of pre-stress

β is the slenderness ratio

v_p is solvent penetration velocity

t^c is critical value of immersion time

2.5 Poly (lactic-*co*-glycolic acid)

In past two decades as a base material, poly (lactic-*co*-glycolic acid) (PLGA) has attracted substantial interest for biomedical applications because of it favorable properties such as 1) Biocompatibility; 2) Ability to tailor degradation rate by changing comonomer ratio and molecular mass; 3) approved by U.S. Food and Drug Administration (FDA) for clinical use in humans; and 4) surface modification potential for better response to biological system[37, 38].

Amongst all the biomaterials, application of the biodegradable polymer poly lactic-*co*-glycolic acid (PLGA) has shown immense potential as a drug delivery carrier and as scaffolds for tissue engineering. PLGA have been extensively studied as delivery vehicles for drugs, proteins and various other macromolecules such as DNA, RNA and peptides. PLGA is a material of choice for making implantable therapeutic medical devices owing to its shape memory effect near body temperature and bio-degradability.

2.5.1 Degradation PLGA

Hydrolysis of ester linkages leads to bulk the degradation of the PLGA in aqueous medium. Gentile P. *et al.* [37] have described degradation of PLGA in four steps: (1) hydration: penetration of water into amorphous phase disrupting the hydrogen bonds and van der Waals forces resulting in the reduction in Tg, glass transition temperature; (2) degradation initiation: molecular weight reduction due to cleavage of covalent bonds; (3) degradation continuation: degradation auto-catalyzed by the carboxylic end groups cause massive breakage of the backbone covalent bonds lined with mass loss and loss of integrity; (4) solubilisation: further break down of fragments to molecules soluble in the aqueous environment. Figure 2.7 (b) shows *In-vivo* degradation rate for

PLGA copolymer with different monomer ratios[39]. Absence of side methyl group in PGA makes it relatively hydrophilic and allows close molecular packing to form a semi-crystalline structure. Whereas, in case of PLA the it can be either in highly crystalline form (PLLA) or completely amorphous form (PDLA). Presence of side methyl group makes PLA more hydrophobic, making it difficult for water absorption. Due to these attributes of PLA and PGA the PLGA copolymers show distinct degradation profile as the copolymer ratio varies. When PGA copolymerized with PLA, reduces the crystalline amount of PLGA and as a result increase the rate of hydration and causing faster degradation by hydrolysis. PLGA with 50:50 comonomer ration exhibits faster degradation rate. Following figure summarizes the rate of degradation for PLGA as a function of comonomer ratio. PLGA with 50:50 copolymer ratio exhibit fastest degradation rate of 1-3 weeks [38, 39].

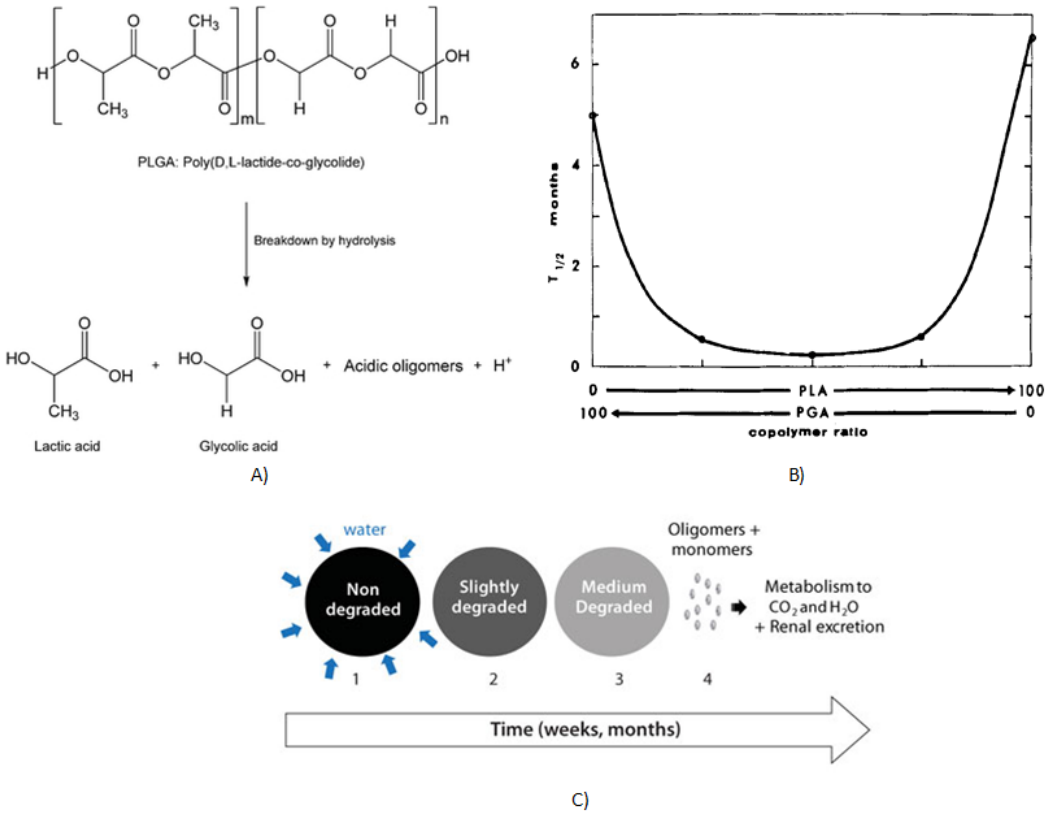

Figure 2.7 Degradation mechanism of PLGA. (a)Degradation products; (b) Effect of copolymer ratio on degradation (c) mechanism of degradation

2.5.2 Shape memory properties of PLGA

Wong YS *et al.* [40, 41]have reported the shape memory effect in uncroslinked PLGA. Effect of three main parameters temperature, time and stress level for shape memory programming have been explored in their work. The main findings are the shape memory effect in PLGA is due to molecular entanglements and transition of the chains from rubbery to glassy state. The factors which cause inter-molecular slippage will results in permanent deformation and hence the reduced shape recovery. Elastic strain is the reason for recovery of the polymer. This elastic strain is due to the reversible uncoiling and orientation of the molecules, which produces entropy elasticity. When the right stimulus is applied to a temporary shape the stored elastic energy drives the shape recovery of a shape memory polymer. Shape memory effect and biodegradability gives PLGA privilege over other biocompatible materials to be used in medical devices, especially for minimally invasive applications.

Similar shape memory mechanism is reported for high molecular weight (3×10^6 kDa), fully amorphous polynorbornene [42-44]. The glass transition temperature range for the material is 35 to 45°C. The higher molecular weight linear chains cause the entanglements which serves as the physical crosslinks in the in the network and the transition to rubber-elastic state from glassy state impart shape memory properties to the polymer. High stain rates above Tg for shorter time gives better shape recovery until, the total of stretching time $\Delta t_{stretch}$ and cooling time Δt_{cool} is much shorter than the time it would take the stretched network to relax $\Delta t_{relaxation}$ ($\Delta t_{stretch}+\Delta t_{cool}\ll\Delta t_{relaxation}$) [45]

Table 2.2 Properties and applications of PLGA copolymers with different monomer ratios [46-55]

Polymer	Modulus (GPa)	Elongation (%)	Solvent	Cristallinity (%)	Degradation Time (Weeks)	Applications
Polyglycolide/ Polyglactine	7.0	15–20	Hexafluoroispropanol	45–55	6–12	Suture anchors, meniscus repair, medical devices, drug delivery, orbital floor Fracture fixation,
Poly(L-lactide)	2.7	-	Benzene, THF, dioxane	37	12–18	interference screws, suture anchors, meniscus repair
Poly(D,L-lactide)	-	3–10	Methanol, DMF	Amorphous	11–15	Orthopaedic implants, drug delivery
Poly(D,L-lactide-*co*-glycolide) 85/15	2.0	3–10	Ethyl acetate, chloroform, acetone, THF	Amorphous	5–6	Interference screws, suture anchors, ACL reconstruction
Poly(D,L-lactide-*co*-glycolide) 75/25	2.0	3–10	Ethyl acetate, chloroform, acetone, DMF, THF	Amorphous	4–5	Plates, mesh, screws, tack, drug delivery
Poly(D,L-lactide-*co*-glycolide) 50/50	2.0	3–10	Ethyl acetate, chloroform, acetone, DMF, THF	Amorphous	1–2	Orthopaedic implants, drug delivery
Poly (L-lactide-*co*-glycolide) 10/90	-					

2.6 Radiopacity and radiopaque fillers

Endovascular embolization treatment is carried out under guidance of X-ray fluoroscopy. Radiopacity of the embolic device is crucial for monitoring deployment and accurate positioning of the device[56, 57]. Generally, polymers are radio-transparent as they are composed of, carbon, oxygen, hydrogen and nitrogen, elements having relatively low Atomic Mass (Z) as well as low electron density and specific gravity. Radiopacity is attained by adding heavy elements into base polymer matrix. Commonly used elements are iodine derivative, barium sulfate, bismuth compounds and tantalum etc. These compounds can be dispersed in polymer matrix by melt- or solvent-blending techniques and iodine compounds can be grafted permanently to the polymers [58-62]. Bismuth oxychloride is the effective radiopacifier as it produces bight and sharp images with higher contrast compared to barium sulfate [63]. Radiopacity is related to density and thickness as follows:

$$\boldsymbol{Radiopacity} = \mathbf{exp}[(\boldsymbol{\mu/\rho})(\boldsymbol{\rho t})] \quad 2.3$$

where (μ/ρ) is mass coefficient of attenuation; ρ is density of sample; and t is thickness of sample.

μ, x-ray absorption coefficient, is inherent property of the material dependent on the atomic mass of the element.

$$\boldsymbol{\mu = K\lambda^3 Z^4 + 0.2} \quad 2.4$$

where Z is atomic number of the element; λ is wavelength of x-ray beam; K is constant; and 0.2 is the average scattering coefficient

Table 2.3 presents the value of Z and μ and ρ for some of the radiopaque filler materials[64].

Table 2.3 Properties of some common radiopaque fillers

Compound	Density, ρ	element	Atomic number, Z	Mass attenuation coefficient (at 100KV), μ/ρ
	g/cm^3			cm^2/g

Barium Sulfate	4.5	Barium	56	2.196
Bismuth Oxychloride	7.7	Bismuth	83	5.739
Tantalum	16.6	Tantalum	73	4.302
Iodine	4.933	Iodine	53	1.942

2.6.1 Bismuth compounds in medical applications

Bismuth compounds have been used in medicine for centuries. Reports have mentioned the use of bismuth oxychloride in the treatment of syphilis and yaws, in conjunction with penicillin and organic arsenicals. Bismuth oxychloride also been used in the treatment of hemorrhoids for its local protective action, as an ointment (5 per cent) as suppositories (10 grains). In another medical application bismuth oxychloride, was injected intramuscularly it was slowly absorbed and found to have a spirocheticidal action[65].

2.6.1.1 Bismuth compounds as radiopacifier

Bismuth compound owing to their higher density and good compatibility with various polymers are gaining attention in medical device field[66].

Bismuth subcarbonate offers more radiopacity than barium sulfate and can be used in smaller amounts for similar results. It is white in a color like barium, but it is more difficult to color because of its higher tinting strength. The use of bismuth subcarbonate is limited because of heat stability issues – it begins to degrade at 225^0C (437^0F) – and it is difficult to disperse, this leads to rough surfaces in finished products. It is also not compatible with certain polymers, such as thermoplastic polyurethanes (TPUs).

The use of bismuth oxychloride in medical devices has been on the increase because it offers many advantages over other options. It offers much better heat stability than bismuth subcarbonate (begins decomposing at 600^0C or 1112^0F) and is much easier to disperse. The surface of plastics filled with bismuth oxychloride is typically smooth

and silky, as is the powder itself. Bismuth oxychloride is known to be sensitive to UV light but there have been advances in stabilizing it and there are powders available with better UV stability. Bismuth oxychloride is compatible with many polymers, including TPUs. Various reports mention uses of bismuth oxychloride as radiopacifier for medical devices. Polycarbonate polyurethane based venous access devices with bismuth oxychloride as a radiopacifier have showed enhanced strength and retention of mechanical properties on exposure to aqueous fluids at body temperature[67].

Bismuth trioxide is the densest of the bismuth powders -so it offers high radiopacity- but is naturally yellow in color, making it difficult to color. At higher temperatures, it can turn brown, which limits the compounding options. Bismuth trioxide also is known for leading to rough surfaces for tubing, which limits applications.

References

[1] Guan Y-S, He Q, Wang M-Q. Transcatheter arterial chemoembolization: history for more than 30 years. ISRN gastroenterology. 2012;2012.

[2] Lencioni R, Petruzzi P, Crocetti L. Chemoembolization of Hepatocellular Carcinoma. Semin intervent Radiol. 2013;30:003-11.

[3] Goldberg SN, Ahmed M. Minimally invasive image-guided therapies for hepatocellular carcinoma. Journal of clinical gastroenterology. 2002;35:S115-S29.

[4] Lencioni R, Crocetti L. Local-regional treatment of hepatocellular carcinoma. Radiology. 2012;262:43-58.

[5] Miraglia R, Pietrosi G, Maruzzelli L, Petridis I, Caruso S, Marrone G, et al. Efficacy of transcatheter embolization/chemoembolization (TAE/TACE) for the treatment of single hepatocellular carcinoma. World Journal of Gastroenterology: WJG. 2007;13:2952.

[6] Roche A, Franco D, Dhumeaux D, Bismuth H, Doyon D. Emergency hepatic arterial embolization for secondary hypercalcemia in hepatocellular carcinoma. Radiology. 1979;133:315-6.

[7] Lau W-Y, Lai EC. Hepatocellular carcinoma: current management and recent advances. Hepatobiliary Pancreat Dis Int. 2008;7:237-57.

[8] Poursaid A, Jensen MM, Huo E, Ghandehari H. Polymeric materials for embolic and chemoembolic applications. J Controlled Release. 2016;240:414-33.

[9] Vaidya S, Tozer KR, Chen J. An Overview of Embolic Agents. Seminars in Interventional Radiology. 2008;25:204-15.

[10] Golzarian J. An Overview of Embolics - how and when to use embolic agents for optimal clinical outcomes. Endovascular Today. 2009.

[11] Lindstrom PA. Complications from the use of absorbable hemostatic sponges. AMA Archives of Surgery. 1956;73:133-41.

[12] Leng J, Lu H, Liu Y, Huang WM, Du S. Shape-memory polymers—a class of novel smart materials. MRS Bull. 2009;34:848-55.

[13] Behl M, Lendlein A. Shape-memory polymers. Mater Today. 2007;10:20-8.

[14] Behl M, Zotzmann J, Lendlein A. Shape-Memory Polymers and Shape-Changing Polymers. In: Lendlein A, editor. Shape-Memory Polymers: Springer Berlin Heidelberg; 2010. p. 1-40.

[15] Huang WM, Ding Z, Wang CC, Wei J, Zhao Y, Purnawali H. Shape memory materials. Mater Today. 2010;13:54-61.

[16] Rimmer S. Biomedical hydrogels: Biochemistry, manufacture and medical applications: Elsevier; 2011.

[17] Peppas NA, Ottenbrite RM, Park K, Okano T. Biomedical applications of hydrogels handbook: Springer Science & Business Media; 2010.

[18] Zalipsky S, Harris JM. Introduction to chemistry and biological applications of poly (ethylene glycol). Poly (ethylene glycol). 1997;680:1-13.

[19] Kasko A. Degradable Poly (ethylene glycol) Hydrogels for 2D and 3D Cell Culture. Aldrich Materials Science. 2013:67-75.

[20] Mironi-Harpaz I, Wang DY, Venkatraman S, Seliktar D. Photopolymerization of cell-encapsulating hydrogels: Crosslinking efficiency versus cytotoxicity. Acta Biomater. 2012;8:1838-48.

[21] Browning M, Cereceres S, Luong P, Cosgriff‐Hernandez E. Determination of the in vivo degradation mechanism of PEGDA hydrogels. Journal of Biomedical Materials Research Part A. 2014;102:4244-51.

[22] Lynn AD, Kyriakides TR, Bryant SJ. Characterization of the in vitro macrophage response and in vivo host response to poly(ethylene glycol)-based hydrogels. Journal of Biomedical Materials Research Part A. 2010;93A:941-53.

[23] Cui Y, Tan M, Zhu A, Guo M. Mechanically strong and stretchable PEG-based supramolecular hydrogel with water-responsive shape-memory property. J Mater Chem B. 2014;2:2978-82.

[24] Rolando B, Daniela P. Hydrogels: Characteristics and Properties. Scaffolds for Tissue Engineering: Pan Stanford Publishing; 2014. p. 337-85.

[25] Johnson A, Karpatkin MH, Newman J. Clinical Investigation of Intermediate‐and High‐Purity Antihaemophilic Factor (Factor VIII) Concentrates. British journal of haematology. 1971;21:21-41.

[26] Smyth HF, Carpenter CP, Weil CS. The toxicology of the polyethylene glycols. Journal of the American Pharmaceutical Association. 1950;39:349-54.

[27] Herold DA, Keil K, Bruns DE. Oxidation of polyethylene glycols by alcohol dehydrogenase. Biochem Pharmacol. 1989;38:73-6.

[28] Szycher M, Sharma CP. Blood compatible materials and devices: perspectives towards the 21st century: CRC Press; 1990.

[29] Deible CR, Petrosko P, Johnson PC, Beckman EJ, Russell AJ, Wagner WR. Molecular barriers to biomaterial thrombosis by modification of surface proteins with polyethylene glycol. Biomaterials. 1998;19:1885-93.

[30] Gombotz WR, Guanghui W, Horbett TA, Hoffman AS. Protein adsorption to poly (ethylene oxide) surfaces. Journal of biomedical materials research. 1991;25:1547-62.

[31] Harris JM. Poly (ethylene glycol) chemistry: biotechnical and biomedical applications: Springer Science & Business Media; 2013.

[32] Browning MB, Cosgriff-Hernandez E. Development of a biostable replacement for PEGDA hydrogels. Biomacromolecules. 2012;13:779-86.

[33] Knop K, Hoogenboom R, Fischer D, Schubert US. Poly (ethylene glycol) in drug delivery: pros and cons as well as potential alternatives. Angew Chem Int Ed. 2010;49:6288-308.

[34] Harris Z, Zalipsky S. Poly(ethylene Glycol): American; 1997.

[35] Chen D, Yoon J, Chandra D, Crosby AJ, Hayward RC. Stimuli-responsive buckling mechanics of polymer films. J Polym Sci, Part B: Polym Phys. 2014;52:1441-61.

[36] Zhao Y, Chun Wang C, Min Huang W, Purnawali H. Buckling of poly(methyl methacrylate) in stimulus-responsive shape recovery. Appl Phys Lett. 2011;99:131911.

[37] Gentile P, Chiono V, Carmagnola I, Hatton PV. An Overview of Poly(lactic-co-glycolic) Acid (PLGA)-Based Biomaterials for Bone Tissue Engineering. International Journal of Molecular Sciences. 2014;15:3640-59.

[38] Makadia HK, Siegel SJ. Poly Lactic-co-Glycolic Acid (PLGA) as Biodegradable Controlled Drug Delivery Carrier. Polymers. 2011;3:1377-97.

[39] Miller RA, Brady JM, Cutright DE. Degradation rates of oral resorbable implants (polylactates and polyglycolates): Rate modification with changes in PLA/PGA copolymer ratios. Journal of Biomedical Materials Research. 1977;11:711-9.

[40] Wong YS, Stachurski ZH, Venkatraman SS. Modeling shape memory effect in uncrosslinked amorphous biodegradable polymer. Polymer. 2011;52:874-80.

[41] Wong YS, Xiong Y, Venkatraman SS, Boey FYC. Shape memory in un-cross-linked biodegradable polymers. Journal of Biomaterials Science, Polymer Edition. 2008;19:175-91.

[42] Lendlein A, Kelch S. Shape-Memory Polymers. Angew Chem Int Ed. 2002;41:2034-57.

[43] Sakurai K, Kashiwagi T, Takahashi T. Crystal structure of polynorbornene. J Appl Polym Sci. 1993;47:937-40.

[44] Sakurai K, Takahashi T. Strain‐induced crystallization in polynorbornene. J Appl Polym Sci. 1989;38:1191-4.

[45] Mather P, Jeon HG, Haddad T. Strain recovery in POSS hybrid thermoplastics. Polymer Preprints(USA). 2000;41:528-9.

[46] Baino F. Biomaterials and implants for orbital floor repair. Acta Biomater. 2011;7:3248-66.

[47] You Y, Min BM, Lee SJ, Lee TS, Park WH. In vitro degradation behavior of electrospun polyglycolide, polylactide, and poly (lactide‐co‐glycolide). J Appl Polym Sci. 2005;95:193-200.

[48] You Y, Lee SW, Youk JH, Min B-M, Lee SJ, Park WH. In vitro degradation behaviour of non-porous ultra-fine poly (glycolic acid)/poly (L-lactic acid) fibres and porous ultra-fine poly (glycolic acid) fibres. Polym Degrad Stab. 2005;90:441-8.

[49] Holland S, Jolly A, Yasin M, Tighe B. Polymers for biodegradable medical devices: II. Hydroxybutyrate-hydroxyvalerate copolymers: Hydrolytic degradation studies. Biomaterials. 1987;8:289-95.

[50] Bergsma J, De Bruijn W, Rozema F, Bos R, Boering G. Late degradation tissue response to poly (L-lactide) bone plates and screws. Biomaterials. 1995;16:25-31.

[51] Agrawal C, Ray RB. Biodegradable polymeric scaffolds for musculoskeletal tissue engineering. Journal of biomedical materials research. 2001;55:141-50.

[52] Sarazin P, Roy X, Favis BD. Controlled preparation and properties of porous poly (L-lactide) obtained from a co-continuous blend of two biodegradable polymers. Biomaterials. 2004;25:5965-78.

[53] Vert M, Li S, Garreau H, Mauduit J, Boustta M, Schwach G, et al. Complexity of the hydrolytic degradation of aliphatic polyesters. Die Angewandte Makromolekulare Chemie. 1997;247:239-53.

[54] Athanasiou KA, Niederauer GG, Agrawal CM. Sterilization, toxicity, biocompatibility and clinical applications of polylactic acid/polyglycolic acid copolymers. Biomaterials. 1996;17:93-102.

[55] Borden M, Attawia M, Khan Y, Laurencin CT. Tissue engineered microsphere-based matrices for bone repair:: design and evaluation. Biomaterials. 2002;23:551-9.

[56] Kessel D, Robertson I. Interventional Radiology: A Survival Guide: Elsevier Health Sciences UK; 2011.

[57] Catheter Embolization. Radiological Society of North America, Inc; 2014.

[58] Kruft MAB, Benzina A, Bär F, van Der Veen FH, Bastiaansen CWM, Blezer R, et al. Studies on two new radiopaque polymeric biomaterials. Journal of Biomedical Materials Research. 1994;28:1259-66.

[59] Sang L, Wei Z, Liu K, Wang X, Song K, Wang H, et al. Biodegradable radiopaque iodinated poly(ester urethane)s containing poly(ε-caprolactone) blocks: Synthesis, characterization, and biocompatibility. Journal of Biomedical Materials Research Part A. 2014;102:1121-30.

[60] Choi SY, Hur W, Kim BK, Shasteen C, Kim MH, Choi LM, et al. Bioabsorbable bone fixation plates for X-ray imaging diagnosis by a radiopaque layer of barium sulfate and poly(lactic-co-glycolic acid). Journal of Biomedical Materials Research Part B: Applied Biomaterials. 2015;103:596-607.

[61] Agusti G, Jordan O, Andersen G, Doelker É, Chevalier Y. Radiopaque iodinated ethers of poly(vinyl iodobenzyl ether)s: Synthesis and evaluation for endovascular embolization. J Appl Polym Sci. 2015;132:n/a-n/a.

[62] Cabasso I. Radiopaque Polymers. Encyclopedia of Polymer Science and Technology: John Wiley & Sons, Inc.; 2002.

[63] Sastri VR. Plastics in medical devices: properties, requirements, and applications: William Andrew; 2013.
[64] Hubbell JH, Seltzer SM. Tables of X-ray mass attenuation coefficients and mass energy-absorption coefficients 1 keV to 20 MeV for elements Z= 1 to 92 and 48 additional substances of dosimetric interest. National Inst. of Standards and Technology-PL, Gaithersburg, MD (United States). Ionizing Radiation Div.; 1995.
[65] British Pharmaceutical Codex: Pharmaceutical Press; 1954.
[66] Glocker D, Ranade S. Medical Coatings and Deposition Technologies: John Wiley & Sons; 2016.
[67] Davis SA, Lareau R. Polycarbonate Polyurethane Venous Access Devices Having Enhanced Strength. Google Patents; 2010.

Chapter 3 Materials and Methods

3.1 Materials

Purasorb Poly(DL-Lactide-co-Glcolide) (PLGA) with 50:50 monomer ratio and molecular weight of 90 kDa is purchased from Purac biomaterials (now Corbion biomedical). The degradation period for the polymer as mentioned in literature is around 1 to 2 months, which makes it suitable for embolic device application. Polyethylene glycol flakes (Mw 2 kDa), which was used as plasticizer for PLGA and Polyethylene glycol with diacrylate end group (PEGDA) (no. average Mw 10 kDa) for hydrogel synthesis were purchased from Sigma-Aldrich. 2-hydroxy-1-[4-(hydroxyethoxy)phenyl]-2-methyl-1-propanone (Irgacure-2959), a free radical initiator for hydrogel crosslinking and radiopaque fillers Barium Sulfate, Tantalum, Bismuth (III) oxychloride in powder form were purchased from Sigma-Aldrich. Ethanol (absolute for analysis grade) was purchased from Merck KGaA (Germany).

Iohexol (OMNIPAQUE™ 300) is a non-ionic radiopaque contrast agent (liquid) used for opacification of blood vessels for radiographic visualization. We are using Iohexol in order to impart radiopacity to the gel. Lipiodol, ethyl esters of iodized fatty acids of poppy seed oil, is a radio-opaque contrast agent suggested for selective hepatic intra-arterial use in order to imagine tumours in adults with known hepatocellular carcinoma (HCC)[1]. Lipidol is used in our studies for flushing catheter in order to prevent swelling of gel inside catheter.

3.2 Fabrication of Radiopaque PLGA filaments

3.2.1 Sample Naming

The samples had been named according to the type of matrix, radiopacifier and plasticizer and their weight percentage (wt%) used. For example, a sample name PLGA-BO504 represent that PLGA composition with 50 weight percent bismuth(III) oxychloride radiopaque filler and four weight percent PEG plasticizer with respect to PLGA.

Table 3.1 lists the biodegradable PLGA shape memory filaments formulations used in our study. PLGA was dry blended with one of the radiopaque fillers Barium Sulfate, Bismuth Oxychloride or Tantalum and Polyethylene glycol flakes (Mw 2 kDa) (plasticizer) in different weight proportion and then compounded using DSM Xplore twin-screw micro-extruder (DSM, The Netherlands). The processing temperature used was 150 °C and screw speed was set to 100 rpm. Five minutes of mixing time or residence time was given for complete mixing. The filaments were extruded through 0.5mm circular die. The final diameter obtained was in the range 0.65 to 0.70 mm because of die swell. The filaments were stored in desiccator and were used for making embolic device and for individual characterizations such as mechanical, thermal, shape memory, surface properties and radiopacity characterization.

3.2.2 Fabrication of sheet by compression moulding

PLGA filaments of varying compositions formed by the melt extrusion were cut into small strands. The strands were compression moulded into sheet of size 65mm x 50mm x 0.3 mm using hydraulic hot press (Carver, USA). The processing temperature was 150°C and maintained at 10,000 Psi for 5 minutes. The film was cooled down to room temperature and then demoulded. The films were stored in desiccator until further characterizations.

Table 3.1 Different formulations of biodegradable PLGA shape memory polymer

No.	Composition	PLGA	PEG (Mw 2k)	Barium Sulfate	Tantalum	Bismuth Oxychloride
		%	%	%	%	%
1	PLGA 50	100	-	-	-	-
2	PLGA 502	98	2	-	-	-
3	PLGA 504	96	4	-	-	-
4	PLGA BS504	48	2	50	-	-
5	PLGA TT504	48	2	-	50	-
6	PLGA BO504	48	2	-	-	50

7	PLGA BO50	50	-	-	-	50

3.3 PLGA filament characterization:

Different formulation of PLGA with radiopaque fillers and plasticizer were characterized for their thermal and mechanical properties, radiopacity and shape memory behavior.

3.3.1 Thermogravimetric Analysis (TGA)

Thermogravimetric analysis (TGA) was conducted using a TA instrument TGA 2950 (USA). The samples were heated to 800 °C at a rate of 10°C/min under nitrogen atmosphere and the weight loss with temperature was obtained. Residual mass because of radiopaque fillers is calculated from TGA thermograms.

3.3.2 Radiopacity

To examine the degree of radiological visibility of the specimen imparted by the radiopaque fillers, unfilled and filled specimens of 0.7 mm diameter were examined by clinical X-Ray fluoroscopy at Singapore General Hospital, radiology department. The radiographs were captured at the exposure (70 kV, at 41 mA, for 3.2 ms) with the specimen imaged next to a metal radiographic standard.

3.3.3 Differential Scanning Calorimetry (DSC)

Thermal characteristics and transition temperatures of different PLGA formulations were evaluated using differential scanning calorimeter (DSC). Differential scanning calorimeter (TA Instrument DSC Q10, USA) was used to study the thermal behavior of the exruded PLGA filaments. Heat-cool-heat cycle with a rate of 10°C/min was used to scan the temperature range from 0°C to 70°C. Three samples were tested for each formulation. Glass transition temperature (Tg) and onset glass transition temperature were measured from the second heating cycle in order to eliminate effect of moisture

or previous thermal history and to accord it with actual process of making embolic device.

3.3.4 Mechanical Properties

Mechanical characterization of PLGA filaments was carried out by uni-axial tensile testing with a MTS Criterion C42 machine (MTS Systems, USA) with a 50 N load cell and 25 mm/min extension rate at room temperature. Extruded PLGA filaments were cut in 30 mm length (gauge length 10 mm). Elastic modulus and tensile strength at yield were calculated using a provided software. For the elastic modulus the initial linear region of the stress-strain curve within the strain range of 2% is considered.

3.3.5 Shape memory properties of PLGA composite filaments

Thermal shape memory behavior of different PLGA compositions were studied. Although the water induced shape memory effect of the gel is main driving force for actuation of device, it is important to know the effect of thermal shape memory of PLGA backbone on the overall mechanism of recovery. Two types of test were conducted to demonstrate and compare the shape memory behavior of different compositions.

Shape memory of coiled samples

In this test the all the extruded PLGA filaments were wrapped around 4 mm screw and kept in oven at 85°C for 20 min to fix coil shape as permanent shape. The PLGA coil was then warmed using 40°C water and the uncoiled and quenched using ice water to form straight temporary shape. The shape recovery from temporary shape to permanent shape was studied in 37°C water. Three reading were taken for each composition for % recovery in four minutes constant time.

Shape memory of stretched samples

In second test, shape memory programming method and testing conditions were kept similar to that for embolic device programming and testing. PLGABO504 (PLGA+50% Bismuth Oxychloride+ 4% PEG (Mw 2k)) filaments were used to study the effect of different programming temperatures on % recovery and recovery speed. The straight filaments of known length were heated in oven at three different temperatures 60, 70 and 80°C for 20 minutes and followed by stretching by 500% and quenching to room temperature. Then the recovery of samples was observed in 37°C water.

Effect of plasticizer on shape memory behavior of stretched sample at 70°C was studied with the same protocol.

$$\%\ \boldsymbol{Recovery, R} = \frac{\boldsymbol{L_t - L_r}}{\boldsymbol{L_t - L_0}} \times \mathbf{100} \qquad 3.1$$

where Lt is length of temporary shape; L_r is length after recovery, L_0 is length of permanent shape (original length).

3.3.6 Plasma Treatment

Plasma is the partially ionized state of the gas, consisting of neutral atoms, atomic ions, molecular ions, molecules and electrons present in excited and ground states. The charged particles present in the plasma confer high electrical conductivity and it carries quite an amount of an internal energy, which when come in contact with a particular surface, alter the surface properties[2]. Chemical modification of surface occurs by polymer chain scissions followed by formation of broad variety of functional groups, which is also accompanied by physical modification i.e. etching of surfaces forming peaks and valleys. Roughening increases specific surface which helps in mechanical anchoring in addition to chemical functionality of the surface. Plasma treatment is widely used in polymeric biomaterials for increasing hydrophilicity and improving cell adhesion[3, 4].

In this research work oxygen plasma treatment (Figure 3.1) was used to improve the hydrophilicity of the PLGA filaments for better adhesion with PEG hydrogel to be coated for making the embolic plug.

PLGA film with different compositions as described in Table 3.1,were prepared by a compression moulding method. Plasma treatment was carried out in a Covance plasma system with radio frequency generated oxygen plasma (Femto Science, South Korea). After evacuating the air from the chamber, the oxygen gas is passed at the flow rate of 30 standard centimetres cubic per minute (sscm). The plasma is generated at 100W power and pressure of 0.2 torr. Sample was subjected to plasma discharge for the duration of 10 minutes. Plasma treated film was characterized by contact angle measurement to elucidate the effect of plasma on wettability of the surface. Whereas, extruded PLGA filaments, after plasma treatment were used to fabricate embolic device.

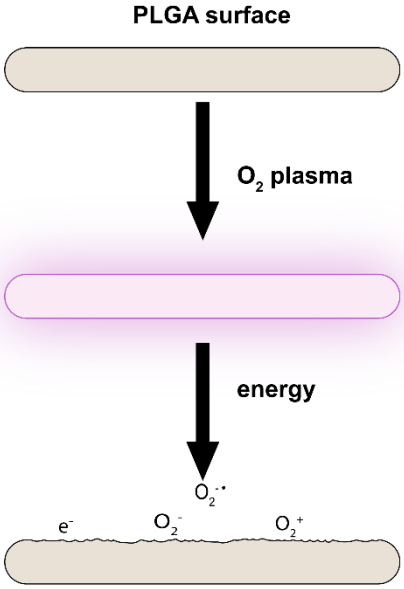

Figure 3.1 Schematic diagram of plasma treatment

3.3.7 Water contact angle measurements

Surface wettability i.e. hydrophilic and hydrophobic properties of a solid surface are characterized by static contact angle measurement. Contact angle depend on various factors, such as surface composition, roughness and energy, surface cleanliness and method of preparation[5]. Good surface wettability i.e. hydrophilic surfaces are marked by lower value of contact angle, usually less than 90 ^{o}.

To study the effect of presence of radiopaque particulate fillers, PEG plasticizer, and multifunctional PEGDA plasticizer on the surface properties of PLGA, contact angle measurements were performed using OCA 15 Pro (Dataphysics, Germany), video-based optical contact angle measuring system. Sessile drop method with 6 μL drop volume of deionized water at 5 μL/s doing rate was used. The contact angle was recorded using SCA 20 image analysis software immediately after depositing the drop on the flat substrate of given PLGA compositions at 25 ± 1 °C. A minimum of five measurements, taken at different positions on the film, were carried out. The average value of contact angles measured on both sides of the drop was used.

3.3.8 Size exclusion chromatography

Molecular weight changes of PLGA were determined by size exclusion chromatography (SEC), with Agilent 1100 series (Agilent Technologies, USA), equipped with a G1262A refractive index detector. All measurements were carried out with a linear PL gel 5 μm mixed-C column maintained at 35 °C. HPLC grade chloroform was used as mobile phase at a flow rate of 1.0 mL/min. Triplicate of sample were used for each characterization.

3.4 Synthesis and characterization of PEG hydrogel

Photo-crosslinking method was used to make hydrogel from macromolecular polyethylene glycol diacrylate solution in water (M_n 10kDa) (PEGDA)[6, 7]. PEGDA powder was dissolved in DI water at room temperature in different weight to volume ratio (5%, 7.5%). Free radical photo-initiator, Irgacure-2959 dissolved in 70% ethanol was added to the PEGDA solution so as to get weight percentage of 0.5%, 1%, 2% and 3% relative to PEGDA. The solution mixture (200 uL for swelling and gel content studies and 150 uL for rheological studies) was then added into 96-wells plate and then cross-linked for 7 minutes under Ultraviolet light (λ=365-nm, Power=12W) (Vilber Lourmat, France) at a 1-cm distance apart.

Hydrogel samples with radiopaque fillers and liquid contrast medium (iohexol) were prepared by same method as above. Three different solid fillers Barium sulfate, Tantalum and Bismuth oxychloride were added and mixed mechanically in PEGDA macromer solution in 10% weight fraction. For the formulations with contrast medium, 2.5, 5, 10, 20 and 30% v/v of contrast medium were added to DI water and then PEGDA is dissolved in it.

3.5 Characterization of PEG hydrogels

Different formulations of PEGDA hydrogel were characterized for their swelling behavior, gel content, rheology, radiopacity, thermal behavior and shape memory properties.

3.5.1 Swelling Characteristics

Photo-crosslinked hydrogel samples were washed in DI water for 24 hours to wash out the unreacted monomer or initiator and then dried for 48 hours at 40 °C. The dried hydrogel samples were dipped in DI water and the changes in weight because of water absorption with time were recorded. Three reading were taken for each formulation.

$$\boldsymbol{Swelling\ Ratio} = \mathbf{1} + \frac{(\boldsymbol{W_t - W_i})}{\boldsymbol{W_i}} \times \boldsymbol{\rho_i} \qquad 3.2$$

Where, W_i is initial weight of dry hydrogel; W_t is weight of swollen hydrogel at time, t; ρ_i is the density of dry weight of hydrogel (volume calculated using ImageJ analysis software).

3.5.2 Gel Fraction

Photo-crosslinked hydrogel samples were dried for 48 hours at 40°C. The weight of the dry samples is recorded (W_i) and then it was soaked in DI water for 48 hours for washing off uncroslinked macromers. The gel was then dried for 48 hours at 40°C, and

the dry weight of the gel is recorded (W_f). The gel fraction, which is indication of degree of crosslinking, is then calculated in percentage as Readings were taken in triplicates.

$$\boldsymbol{Gel\ fraction}\ (\%) = \frac{\boldsymbol{W_f}}{\boldsymbol{W_i}} \times \mathbf{100} \qquad 3.3$$

where W_i is initial weight of dry hydrogel; W_f is weight of dry insoluble part.

3.5.3 Rheology

Crosslinking density and the mechanical properties of hydrogel were evaluated using cone and plate rheometer (Anton Paar Physica MCR 501, Germany GmbH). An amplitude sweep from 1% to 100% was carried out at constant frequency of 1 Hz to find the linear viscoelastic region (LVR) for each sample. The amplitude value was chosen from linear viscoelastic region and was set constant while performing frequency sweep from 0.1 Hz to 10 Hz. The response of shear storage modulus (G') and shear loss modulus (G'') to the frequency was plotted by software. Both these tests were carried out at 25°C and for each formulation three samples were tested.

3.5.4 Radiopacity

To examine the degree of radiological visibility of the specimen imparted by the radiopaque fillers, unfilled and filled specimens of 0.7 mm diameter were examined by clinical X-Ray fluoroscopy at Singapore General Hospital, radiology department. The radiographs were captured at the exposure (70 kV, at 41 mA, for 3.2 ms) with the specimen imaged next to a metal radiographic standard.

3.5.5 Differential Scanning Calorimetry (DSC)

Differential Scanning Calorimetry (DSC) of unstreched dry hydrogel sample was carried out on differential scanning calorimeter (TA Instruments DSC Q10, USA) in order to identify the transition temperature for the shape memory programming.

Further DSC of the hydrogel filaments stretched to a different ration is examined. The DSC scan was obtained by heat-cool-heat cycles from 0°C to 90°C at the heating and cooling rate of 10°C per minute. The transition temperature and the enthalpy were analysed using TA universal software. Three samples of each hydrogel compositions were tested.

3.5.6 Shape Memory Behaviour

Hydrogel samples were prepared by photo-crosslinking method using transparent plastic straw with 6mm ID as the mould. The crosslinked hydrogel was taken out from the straw and dried at 40 °C for 48 hours. The known length of the dry hydrogel was heated at 70°C for 20 minutes and then hand-stretched inside oven to the drawing ration of 3, 5, 6, 7 and 8. The samples were cooled down to the room temperature to fix new shape and then the stresses were removed. Thick ends of the samples were trimmed, and the hydrogel filaments were used for water induced shape recovery studies.

Equal lengths of samples with different drawing ratio were immersed in water maintained at 37°C and recovery (free recovery) process of the samples is inspected with time

3.6 Device Fabrication using polymer-hydrogel composite

Fabrication of biodegradable embolic device composed of polymer-gel composite was carried out in two steps. The first step was to coat PEG hydrogel on PLGA backbone and second step was to program the device for water induced shape memory effect.

3.6.1 Coating of PEG hydrogel on PLGA filament

In first step PEG hydrogel precursor solution was prepared by method mentioned earlier. Extruded radiopaque PLGA filaments (diameter 0.65-0.7mm) subjected to oxygen plasma as described in section. The plasma treated PLGA composite filament was held straight at the center of transparent plastic mold (6mm inner diameter and 140mm

length) by using clips. The both ends of mold were sealed with foam tape having hole at the center to allow passage of PLGA filament. Then the precursor solution was transferred into the mold using syringe and needle by pricking another hole in the end of the mold. The whole setup was kept for crosslinking for 7 minutes under ultraviolet light (λ=365-nm, Power=12W) (Vilber Lourmat, France) at a 1-cm distance apart. The cross-linked gel coated PLGA filament was taken out by cutting the thin mold out and kept for drying at 40°C for 48 hours. The dry sample length was in the range 110±5 mm and diameter after drying was 2.3±2mm.

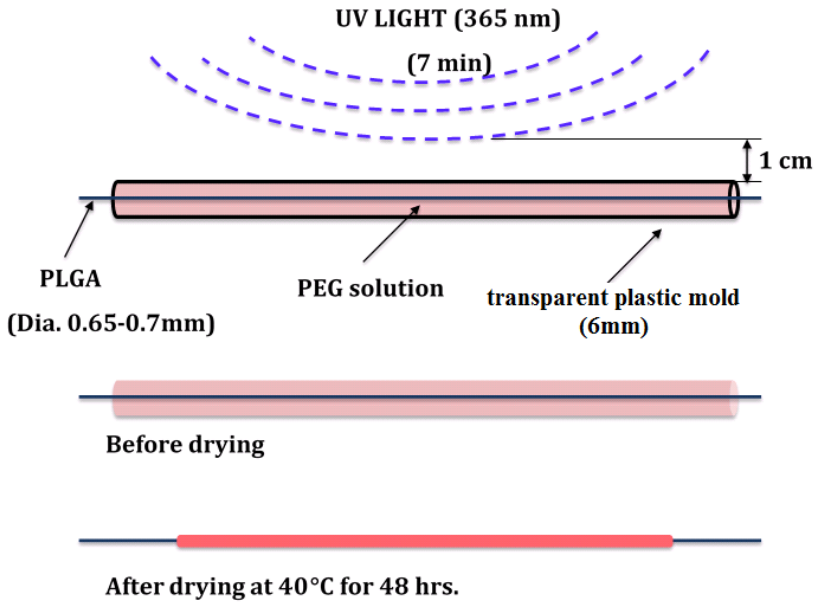

Figure 3.2 method of coating PEG hydrogel on PLGA filament

3.6.2 Shape memory programming for water induced buckling

Figure 3.3 illustrates the steps involved in programming water induced shape memory for polymer-hydrogel composite. For the shape memory programming the sample was heated in the oven at 70°C for 20 minutes. The programming temperature has to be above the transition temperature for both PLGA and PEG. Then the composite was stretched to required deformation strain (500%) and then quenched to the room temperature releasing the stress. The diameter of the final sample was in range 0.8-0.85

mm. These samples were cut in desired length after trimming the holding portion on both the ends and used for *in-vitro* flow studies.

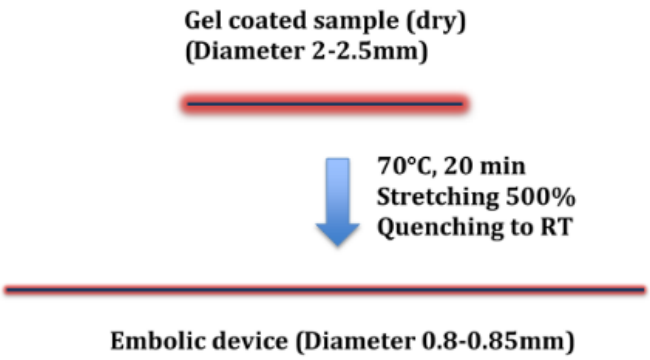

Figure 3.3 Shape memory programming of polymer-hydrogel composite

3.7 Interfacial shear strength between radiopaque PLGA filament and PEGDA hydrogel using Pull-off test

The experiment was designed to study the interfacial bonding strength for a composite consisting extruded radiopaque PLGA filament coated with PEG hydrogel. The effect of plasma treatment on the interfacial bonding strength was evaluated. The PLGA sample sets were prepared as shown in the Table 3.2 below.

Table 3.2 PLGA compositions for plasma treatment

PLGA filaments via extrusion	PLGA	BiOCl	PEG (Mw 2k)	Plasma Treatment time (100W)
PLGA BO504 (control)	48	50	2	-
PLGA BO504P	48	50	2	10 min

The PLGA filaments of diameter 0.7 ± 0.02 mm were coated with PEG hydrogel (7.5% w/v, 2% initiator w/w, and 7-minute UV exposure) using same protocol and composition of PEG hydrogel as described earlier.

Pull-off test was carried out in tensile mode using TCD110 Series Force Measurement System (Chatillon Force Measurement Products, USA) with a 10N load cell and a crosshead speed of 3 mm/min. Measuring length of 30 mm was employed for all the samples. Interfacial shear force generated, and corresponding extension were recorded. The maximum load required delaminate the PLGA filament from the hydrogel coating for was reported. The experimental arrangement for the test is illustrated in Figure 3.4.

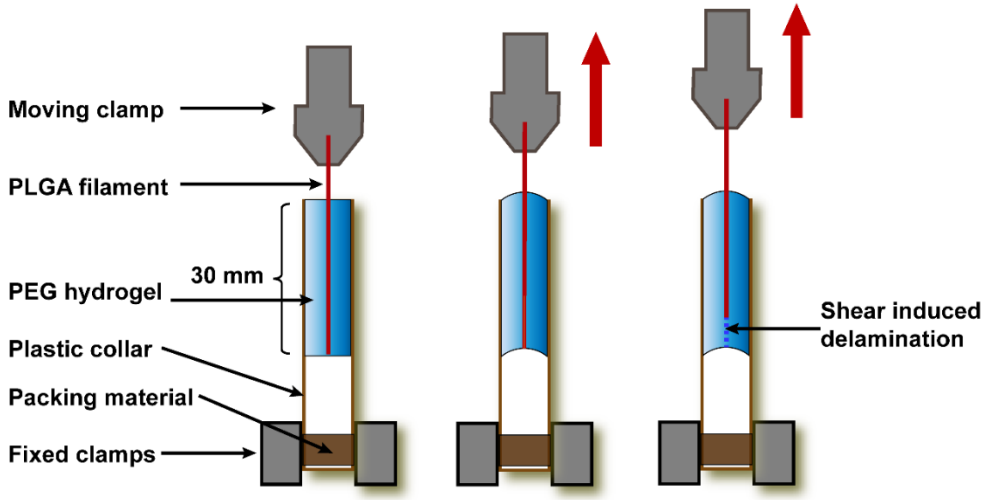

Figure 3.4 Experimental setup for the pull-off test

3.8 Scanning Electron Micrography of PLGA composite

To understand the interactions between the radiopaque fillers and PLGA matrix as well as the interfacial adhesion between PLGA filament and coated hydrogel, morphological analysis was performed with the scanning electron microscope (SEM; JSM-6360A JEOL, Japan) operating voltage 5kV and field emission scanning electron microscope (FESEM; JSM-6340F JEOL, Japan) operating voltage 3 kV respectively. The samples were cut, and the cross-sectional surface were sputter coated with platinum (JFC-1600 JEOL, Japan) for 60 seconds. Only one representative SEM micrograph is shown.

3.9 *In-vitro* studies of device in flow system

In-vitro flow system (Figure 3.5) was designed to study the deployment and actuation of the device in water at various flow rate through different sizes of tubing's resembling to actual blood vessel network. Tubing's (Masterflex Tygon™), peristaltic pump (Masterflex L/S) and fittings were purchased from Cole-Parmer. Figure 3.5 shows the design of the flow system.

Different tubing's sizes matching to the blood vessels to be embolized can incorporated in the flow system. Flow rate range for the peristaltic pump is 0.06 to 2300 mL/min.

For initial *in-vitro* flow studies the Tygon tube with internal diameter 3.175mm and flow rate of 120 mL/min was used. 4 French (Internal Diameter 0.97mm) catheter was pierced inside the tube to facilitate the delivery of the device. Before introducing the device into catheter, either catheter was flushed with lipidol oil or the device is washed with lipidol oil to avoid swelling of device in catheter. The device was loaded in the catheter using loader and pushed till the end using guide wire.
The recovery/actuation of the device is monitored visually (NTU, Singapore) as well as under X-ray fluoroscopy (SGH, Singapore). Time to start the recovery of the embolic device was recorded along with the monitoring reduction in the flow, until the flow stops completely.

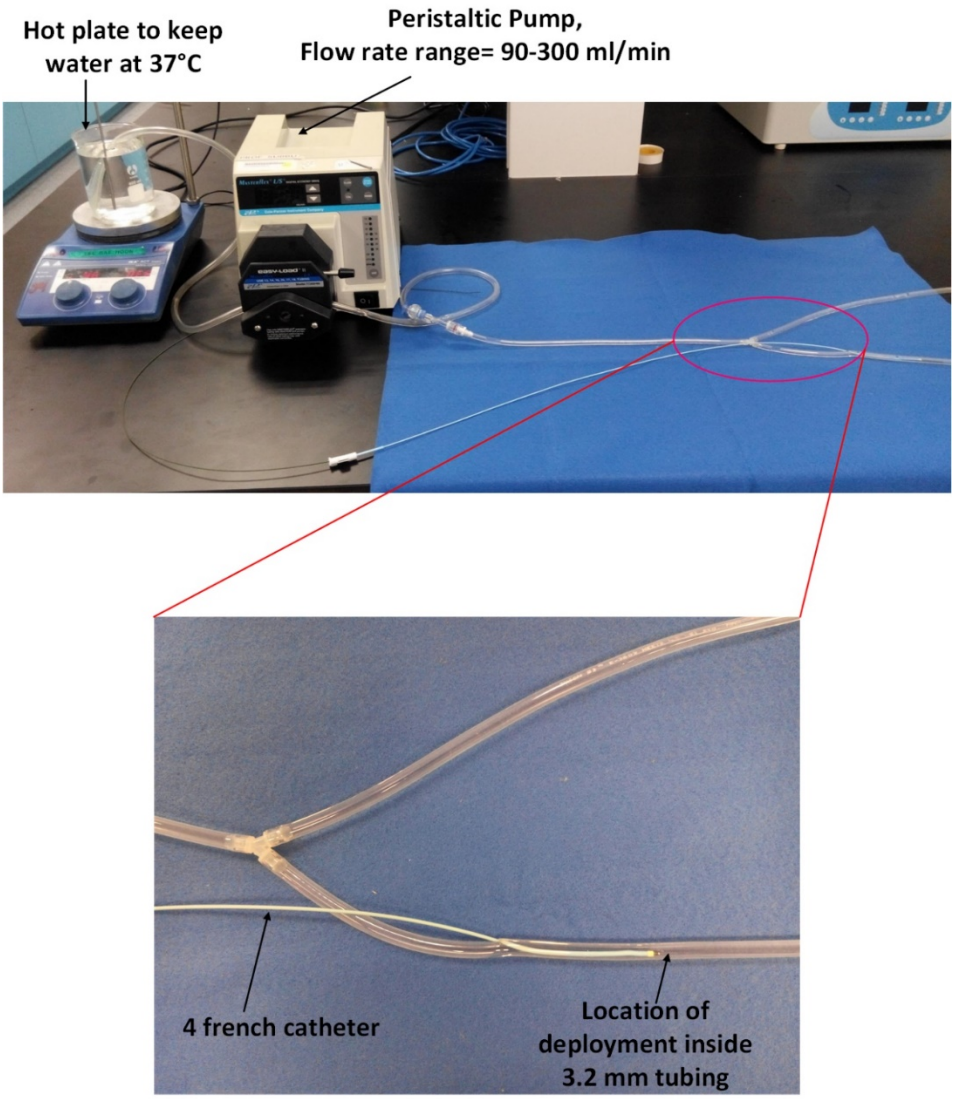

Figure 3.5 simulated blood flow experimental model

3.10 Water-responsive Shape Recovery Induced Buckling in Biodegradable Photo-crosslinked Polyethylene Glycol (PEG) Hydrogel

3.10.1 Preparation of hydrogel filaments

PEGDA hydrogel were synthesized using method and formulation as described in section 3.4. Different sized transparent plastic moulds were used to photo-crosslink the hydrogels to prepare hydrogel filaments with different diameter. Table presents the diameters of PEG hydrogel sample in wet state and in dry state after drying at 37 °C incubator for 48 hours.

Table 3.3 Diameters of PEG hydrogel in wet and dry state

Wet state, (mm)	Dry state (mm)
3.85	1.50
4.45	1.80
5.95	2.45
7.20	2.75

3.10.2 Shape memory programming

Dry PEG samples were heated in an oven and maintained at 70 °C (above its Tm) for 20 minutes and then stretched to the different programming strains under considerations viz. 300, 400, 500, 600 and 700 % strain. The applied constraint was removed, only after the stretched samples were cooled back to the room temperature.

3.10.3 Effect of programming strain on the mechanical properties of dry hydrogel

A MTS Criterion C42 Machine (MTS Systems, USA) with a 50 N load cell was used to investigate the mechanical properties of dry samples with gage length of 30 mm at 25°C. Uni-axial tensile tests were carried out at a strain rate of 5.56×10^{-3}/s.

3.10.4 Mechanical properties of wet hydrogels

Hydrogel samples with different starting diameter in dry state were hydrated in DI water at 37 ºC for 15 minutes until it became all hydrated. The dimensions of the samples were noted for the subsequent stress-strain calculations. These samples were then characterized using uniaxial tensile test on MTS Criterion C42 machine with the same testing parameters as mentioned in section 3.3.4.

3.10.5 Cyclic tensile testing of dry hydrogel at 70 ºC.

Cyclic tensile test was carried using MTS Criterion C43 Machine (MTS Systems, USA) with a 500 N load cell and a heating chamber. A dry hydrogel sample with 2.45 mm

diameter and 10.5 mm gage length was fixed between the two clamps inside the heating chamber set at 70ºC. Cyclic tensile test for three different strains points (300%, 500% and 700%, in ascending order) was then carried out at a strain rate of 0.079/s using multicycle to different strain point module in MTS software.

3.10.6 Determination of recovery force generated in hydrogel during water induced buckling of hydrogel

In order to find the recovery force generated by sample at 37°C when immersed in water, iso-strain test is carried out using MTS Criterion C42 machine with MTS Bionix® EnviroBath setup. The sample in temporary shape is fixed between two grips inside an EnviroBath and then deionized water at 37°C is circulated. The force generated by the sample is monitored with the time until the sample is completely transparent and solvated.

3.10.7 Determination of time to cause water induced buckling of a hydrogel

Similar setup as described in 3.10.6, except fixing the one end of the sample in upper grip and second end free to deflect, is used for calculating buckling time for the samples. Buckling time is recorded as the time at which sudden change in the configuration of sample such as bending, or coiling takes place.

3.11 Embolic device feasibility and safety studies

3.11.1 Shelf-life studies for the device

A medical device is used to address various conditions ranging from relieving minor irritations to emending life threatening conditions. A probability that the device will perform as desired at the time it is manufactured is high if the device design and manufacturing processes are done adequately. However, how long after manufacturing the device will maintain the ability to fully perform the intended function is affected by

various naturally occurring factors[8]. Shelf life is the time duration or period during which a device and all its active ingredients will remain stable suitable for intended use. The embolic device in this research developed using biodegradable polymers so it is important to study the shelf life of the device as whole with respect to its intended functionality, material and mechanical stability[9].

Embolic plug sealed in package were exposed ETO sterilization and then sterilized pack stored at 25^0C and 35% relative humidity in a desiccator. The samples were taken out at four different timepoints as day 0, day 30, day 90, and day 180 and characterized by following methods.

3.11.1.1 Mechanical Test:

Mechanical test of the embolic device is carried out using standard method as described in as per the ASTM F1635–16 and ASTM D638 [10, 11]. MTS Criterion C42 machine (MTS Systems, USA) with a 250 N load cell and 25 mm/min extension rate is used to carry out uni-axial tensile testing at room temperature. MTS advantage pneumatic grip (100 N) with 5 bar clamp pressure is employed to avoid slippage of the sample. Sample length of 35 mm length (gauge length 20 mm) is used. The tensile yield strength was calculated by dividing the load at yield point in newtons by the average original cross-sectional area in the gage length segment of the specimen in square metres. Elastic modulus is determined considering initial linear portion of the stress-strain curve.

3.11.1.2 Water induced shape recovery

Water induced shape recovery studies of the embolic plug in 37 ^{0}C DI water is carried using MTS Criterion C42 Machine with MTS Bionix® EnviroBath setup (MTS Systems, USA). The 37 ^{0}C DI water was circulated through the chamber using polyscience circulating water bath system (PolyScience, USA). The time required for the water induced shape recovery was noted for each sample.

3.11.1.3 Swelling of PEGDA hydrogel coating

The hydrolytic degradation of the acrylate esters in crosslinked PEG hydrogel results in the breakage of crosslinks, which is reflected in the increased swelling ratio[12-14]. The swelling ratio of the hydrogel coating part of the embolic device is calculated as described earlier.

3.11.1.4 Molecular weight of PLGA core filament.

The embolic plug was immersed in DI water at 37 ^{0}C. Upon complete shape recovery of the device and swelling of hydrogel, the PLGA filament was pulled out from the core and dried it at 37 ^{0} using vacuum oven for 48 hours. Then molecular weight of PLGA filament was determined by size exclusion chromatography as described earlier.

3.12 *In-vitro* degradation of the embolic plug

The individual components (PLGA filaments and PEGDA hydrogels) and prototypes (20 mm × 0.8 mm) were subjected to hydrolytic degradation *in vitro*. In brief, the samples were incubated with 5 ml of phosphate buffered solution (pH 7.4) in an incubator at 37 °C. The buffered solution was replaced every 5 days. The degraded samples were washed thoroughly with distilled water then dried to constant weight in vacuum at 37 °C, finally weighted. The percentage of weight loss was calculated according to:

$$\boldsymbol{Weight\ loss}\ (\%) = \left[\frac{W_t - W_0}{W_0}\right] \times 100\% \qquad 3.4$$

where W_t and W_0 are the dry weight of the sample on day t and day 0, respectively.

3.13 Sterilization of the device:

Embolic plugs were separately packed in Corning™ Falcon™ round-bottom polystyrene tubes with snap cap having few holes for the entry of ETO gas. The tubes were then packed in Seal and Peel® sterilization pouches (Andersen Products, Inc, USA). ETO sterilization was achieved in a 100% ethylene oxide atmosphere at 30°C for 24 h followed by 2 h ventilation using EOgas 4 (Andersen Products, Inc, USA). No change in the dimensions of the sample were observed.

3.14 Cytotoxicity

The direct contact mode was used to perform in vitro cell cytotoxicity test. In this study, mouse fibroblasts (L929) were cultured with low-glucose Dulbecco's Modified Eagle's Medium (DMEM) containing L-glutamine (Sigma Aldrich, USA) supplemented with 10% fetal bovine serum (FBS) (PAA, Pasching, Austria) and 1% antibiotic/antimycotic solution (PAA, Pasching, Austria) in a CO2 incubator at 37 ^{0}C. The fibroblasts (L929 cells) were harvested using enzymatic digestion and subcultured in 24-well plates at densities of 7.5 x 10^4 cells per well. The embolic device test samples (developed embolic plugs, 0.35 cm in length) were sterilized using ethylene oxide (EtO). The day after cell seeding, the sterilized specimens test samples (n = 3) were co-cultured with L929 and the media were changed daily. At predetermined time points, cell morphology was observed, and cell viability was quantified with PrestoBlue® assay (Life technology, Singapore) according to the manufacturer's instruction with a monolayer of L929 and Gelfoam® (Pfizer, USA) as controls.

3.15 In vivo feasibility study to assess embolization efficacy in rabbit model

An in vivo feasibility study was performed on 4 adult New Zealand white rabbits according to the National Advisory Committee on Laboratory Animal Research (NACLAR) guidelines and Institutional Animal Care and Use Committee approval was obtained (IACUC #2015/SHS/1063). The aim of the feasibility study was to assess the feasibility of prototype deployment in the in vivo setting. The New Zealand rabbit was chosen due to its adequate size and similar tissue response as humans. The rabbits were sedated with intramuscular ketamine and xylazine, followed by maintenance general anesthesia with inhalational sevoflurane. The femoral artery of each rabbit was exposed surgically and a 4F vascular sheath inserted (Cordis, Warren, NJ). A 4F x 65cm Berenstein catheter (Cordis, Warren, NJ) was used to perform angiography and catheterize a suitable artery for embolization. Upon gaining access to the target vessel, lipiodol was used to flush the catheter before loading the prototypes, so as to prevent intra-catheter expansion of prototype which can block the catheter. The prototype was loaded into the catheter and pushed out of the catheter tip by a guide wire. A short

segment of the prototype was left within the catheter tip while allowing the exposed portion of prototype to undergo shape recovery and swelling. Continuous fluoroscopy was performed to assess the shape recovery of the deployed segment. The remaining short segment was later pushed out once shape recovery and swelling of the deployed segment was well on the way. Digital-subtraction angiography was used to assess for occlusive effect of the deployed prototype. The rabbits were euthanized with overdose injection of pentobarbital at the end of the study. Dissections with explant of the embolized carotid arteries were performed to visually inspect the artery and prototype in 2 of the 4 rabbits.

References

[1] LIPIODOL® (ethiodized oil) Injection. Guerbet; 2014.

[2] Friedrich J. The plasma chemistry of polymer surfaces: advanced techniques for surface design: Wiley Online Library; 2012.

[3] Wan Y, Qu X, Lu J, Zhu C, Wan L, Yang J, et al. Characterization of surface property of poly (lactide-co-glycolide) after oxygen plasma treatment. Biomaterials. 2004;25:4777-83.

[4] Tallawi M, Rosellini E, Barbani N, Cascone MG, Rai R, Saint-Pierre G, et al. Strategies for the chemical and biological functionalization of scaffolds for cardiac tissue engineering: a review. Journal of the Royal Society Interface. 2015;12:20150254.

[5] Jung YC, Bhushan B. Contact angle, adhesion and friction properties of micro-and nanopatterned polymers for superhydrophobicity. Nanotechnology. 2006;17:4970.

[6] Mironi-Harpaz I, Wang DY, Venkatraman S, Seliktar D. Photopolymerization of cell-encapsulating hydrogels: Crosslinking efficiency versus cytotoxicity. Acta Biomater. 2012;8:1838-48.

[7] Hagel V, Haraszti T, Boehm H. Diffusion and interaction in PEG-DA hydrogels. Biointerphases. 2013;8:36.

[8] Clark GS. SHELF LIFE OF MEDICAL DEVICES. Food and Drug Administration 1991.

[9] ASTM F2902 Standard Guide for Assessment of Absorbable Polymeric Implants. ASTM international; 2016.

[10] ASTM D638 - Standard Test Method for Tensile Properties of Plastics. ASTM international; 2014.

[11] ASTM F1635 - 16 Standard Test Method for in vitro Degradation Testing of Hydrolytically Degradable Polymer Resins and Fabricated Forms for Surgical Implants. ASTM international; 2016.

[12] Browning M, Cereceres S, Luong P, Cosgriff‐Hernandez E. Determination of the in vivo degradation mechanism of PEGDA hydrogels. Journal of Biomedical Materials Research Part A. 2014;102:4244-51.

[13] Browning MB, Cosgriff-Hernandez E. Development of a biostable replacement for PEGDA hydrogels. Biomacromolecules. 2012;13:779-86.

[14] Lynn AD, Kyriakides TR, Bryant SJ. Characterization of the in vitro macrophage response and in vivo host response to poly(ethylene glycol)-based hydrogels. Journal of Biomedical Materials Research Part A. 2010;93A:941-53.

Chapter 4 Material Characterization and Embolic Device Fabrication

4.1 Introduction

In this chapter properties of individual materials used for making a biodegradable embolic device were explored. PLGA and PEG were chosen as two materials based on their favorable degradation period and ability to be programmed for water induced shape memory for PEG and thermoresponsive shape memory for PLGA around body temperature. With the objective of making polymer-hydrogel composite, where the polymer (PLGA) modified with radiopaque fillers impart radiopacity to the device and will assist in the shape recovery of the device at body temperature. Whereas, the hydrogel primarily actuates the shape recovery of the device by water induced buckling and simultaneously it expands and accomplishes the mechanical blocking of the blood vessel

PLGA and PLGA composite with particulate radiopaque fillers and plasticizers were prepared and characterized for mechanical properties, thermal properties, shape memory function, wettability, and radiopacity

PEG hydrogel was synthesized and the parameters for optimum properties were identified by rheology, swelling, shape memory characterizations.

A novel method of making polymer-hydrogel composite by coating PEG hydrogel on the radiopaque PLGA filament was established and improvised.

Finally, the underlying mechanisms of water induced shape recovery of the embolic device is elucidated.

4.2 Characterization of PLGA composite filament

The radiopaque PLGA filaments were fabricated using melt extrusion as described earlier. Different formulation of PLGA with radiopaque fillers and plasticizer were characterized for their thermal and mechanical properties, radiopacity and shape memory behavior.

4.2.1 Thermogravimetric analysis (TGA)

Radiopaque filler loading Percentage, theoretical and actual, are tabulated in the Table 4.1. The residual mass remaining after complete degradation of PLGA at 500°C is considered for calculating actual loading of the percentage.

Table 4.1 Filler content and the characteristics of fillers in radiopaque PLGA composites.

Formulation	Filler type	Input loading %	Actual loading %	Density of filler g/cm^3
PLGA-BS502	Barium sulfate	50	45.36 ± 0.10	4.50
PLGA-TT502	Tantalum	50	50.03 ± 0.16	16.69
PLGA-BO502	Bismuth oxychloride	50	44.75 ± 0.32	7.78

4.2.2 Radiopacity of PLGA filaments modified with radiopaque fillers

Radiopacity for embolic plug is essential requirement as the process of embolization is guided under X-ray fluoroscopy. Polymeric materials are inherently radiotransparent and are generally hard to detect under x-ray diagnostic imaging, which limits their applications in medical devices. It is well known that radiopaque fillers such as barium sulphate, tantalum and bismuth compounds are usually blended into the polymer in a 30 to 60 wt.% range to provide the required radiopacity [1-3]. Therefore, PLGA filaments with various radiopaque fillers were fabricated via melt blending twin-screw micro-extruder and their actual filler contents were reported in Table 4.1. The relatively

small standard deviation (0.1 – 0.3%) in the actual loading suggests consistent filler content in the individual filament samples. Radiographs of the PLGA compounds with different radiopaque fillers are obtained by X-ray fluoroscopy as described in section are shown in the Figure 4.1. PLGA without any radiopaque filler is completely radio-transparent to x-rays. Addition of radiopaque fillers impart visibility to the PLGA filaments. PLGA filament filled with barium sulfate has less radiopacity than those filled with tantalum and bismuth oxychloride. This could be attributed to the higher specific gravity of bismuth oxychloride (7.7) and tantalum (16.6) as compared to barium (4.5). bismuth compound and tantalum can produce a brighter, sharper and higher-contrast image on fluoroscope than does barium sulfate [4]. Besides, maximum loading without processing difficulties is possible with tantalum and bismuth oxychloride as compared to barium sulfate owing to their higher densities. Attempt was made to make PLGA filaments with even higher loading of bismuth oxychloride, but the filaments were comparatively brittle, and it might pose adverse effect during subsequent shape memory programming.

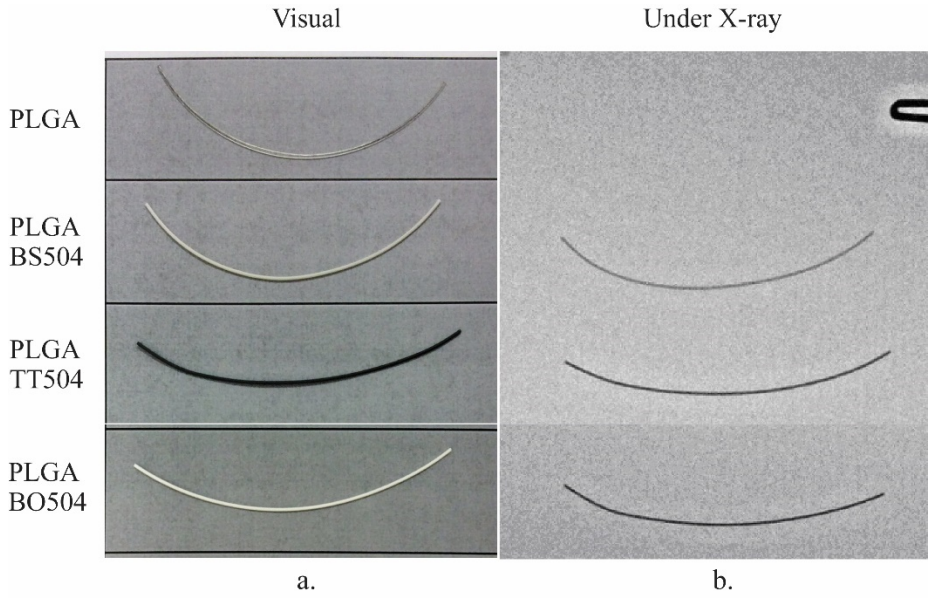

Figure 4.1 Visual (a), and radiographic (b) imaging of PLGA filaments with different radiopaque fillers

4.2.3 Differential Scanning Calorimetry (DSC)

To design a better device and to utilize the properties of PLGA apart from is favorable degradation rate, it is necessary to understand the thermal, mechanical and biological properties of PLGA. The glass transition temperature for neat PLGA is well above the physiological body temperature i.e. 37°C. In order to utilize glass transition temperature of PLGA as transition temperature for shape memory, it is favorable to have its Tg slightly below the human body temperature for the design of clinical devices [5, 6]. To achieve that PEG (2 kDa) was chosen as a low molecular weight plasticizer owing to its biocompatibility.

Following Figure 4.2 shows the DSC thermograms indicating glass transition onset, Tg1 and transition temperature, Tg of neat PLGA (50/50) and PLGA compounded with plasticizer (PEG 2kDa) and/or radiopaque particulate fillers barium sulfate (BS), Bismuth Oxychloride (BO) and Tantalum (TT). The glass transition temperature for neat PLGA is well above the physiological body temperature i.e. 37°C (Figure 4.3). The decrease in glass-transition temperature-Tg, as expected, with addition of PEG plasticizer is observed. The glass transition temperature for neat PLGA is 41.05°C with addition of 2% and 4% of Plasticizer Tg dropped to 38.87°C and 35.21°C respectively. Plasticizers are low molecular weight compound having Tg lower than the base materials to which it is added. Addition of plasticizer creates disorder in the molecular arrangement resulting in the increased mobility of molecules[7, 8]. No melting Peak is observed which confirms that the PLGA (50/50) is completely amorphous co-polymer.

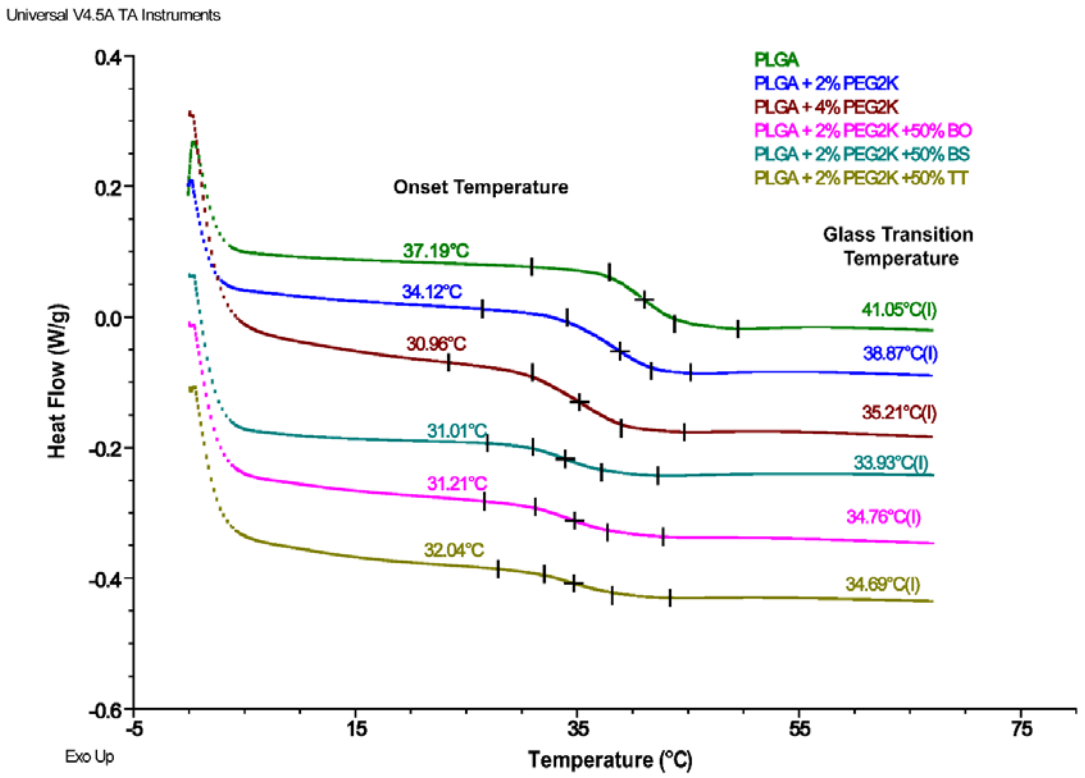

Figure 4.2 Differential scanning calorimetry thermograms of various PLGA compositions.

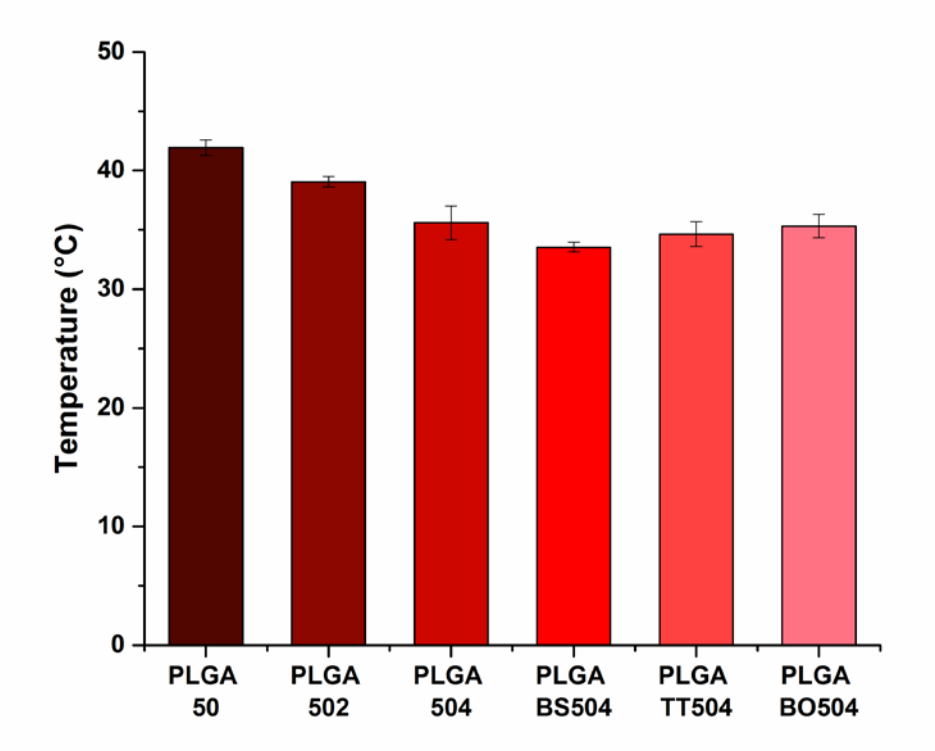

Figure 4.3 Glass transition temperature of various PLGA compositions.

The effect of addition of different types of radiopaque fillers on the transition temperature of the plasticized PLGA is investigated. Effect of radiopaque fillers on the

transition temperature is statistically insignificant. (*p*-value > 0.05). However this slight reduction in the ,Tg is might be because the weakening of van der Waals interaction within polymer chains due to presence of high concentration (50%) of radiopaque fillers. The reduction in the molar mass of polymer due to high shear forces in melt compounding with filers could also cause the drop in Tg [9, 10]. No change in transition temperature-Tg indicate that no active interaction is taking place between filler and polymer matrix. With addition of radiopaque fillers glass transition step height ΔC_p is reduced which signifies the reduction of overall polymer content in the composition[11].

4.2.4 Mechanical properties of PLGA

Following Figure 4.4 delineates the mechanical properties for different PLGA compositions. With addition of plasticizer to the PLGA the tensile strength and tensile modulus of the filaments dropped significantly. Incorporation of plasticizer increases the molecular disorder due to creation of free volume within polymer network. A plasticized polymer would therefore be more compliant and would need lower force to cause deformation compared to one without plasticizer [12-14]. Hence, lower tensile strength and Young's modulus of the plasticized PLGA was expected. On the contrary, the addition of radiopaque fillers into the plasticized PLGA has no significant effect on the Young's modulus but decreased the tensile strength significantly by 30%, irrespective of filler type. A similar trend has been observed by Liu *et al* [15] and it may be attributed to reduced matrix volume, particle agglomeration and insufficient stress transfer between the particle-matrix interface due to poor interface adhesion [16, 17]. Radiopaque fillers in addition to imparting radiopacity to the embolic device, retain the modulus of the composite which might be favourable for anchoring effect during water induced shape recovery of the device.

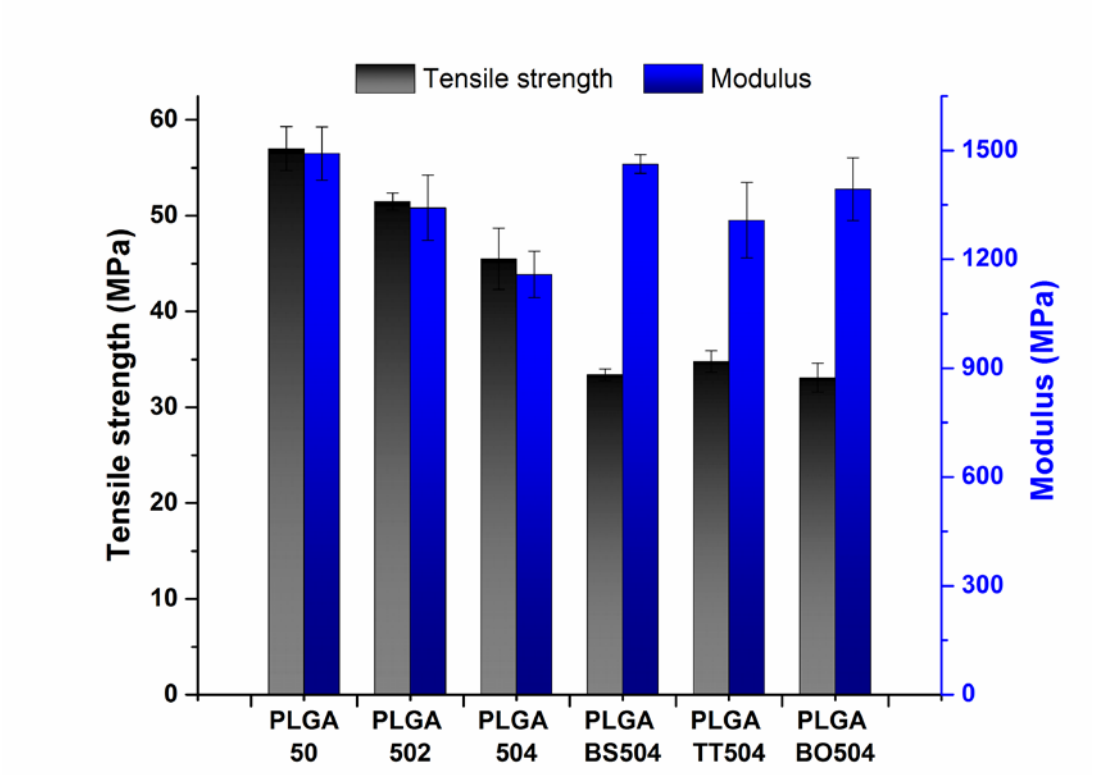

Figure 4.4 Mechanical properties of PLGA composites.

4.2.5 Shape memory properties of PLGA composite filaments

For minimally invasive applications viz Catheter Embolization the use of SME enables the device or plug to be delivered in a low profile, via a micro-catheter, and then recovered to a pre-determined shape after deployment. Evaluation of the shape memory capability of the PLGA composite material, separately and in conjunction with the PEGDA hydrogel is required for the optimization of the SME in embolic plug. As an amorphous polymer, PLGA has evinced SME by having the polymer entanglements as the physical cross-link points determining the permanent shape and glass-rubbery transition to function to hold the temporary shape as well as to actuate shape recovery [18, 19]. However, there is little work done on the effect of additives, such as a plasticizer, on the shape memory ability of amorphous PLGA. Figure 4.5 depicts the shape recovery behavior of the PLGA composites after immersion in DI water at 37 °C for 4 minutes. For all PLGA composites studied, their shape fixities were approximately 100%. As shown in Figure 4.5, the recovery ratio, R_r of the neat PLGA filament was 23% and the R_r improved with the introduction of the PEG plasticizer. This result was mainly ascribed to the lowering of glass transition temperatures of the PLGA from 42

°C to 36 °C with the addition of 4 wt.% plasticizer. For plasticized PLGA the polymer molecular chains gain full mobility at the experimental temperature i.e. 37 °C and an elastically recovery to the original shape. It is noteworthy the there was only slight reduction in R_r with the addition of high filler content to the plasticized PLGA and it may be ascribed to the fact that the presence of radiopaque filler hinders the mobility of the polymer chains, thus reducing the degree of shape recovery.

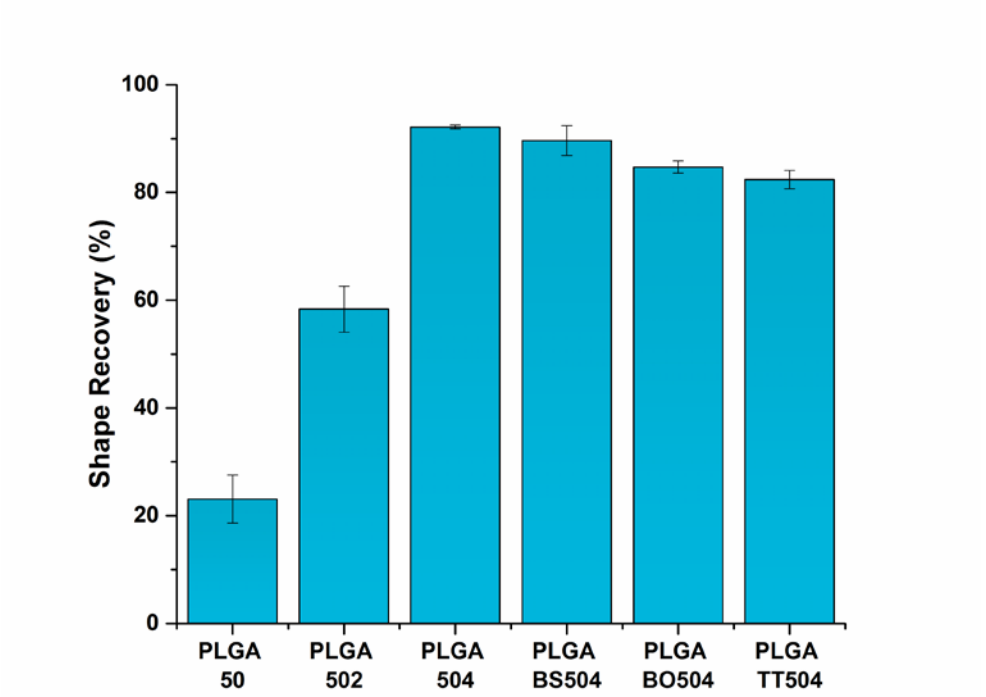

Figure 4.5 Shape memory behavior of PLGA composites after immersion in DI water at 37 °C for 4 minutes

Figure 4.6 demonstrated water-responsive SME of PLGA composite filament. The permanent shape is that of coil, which has been stretched into a straight strip at 70 °C, and the temporary shape were then fixed by quenching. However, when it was immersed in water at 37 °C, it recovered to its original coil shape within 100 second.

Figure 4.6 Water-responsive shape recovery from temporary shape (straight strip) to the permanent shape coil for PLGA BO504 on immersion in DI water at 37 °C a) illustraion, and b) progressive images during recovery preocess.

PLGA composite with 4% PEG (w/w) plasticizer and 50% bismuth oxychloride (w/w) (PLGA BO504) was used to carry out further characterizations owning to its better radiopacity, dimensional stability and uniformity of the extruded filaments and intermediate density between barium sulfate and tantalum.

4.2.6 Plasticization effect of water and its role in enhancing shape memory effect

It is also noteworthy that shape recovery of PLGA occurred due to the combination of water- and thermal-induced SME by sample immersion in water at 37 °C, mimicking the *in vivo* situation. In addition to the thermal shape recovery activated at 37 °C, the water molecules diffuse into the polymer matrix and act as a plasticizer [20, 21], essentially lowering the T_g enough to enable greater shape recovery. To verify this a comparative experiment have been done to study recovery of PLGA BO504 in both the

dry and wet states. It was observed that the recovery in 37 ^{0}C water was significantly higher (81.1 ± 0.9 %) compared to the recovery in dry state/air (72 ± 0.7 %) in 37 ^{0}C oven ($p < 0.05$). To quantify this effect water absorption studies in 37 °C DI water were carried out for PLGA BO504 filament. Water absorption at timepoints, specifically 2 hr. and 24 hr., was measured using change in weight of the sample and is expressed as the percentage of original weight. Water absorption was found to be 1.7 ± 0.3 % at 2 hours and 5.5 ± 0.4 % at the end of 24 hours. DSC results of the samples after 24 hours of hydration in DI water at 37 ^{0}C evinced significant depression in glass transition temperature from 35.3 ± 0.99 ^{0}C to 32.67± 0.28 ^{0}C. The plasticizing effect by the water absorbed into the polymeric matrix is reversible, simple drying returns the Tg of samples to near original values[22].

4.2.7 Effect of programming temperature on shape recovery

Programming temperature is important consideration while designing a device with shape memory effect. Amount of shape recovery is dependent on the programming temperature, and can be tailored using optimum range of temperature[18, 19]. It is hypothesized that higher the deformation temperature (above the glass transition temperature of PLGA) used for the programming of the shape memory effect, lesser will be the recovery percentage. Therefore, it is important to study the shape recovery of radiopaque PLGA composite material at different possible programming temperatures that can be used to fix the temporary shape of the embolic plug. Deformation temperatures were chosen above the melt transition temperature of the dry PEG hydrogel i.e 55 °C. PLGA BO504 composite filaments were uniaxially stretched to 500% deformation strain at three different temperatures viz. 60, 70 and 85 °C and then quenched to room temperature to fix the temporary shape. Shape fixity was approximately 100% for all the samples. Figure 4.7 represent the recovery percentages of shape recovery in 37 °C DI water for the abovementioned samples. It is observed that with increase in deformation temperature the % shape recovery decreased which is due to not-elastic permanent deformation owing to increased mobility molecular chain at higher temperature[23, 24]. For the samples deformed at 60 and 70°C, at end of 12 hours same recovery is observed approximately 95 ± 1.5 %, whereas for samples deformed at 80°C final shape recovery obtained was 84 ± 1.2 %.

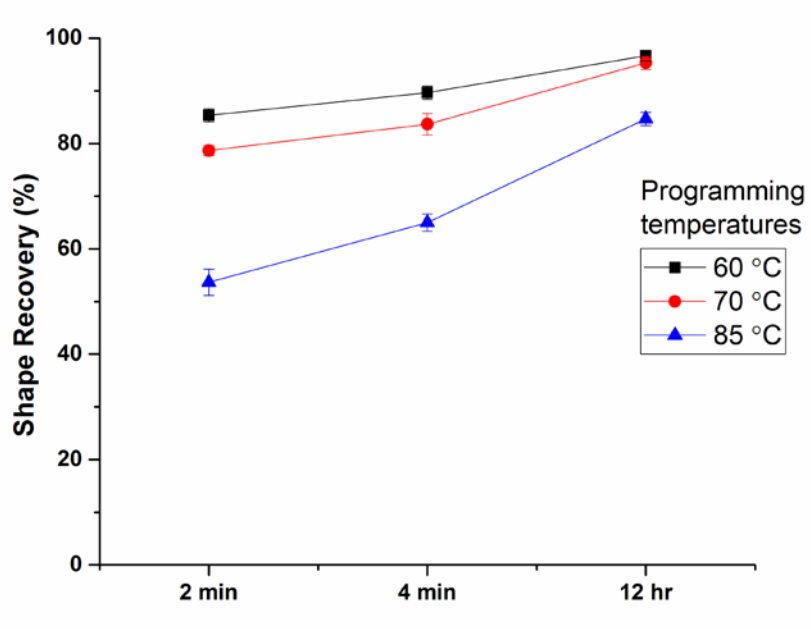

Figure 4.7 Effect of programming temperature on shape recovery of PLGA composite filament

This effect can be explained as follows: PLGA is an amorphous thermoplastic. There are no chemical bonding between the molecular chains. The permanent shape is defined by the molecular entanglements. When a load is applied, the molecular chain may slip past its neighbour to give a permanent deformation. At high temperature, due to increase mobility of the molecules the slippage is easier[24]. Thus, the permanent deformation is higher in the sample programmed at 85 ^{0}C as compared to 60 and 70 ^{0}C.

4.2.8 Water contact angle for various PLGA compositions

The Figure 4.8 and Figure 4.9 show the contact angle measurements for various PLGA composition. Reduction in the contact angles, from 81$\pm$ 1^{o} to 69 $\pm$ 1^{o} is observed with addition of 4% PEG (Mw = 2k) plasticizer to the PLGA. Addition of PEG, which is hydrophilic, improves the wettability of the surface[25-28]. Radiopaque composition of PLGA with 50% bismuth oxychloride shows reduced contact angle of 70 $\pm$ 1^{o}. This can be associated with the increased surface roughness with the addition of particulate fillers[29, 30]. For PLGA BO504 where both plasticizer and radiopaque filler are present, the contact angle further dropped to 67 $\pm$ 1^{o}. This small decline in contact angle

value compared to the PLGA compositions where either plasticizer or filler alone is present, could be synergistic effect of hydrophilic PEG fraction and surface roughness. Contact angle for plasma treated PLGA BO504 surface decreased to 43 $\pm$ 1^{o}. This is due to the formation of oxygen-containing functional groups improving wettability of the surface on plasma treatment as well as improved specific surface area because of surface etching [29, 31-33]. Strong interactions of ions, radicals, electrons and neutral molecules in plasma with polymer surfaces induce chemical and physical modifications of the surfaces resulting into more hydrophilic surface.

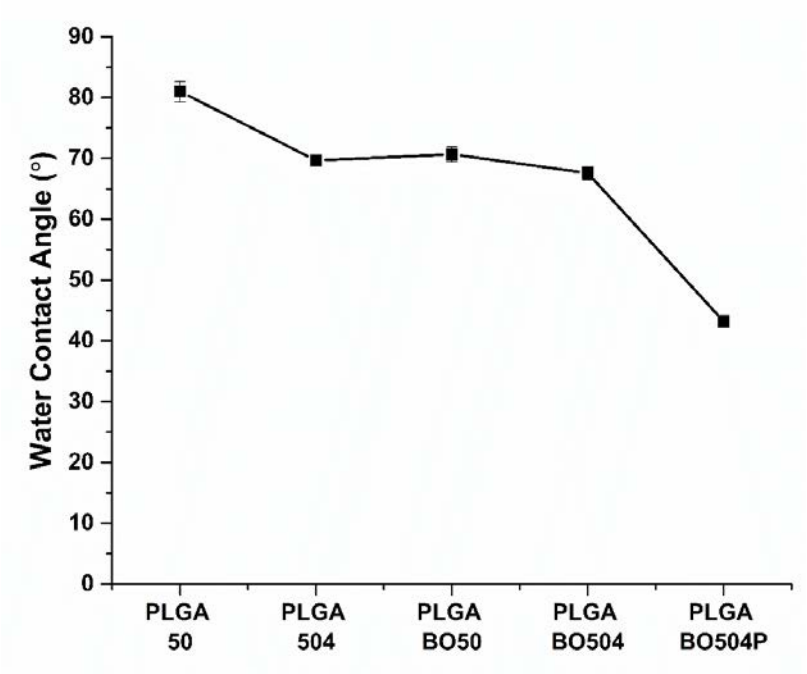

Figure 4.8 Water contact angle for various PLGA compositions

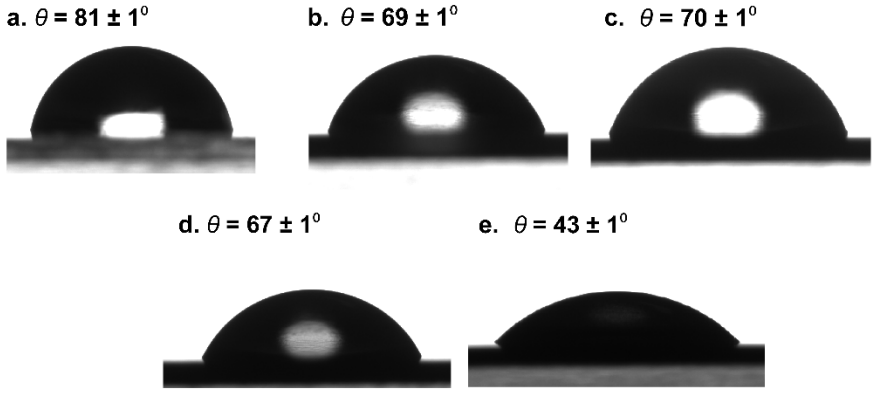

Figure 4.9 Water contact angle for PLGA (a); PLGA + 4% PEG plasticizer (b); PLGA + 50% BiOCl (c); PLGA + 4% PEG plasticizer + 50% BiOCl (d); PLGA + 4% PEG plasticizer + 50% BiOCl plasma treated for 10 minutes (e).

4.3 PEG hydrogel characterization

In this section effect of different parameters on properties of PEG hydrogel have been reported and discussed

4.3.1 Effect of initiator percentage on Swelling of PEG hydrogel

Figure 4.10 delineate the effect of different initiator percentages on swelling properties of the PEG hydrogel synthesized using 7.5% of PEGDA (Mn 10kDa). Hydrogel prepared with 0.5% initiator gives maximum swelling ratio of 31.4. For 1% initiator content the swelling ratio drops to 29, with further increase in initiator percentage to 2% and 3% there is no significant change in swelling ratio. The increase of initiator to macromere ratio results in increased crosslink density and decreased swelling ratio as a result of reduced probability of formation of cyclic crosslinks and multiple crosslinking reactions[34, 35]. Various studies have reported the power law relation between swelling and cross-linker concentration [36, 37]. Less swelling ratio is indication of compaction of the gel crosslink structure i.e. reduction in pore size of the gel. For PEG hydrogel with 5% concentration and initiator amount of 2% swelling ratio

is 39, owing to the loosely bound crosslink structure since the number of effective acrylate groups per volume, taking part in crosslinking reaction, are less compared to 7.5% PEGDA concentration.

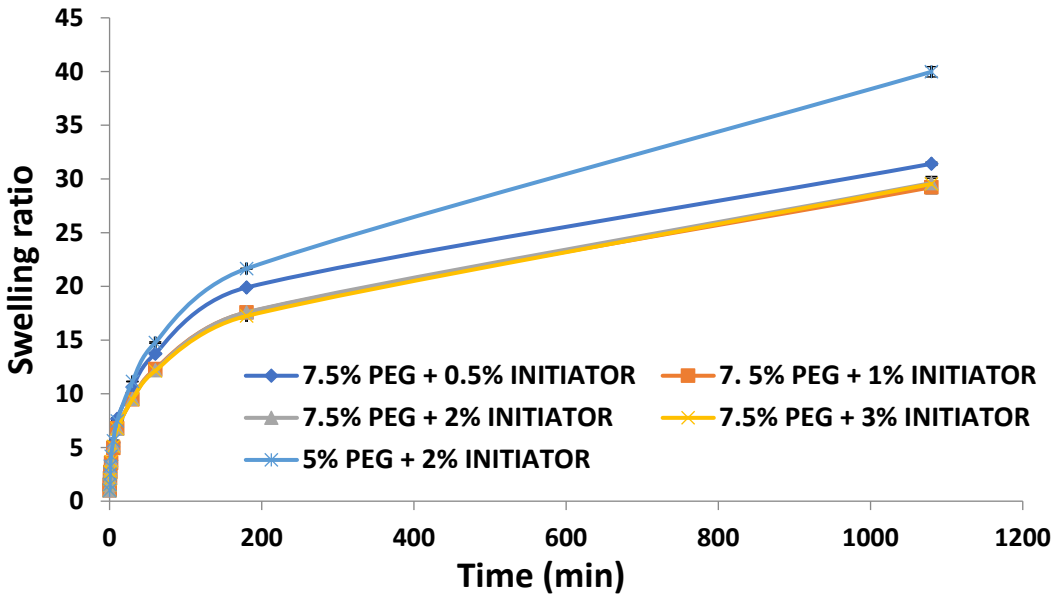

Figure 4.10 Effect of initiator content on swelling of PEG hydrogel

4.3.2 Effect of initiator percentage on Gel content of PEG hydrogel

Figure 4.11 shows the change in gel fraction with initiator amount. Hydrogel is 3-dimensional network formed by crosslinked macromers (gel) and small fraction macromers not attached to network (sol). Maximum gel fraction (100%) corresponds to maximum extent of crosslinking reaction, and it depends on the concentration of polymer, initiator concentration, size of sample and time of reaction[35]. In our studies Gel fractions for hydrogel synthesized using 0.5, 1, 2 and 3% (w/w) of photo-initiator are 71.16, 84.72, 86.29 and 86.07 respectively. With 2 and 3% of initiator the gel fraction is statistically same (*p*-value 0.625) this is because maximum crosslinking is achieved with 2% initiator and further addition of initiator does not form more crosslinks. It is well-known phenomena that at certain threshold value for cross-linker the gel content is maximum and above threshold value there is no significant change in the gel-content which agrees with our results.

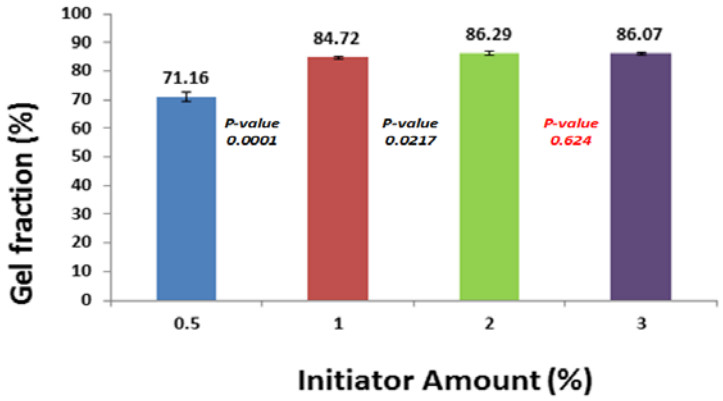

Figure 4.11 Effect of initiator content on gel fraction of the hydrogel

4.3.3 Rheology of the PEGDA hydrogel

Figure 4.12 depicts the shear storage modulus (G') for various PEG hydrogel compositions obtained by frequency sweep at room temperature. The storage modulus values are almost constant at all frequencies except at higher frequencies. Initiator amount has significant effect on the mechanical properties. As the initiator amount increased from 0.5% to 3% the storage modulus increased from 320 Pa to 795 Pa at 1 Hz frequency. The response of storage modulus to initiator amount is linear and higher till 2% initiator amount after which the modulus value increased marginally (*p*-value 0.6). These findings are in consonant with swelling and gel fraction results. The rise in modulus is on account of increased crosslinked densities and formation of the hydrogel with the initiator amount. Increase in crosslink density was reflected in the decreased tanδ values which signifies the ratio of elastic modulus to viscous (loss) modulus. Lesser the tanδ value stronger is the gel[38].

For same initiator concentration (2%) and same molecular weight of PEGDA (10 kDa), as the concentration of PEGDA decreased from 7.5% to 5% the storage modulus is dropped from 746 Pa to 260 Pa. Similar drop in modulus to 208 Pa is observed when molecular weight of PEGDA increased from 10 kDa to 20 kDa at same initiator content of 2%. The possible reason for these behaviors is formation loosely bound crosslinked structure. As the concentration of PEGDA macromers decreases number of acrylate groups per volume decreases as well as probability of physical entanglement formation decreases which results in reduced storage modulus. On the similar line as the

molecular weight of PEGDA macromers increases the effective photo-crosslinkable acrylate group decreases for given mass.

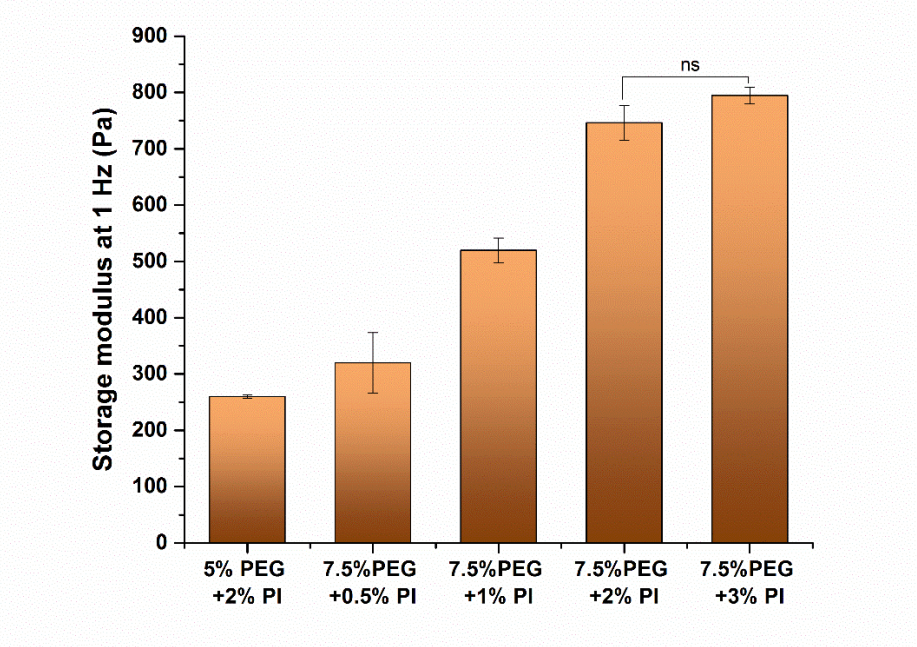

Figure 4.12 Effect of initiator on storage modulus of PEG hydrogel (PI- photoinitiator).

From the swelling, gel fraction and rheology result, the hydrogel formulation with 7.5% concentration of PEGDA macromers of 10 kDa molecular weight and 2% of Irgacure 2959 photo-initiator crosslinked for 7 minutes is fixed as optimum formulation of the hydrogel for further studies.

4.3.4 Radiopacity of PEGDA hydrogel with radiopaque fillers.

As the final application of device demands the radiopacity in our studies we incorporated different radiopaque fillers in the hydrogel. The effects of these fillers are discussed here. The radiopaque fillers are added to improve the visibility of the gel in dry and wet state.

Following Figure 4.13 and Figure 4.14 illustrates the improvement in radiopacity for the hydrogel in dry and wet state observed under X-ray fluoroscopy.

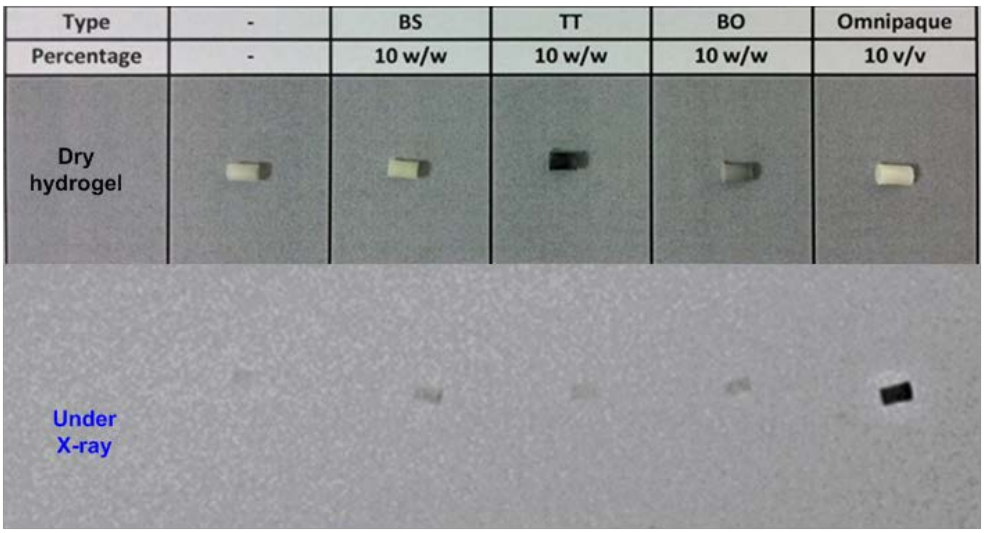

Figure 4.13 Radiopacity of 7.5% PEG hydrogel in dry state with different radiopaque fillers under x-ray fluoroscopy BS- Barium Sulfate; TT-Tantalum; BO-Bismuth Oxychloride

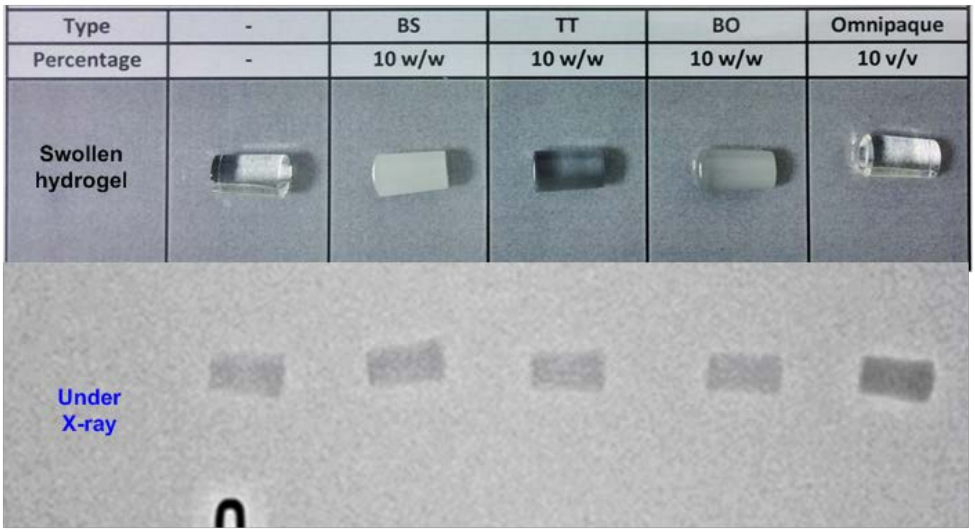

Figure 4.14 Radiopacity of 7.5% PEG hydrogel in wet state with different radiopaque fillers under x-ray fluoroscopy

Dry hydrogel without any radiopaque fillers is hardly visible under X-ray. Even addition of particulate fillers BS- Barium Sulfate, TT-Tantalum or BO-Bismuth Oxychloride does not impart sufficient visibility under X-ray. With addition of 10% v/v (40% w/w) Omnipaque, which is iodine based contrast agent, effect on radiopacity is multifold. For wet/swollen hydrogel without any radiopacifier there is slight radiopacity owning to size or volume of the gel and it remains unchanged on further addition of radiopaque fillers. The reason may be that the weight fraction of radiopaque fillers decreases for swollen hydrogel and since the radiopacity for mixture or blend is

directly proportional to density of the material, weight fraction of radiopaque component and thickness. Omnipaque contrast agent gives maximum radiopacity in wet state too since the higher loading is possible. So only effective way to impart opacity to hydrogel is to add the contrast agent to Gel but its effect on swelling behavior is important to study.

4.3.5 Thermal analysis of PEG

Figure 4.15 shows the DSC heating scans for PEG hydrogel (10kDa Mw, 7.5% w/v, 2% initiator) pre-stretched to 400%, 500%, 600% and 700% at 70°C. (DSC scan rate 10°C/min). The enthalpy (ΔHm) associated with crystal melting can be determined from the area under the melting endotherm, and the crystallinity in the sample can be estimated as follows [39].

$$\chi_c = \frac{\Delta Hm}{\Delta Hc} \times 100\% \quad 4.1$$

where ΔHc is the enthalpy of melting of 100% crystalline PEG, which is 166.4 J/g as taken from the previous literature[40]

Table 4.2 Thermal properties and crystallinity of PEG hydrogel stretched to different ratio.

Pre-stretch strain (%)	Onset melting, Tm1 (°C)	Peak Melting, Tm (°C)	Crystallinity %
unstretched	53	61.5	72.53
400	55.3	59.5	67.42
500	55.7	60.3	63.40
600	54.4	59.0	64.06
700	54.9	59.3	67.12

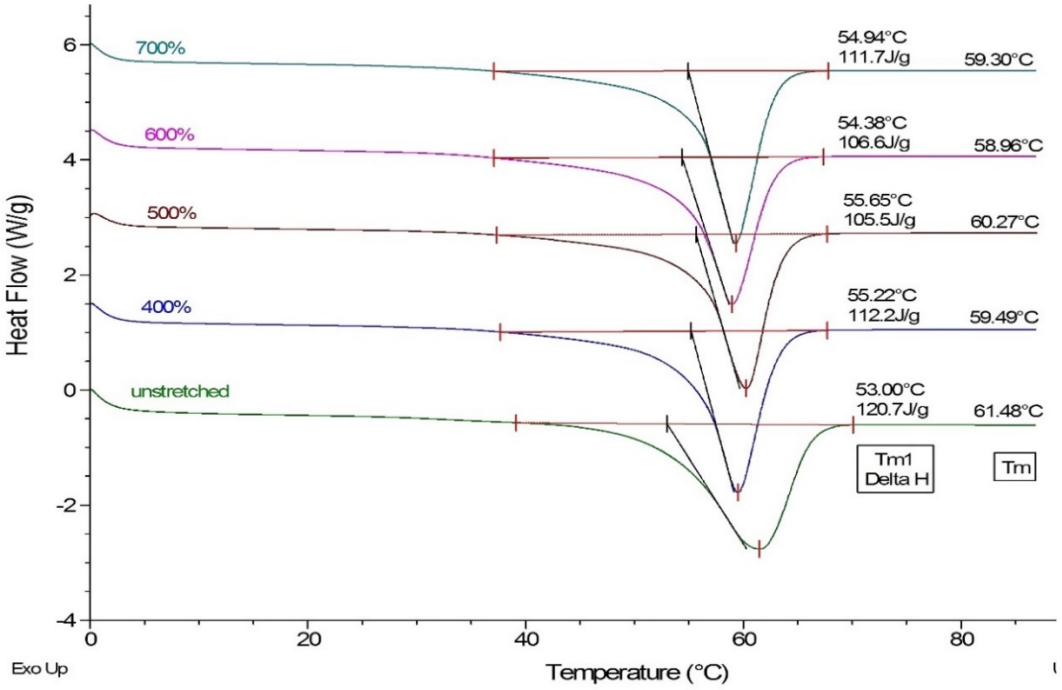

Figure 4.15 DSC thermograms of the PEG hydrogel pre-stretched to different ratio

From DSC scan, no increase in crystallinity with the deformation strain is noticed. Broad melting peak is observed for unstretched sample while for stretched sample the peak is relatively sharp narrow. This is reasonable. For the unstretched sample, the crystallization peak is corresponding to crystals formed from solution (by dehydration). The mobility of molecules in the solution is higher compared to melt state so the crystals of long order are formed thus highest melting temperature is observed in case of unstretched sample. Solution crystallization is slow process so wide crystal distribution is pronounced[41]. For stretched samples the dry hydrogel is heated to 70°C and then hand stretched to particular deformation strain and cooled it down to room temperature, so associated quenching effect retard the crystallization, but stress/strain induced nucleation promote crystallization [42-45]. This explains the narrow melting peak at lower melting temperature owing to formation of small crystals of similar sizes.

4.3.6 Shape Memory Effect and Deformation Strain Limit for PEG hydrogel

The basic working principle behind the recovery/actuation of polymer-hydrogel composite is water induced shape memory and shape change effect of hydrogel. Hence it is important to study these effects individually on both the materials. Figure 4.16

shows the water induced shape memory effect in hydrogel filaments and maximum allowed deformation strain without causing any breaking of gel.

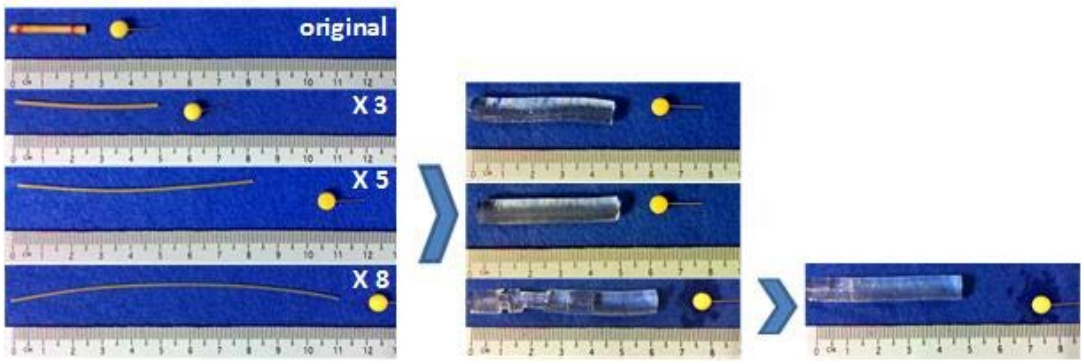

Figure 4.16 Shape memory in PEG hydrogel filaments pre-stretched to different stretching ratio at 70°C

Hydrogel samples stretched 200% (3 times) and 400% (5 times) to its original length show no breaking or delamination of gel layer and 100% recovery is observed. Whereas for sample stretched 700% (8 times) of its original length, there is delamination and breaking of gel. The original diameter for unstretched dry gel was 2.4 mm and diameter after stretching samples to 200%, 400% and 700% were 1.36mm, 1.05mm and 0.83 respectively.

The time taken for complete recovery increases as the thickness or diameter of the sample increases. The buckling starts earlier as the deformation strain increases. Time to start buckle for hydrogel samples with deformation strains 200, 400 and 700% are 310sec, 168sec and 71 sec respectively. For the sample with 700% deformation strain, the buckling occurs along with delamination of softened hydrogel from. These results are in accord with the eq. 2.2 in theory of buckling by Huang WM et al., (2011). The possible reason for this behavior can be as follow. As the deformation strain increases, stored elastic energy in the crosslinks i.e. stress, σ increases and the initial radius R of the of the stretched sample decreases [46]. This phenomenon is further explored in chapter 5.

From DSC thermograms it is clear that there is no significant difference between the crystallinity of the samples stretched to different ratios. Once these samples are immersed in water the mobility of molecules on the outer surface increases and the

stored energy in the crosslinks start to apply compressive or pulling force on the softened part, as in case of samples with higher deformation strain, σ is higher and R is smaller sample buckle faster. Similar results have been reported for crosslinked natural rubber, PMMA and crosslinked NBR[47-49]

The limitations on the diameter of device is of concern when buckling phenomena of the hydrogel is to be utilized for actuation of embolic device. In order to make device which can be deployed using 4 French catheter (0.97mm), the dry hydrogel polymer composite, (2.2±0.2) made using 6mm mold, needs to be stretched sufficiently without causing breaking of gel during recovery. The maximum possible extension for current optimized formulation without causing breaking or delamination of while recovery is found to be 500-550 %. The optimized formulation here means 7.5% w/v of 10kDa molecular weight PEGDA with 2% Irgacure 2959 crosslinked under UV light for 7 min.

4.4 Fabrication of the embolic device and preliminary characterization

In this section method to fabricate the embolic foam based on the characterization results of individual constituents i.e. radiopaque PLGA composite and PEG hydrogel, is devised. The preliminary characterizations done here were used for the optimization of the device performance

4.4.1 The concept of the embolic plug prototype

In the design of our embolic plug, it consists of the radiopaque polymer core and the outer hydrogel coating for enhanced occlusion. The polymer core coated with hydrogel can be thermally programmed into a temporary shape, which can be introduced into the selected artery through a micro-catheter, and vascular embolization can be realized by expansion of the device from temporary shape upon contact with body fluid and body temperature by thermal and water-induced SME followed by complete mechanical occlusion due to hydrogel swelling.

In this system, biodegradable SMP plays two roles: one as “carrier” or scaffold for the hydrogel and the other is to provide radio-opacity for device visualization under x-ray imaging. Therefore, PLGA-BO502 is chosen as the core material for it possesses good radio-opacity, mechanical strength and has a glass transition temperature, close to body temperature. Furthermore, the hydrogel provides the driving force for water-induced actuation of device, that eventually leads to mechanical anchoring of the plug and the blocking of the blood vessel. With the selected materials, an embolic plug prototype was fabricated and programmed to possess shape memory by thermally deforming into its temporary shape at 70 °C.

4.4.2 Embolic device prototype fabrication

The embolic device was fabricated using photo-crosslinking of PEG hydrogel over radiopaque PLGA composite as described in section 3.6. Figure 4.17 illustrates the stages in the process of fabrication and shape memory programming of embolic plug. The plug in the final form was for various characterizations

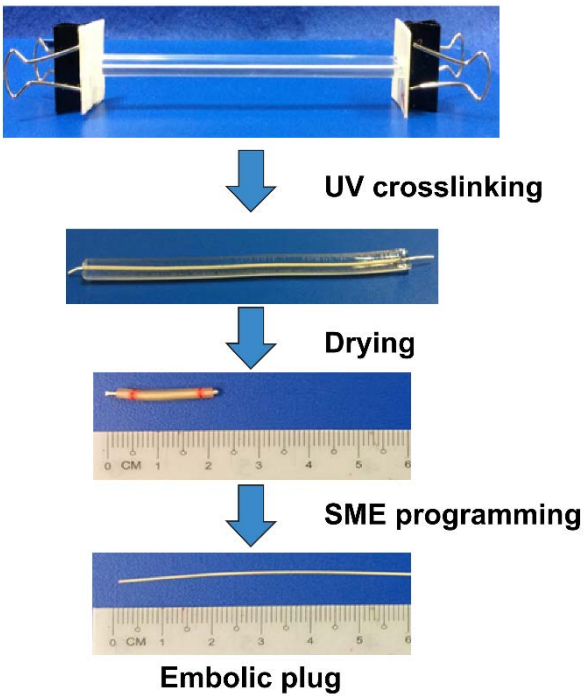

Figure 4.17 Fabrication of the embolic plug

4.4.3 SEM imaging

Following Figure 4.18 shows the SEM micrograph of the cross-sectional view of embolic plug. The concentric coaxial structure of the PLGA composite filament coated with PEG hydrogel can be observed with good bonding at the interphase between PEG hydrogel and PLGA composite filament. The morphological image (at the bottom) indicated uniformly dispersed of bismuth(III) oxychloride lamellae, which usually tend to aggregate forming agglomerates of around 40 µm (Porous BiOCl micro-flowers constructed from ultrathin nano-sheets)[50].

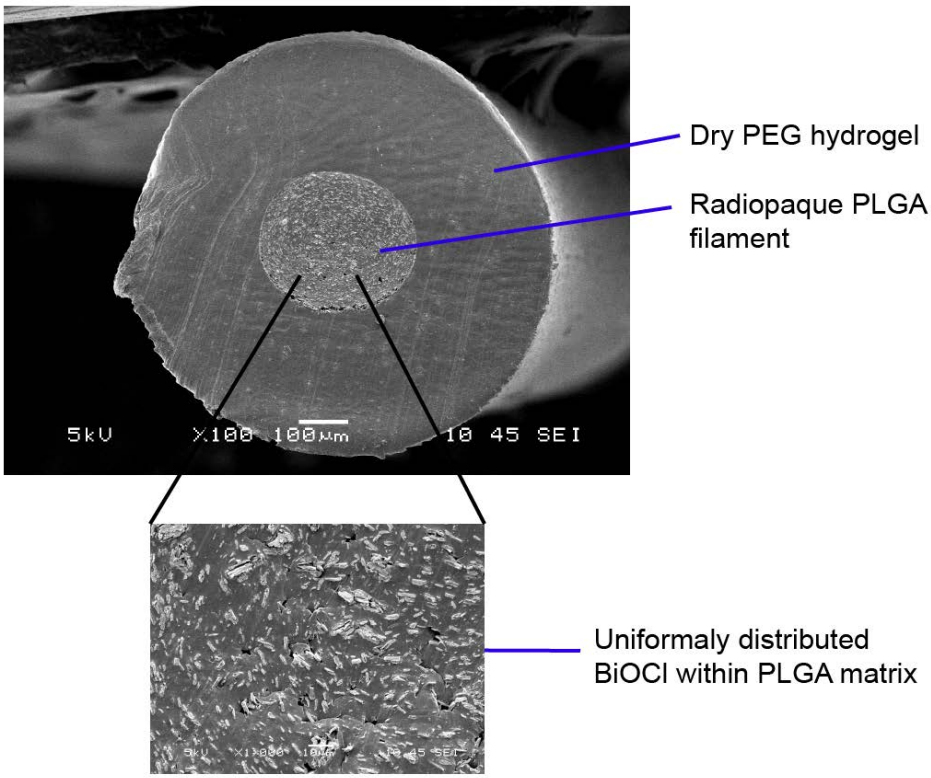

Figure 4.18 SEM Micrograph of embolic device; cross-sectional view (top), morphology of PLGA BO504

4.4.4 Interfacial adhesion between radiopaque PLGA filament and PEG hydrogel

Interfacial shear strength between radiopaque PLGA filament and PEG hydrogel was investigated via pull-off test as described in section

PLGA is comparatively hydrophobic polymer compared to PEG hydrogel. In order to have good adhesion between PLGA composite filament and coated PEG hydrogel, PLGA filament treated with oxygen plasma for 10 min prior to coating of hydrogel. Figure 4.19 shows that the pulling force required to delaminate core PLGA composite filament from the hydrogel, increased by 70% for plasma treated sample. For the control sample i.e. without plasma treatment the pulling force and elongation before delamination occurs was 1.09 ± 0.08 N and 1.73 ± 0.06mm whereas, for plasma treated sample the value was found to be 1.88 ± 0.30 N and 2.83 ± 0.71mm respectively. The results are aligned with the contact angle results and together it infers that plasma treatment improves adhesion strength between PLGA composite filament and PEG hydrogel by improving the surface wettability.

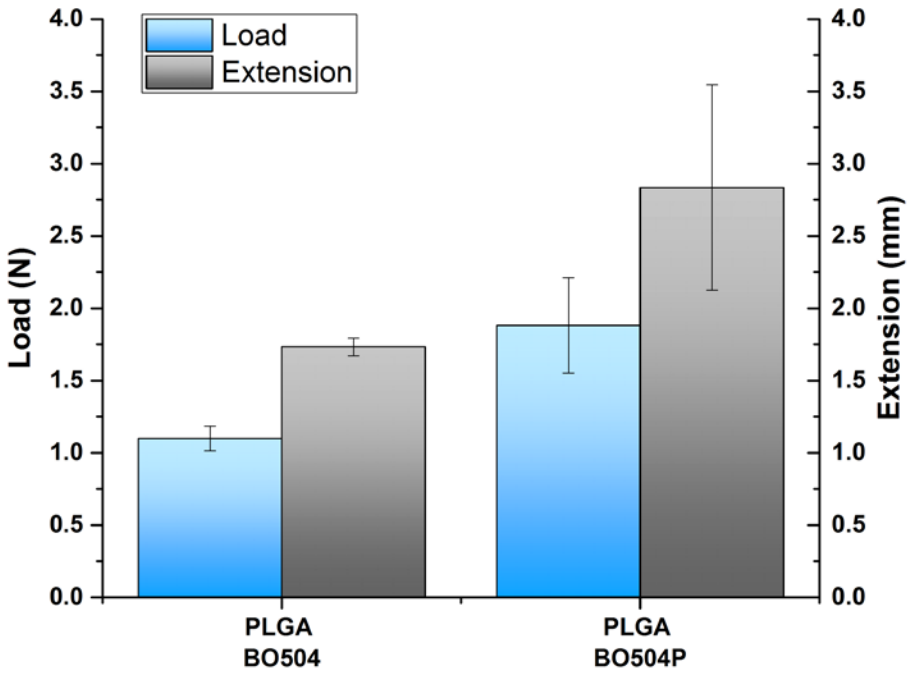

Figure 4.19 Effect of plasma treatment of PLGA composite filament on the interfacial adhesion with PEG hydrogel

4.5 *In-vitro* studies of device in flow system

In the application *in vivo*, the rate of embolization (or plugging) is as important as the extent of plugging; this "embolization efficiency" was tested *in vitro* using a customized flow model to simulate blood flow through an artery. As shown in Figure 4.20 (a), after the developed prototype was deployed via a 4-F catheter (at 0 s), water molecules started diffusing into the system, actuating the water-triggered recovery of the hydrogel coating. Subsequently, the PLGA core started to recover and buckle once the shape recovery of PLGA core overcame the resistance of the PEG hydrogel coating, leading to the anchoring of the device to the vessel wall within 16 s of deployment (as evidenced by significant reduction in the flow rate shown in Figure 4.20 b). At this stage, the device was mechanically locked/anchored onto the targeted site and complete occlusion was achieved with the hydrogel swelling at 120 s. The reduction of fluid flow rate was monitored with time as shown in Fig. 8b. As seen from the figure, there was an initial sharp drop in the flow rate for the first 40 s when the embolic plug started to recover, and the flow was completely stopped at 120 s, corresponding to the complete "embolization" or plugging of the flow channel.

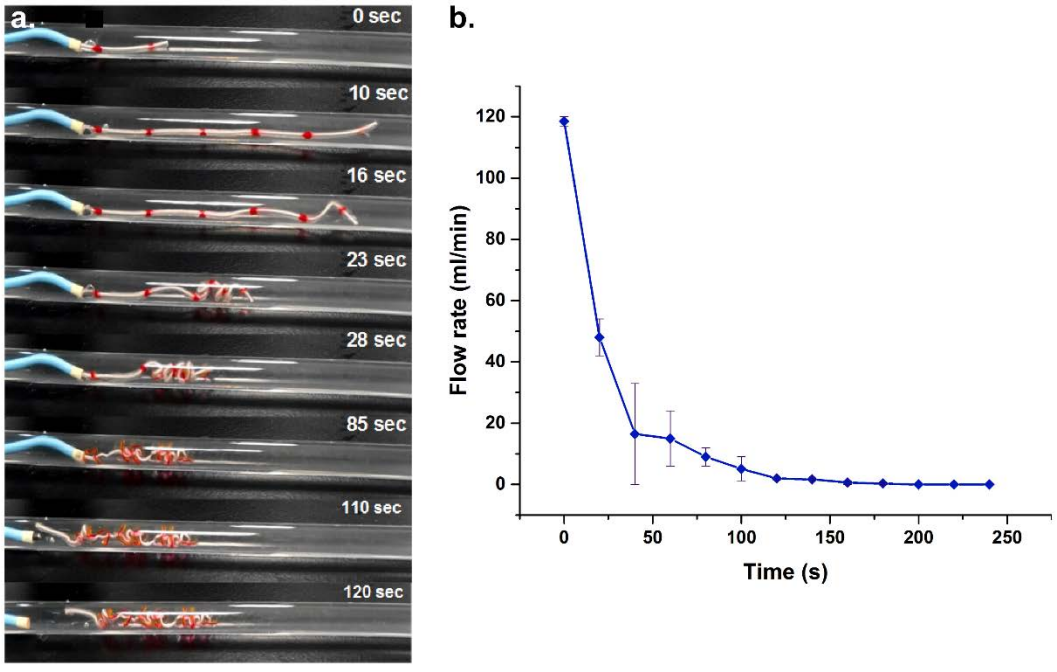

Figure 4.20 (a) *In vitro* embolization by the developed embolic plug, and (b) the reduction of flow rate was monitored with time.

4.6 Effect of programming temperature on final shape of embolic device.

In section 4.2.7 it was seen that the deformation temperature affects the shape recovery of PLGA. PLGA is amorphous polymer, and the shape memory effect is on account of molecular entanglements and transition of the molecular chains from glassy to rubbery state. At higher temperature, because of higher mobility of molecules, intermolecular slippage is prominent which results into permanent deformation[19, 51].

Figure 4.21 shows the embolic devices programmed at different temperatures and corresponding shape recovery to different shape as affected by the programming temperature. It can be observed that at higher temperature (85 ^{0}C and 100 ^{0}C) of programming, PLGA does not recover completely but it forms a zig-zag shape due to differential shrinkage between PEG hydrogel and core filament, which can also lead to delamination of the hydrogel from the filament (e.g. for 100 ^{0}C).

This can be utilized as a tool to fabricate medical device with different core shape and hence the different visibility under X-ray fluoroscopy to differentiate the embolic plugs based on the shape (e.g. in case of biopsy markers)[52].

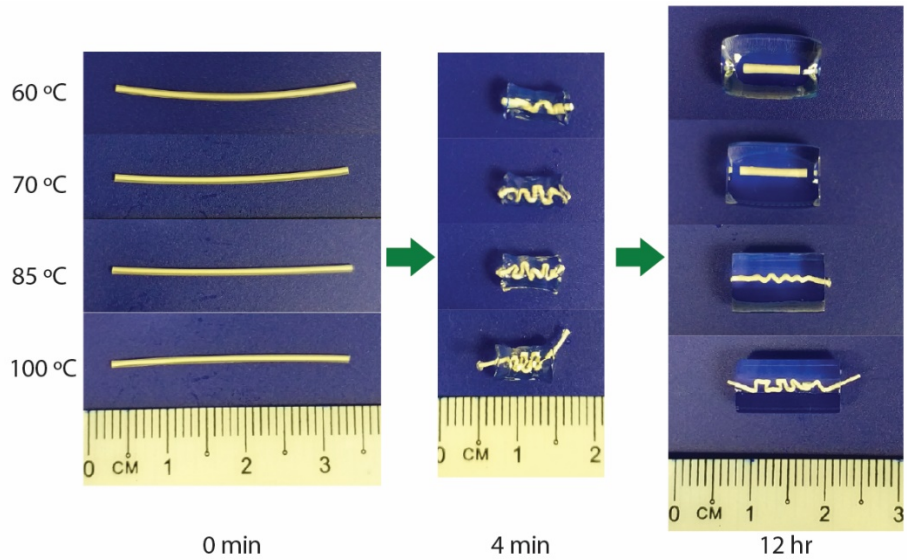

Figure 4.21 Effect of programming temperature on shape recovery of PLGA-PEG hydrogel

4.7 Working mechanism of shape-memory embolic plug

The mechanism of the shape-memory process involved is proposed in Figure 4.22 and is explained below. Molecular entanglements in PLGA and covalent crosslinks in PEG hydrogel are the netpoints responsible for holding the permanent shape, which is that of a straight rod. During the programming process at 70 °C, which is above the melting temperature of PEG crystalline phase, both PEG and PLGA are in an amorphous, deformable state and the molecular chains get oriented along the direction of deformation with loss of entropy. The temporary deformed shape is fixed by the PEG recrystallization and the transition of the PLGA to a glassy state as the temperature is lowered to room temperature. PEG crystallites act as the reversible switch points. Upon immersion in water at 37 °C, water molecules diffuses into the system and as the PEG crystalline phase "dissolves" , the network becomes fully amorphous [53], actuating the shape recovery of PEG in conjunction with swelling. Likewise, when the PEG hydrogel softens sufficiently, the PLGA molecular chains resume mobility and trigger the PLGA shape recovery. By having this water-induced shape recovery mechanism of the PLGA-PEG hydrogel system, the net outcome translates into the creation of an embolic plug that can achieve complete occlusion within 120s *in vitro*. The shape recovery of the PLGA core accelerates the creation of the embolic plug, and gives it mechanical integrity, and radio-opacity.

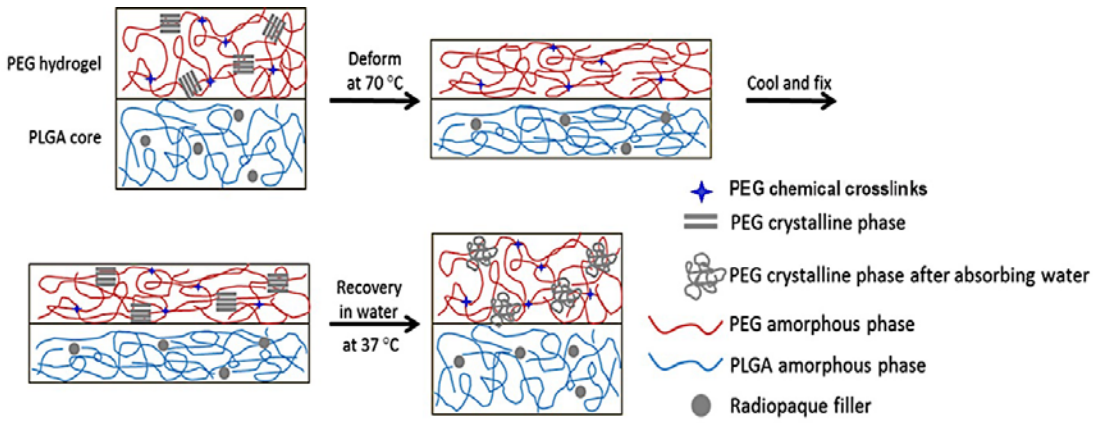

Figure 4.22 Water-responsive shape memory mechanism of the embolic plug.

Conclusion

Individual compositions of PLGA and PEG hydrogel were successfully prepared, modified and characterized to impart required functionality to a final embolic device constructed thereof. From the radiopacity and thermo-mechanical testing it was found that the PLGA formulation with 2% plasticizer and 50% bismuth oxychloride exhibited best properties. Plasma treatment of PLGA composite filament prior to PEG hydrogel coating improved the interfacial adhesion.7.5% (w/v) PEG hydrogel photo-crosslinked using 2% (w/w) Irgacure 2959 initiator was found to be optimum. Pre-stretched hydrogel filaments displayed water-induced shape memory dependent on the deformation strain. The stretching to 600-650% uniaxial strain at 70°C presented faster buckling without breaking of gel.

A bioabsorbable radiopaque embolic plug based on water-triggered shape memory PLGA-PEG hydrogel composite was successfully developed and evaluated with regard to its application as an embolic agent in terms of shape recovery capability, occlusion efficiency, feasibility of delivery *in vitro*. Finally, the underlying mechanism of water and thermoresponsive shape memory effect in the PLGA-PEG hydrogel composite was elucidated.

References

[1] Hampikian JM, Heaton BC, Tong FC, Zhang Z, Wong CP. Mechanical and radiographic properties of a shape memory polymer composite for intracranial aneurysm coils. Materials Science and Engineering: C. 2006;26:1373-9.

[2] Chan WA, Bini TB, Venkatraman SS, Boey YCF. Effect of radio-opaque filler on biodegradable stent properties. Journal of Biomedical Materials Research Part A. 2006;2006:1.

[3] Huang Y, Wong YS, Wu J, Kong JF, Chan JN, Khanolkar L, et al. The mechanical behavior and biocompatibility of polymer blends for Patent Ductus Arteriosus (PDA) occlusion device. Journal of the Mechanical Behavior of Biomedical Materials. 2014;36:143-60.

[4] Shah TM. Radiopaque polymer formulations for medical devices. Medical Device and Diagnostic Industry2000.

[5] Venkatraman SS, Tan LP, Joso JFD, Boey YCF, Wang X. Biodegradable stents with elastic memory. Biomaterials. 2006;27:1573-8.

[6] Metcalfe A, Desfaits A-C, Salazkin I, Yahia LH, Sokolowski WM, Raymond J. Cold hibernated elastic memory foams for endovascular interventions. Biomaterials. 2003;24:491-7.

[7] Gentile P, Chiono V, Carmagnola I, Hatton PV. An overview of poly (lactic-co-glycolic) acid (PLGA)-based biomaterials for bone tissue engineering. International journal of molecular sciences. 2014;15:3640-59.

[8] Dhillon A, Schneider P, Kuhn G, Reinwald Y, White LJ, Levchuk A, et al. Analysis of sintered polymer scaffolds using concomitant synchrotron computed tomography and in situ mechanical testing. Journal of Materials Science: Materials in Medicine. 2011;22:2599-605.

[9] Blanchard L-P, Hesse J, Malhotra SL. Effect of molecular weight on glass transition by differential scanning calorimetry. Can J Chem. 1974;52:3170-5.

[10] Xie Y, Park J-s, Kang S-k. Studies on the Effect of Molecular Weight on the Degradation Rate of Biodegradable Polymer Membrane. 2015.

[11] Mettler Toledo, Interpreting DSC curves; Part 1: Dynamic measurements,. USERCOM 1/2000.

[12] Lim H, Hoag SW. Plasticizer Effects on Physical–Mechanical Properties of Solvent Cast Soluplus® Films. AAPS PharmSciTech. 2013;14:903-10.

[13] Rabek CL, Stelle RV, Dziubla TD, Puleo DA. The Effect of Plasticizers on the Erosion and Mechanical Properties of Polymeric Films. Journal of biomaterials applications. 2014;28:10.1177/0885328213480979.

[14] Kranz H, Ubrich N, Maincent P, Bodmeier R. Physicomechanical properties of biodegradable poly(D,L-lactide) and poly(D,L-lactide-co-glycolide) films in the dry and wet states. J Pharm Sci. 2000;89:1558-66.

[15] Liu Y, Li Y, Chen H, Yang G, Zheng X, Zhou S. Water-induced shape-memory poly(D,L-lactide)/microcrystalline cellulose composites. Carbohydrate Polymers. 2014;104:101-8.

[16] Ofem MI, Umar M. Effect of filler content on the mechanical properties of periwinkle shell reinforced CNSL resin composites. ARPN Journal of Engineering and Applied Sciences. 2012;7:212-5.

[17] Bleach NC, Nazhat SN, Tanner KE, Kellomäki M, Törmälä P. Effect of filler content on mechanical and dynamic mechanical properties of particulate biphasic calcium phosphate—polylactide composites. Biomaterials. 2002;23:1579-85.

[18] Wong YS, Xiong SS, Venkatraman SS, Boey FYC. Shape memory in un-cross-linked biodegradable polymers. Journal of Biomatials Science: Polymer Edition. 2008;19:175-91.

[19] Wong YS, Stachurski ZH, Venkatraman SS. Modeling shape memory effect in uncrosslinked amorphous biodegradable polymer. Polymer. 2011;52:874-80.

[20] Yang B, Huang WM, Li C, Li L. Effects of moisture on the thermomechanical properties of a polyurethane shape memory polymer. Polymer. 2006;47:1348-56.

[21] Du H, Zhang J. Solvent induced shape recovery of shape memory polymer based on chemically cross-linked poly(vinyl alcohol). Soft Matter. 2010;6:3370-6.

[22] Blasi P, D'Souza SS, Selmin F, DeLuca PP. Plasticizing effect of water on poly(lactide-co-glycolide). J Controlled Release. 2005;108:1-9.

[23] McNally G, Ruddy A. Rheological, Mechanical and Thermal Behaviour of Radiopaque Filled Polymers. ANTEC-CONFERENCE PROCEEDINGS-2005. p. 167.

[24] Wong YS, Xiong Y, Venkatraman SS, Boey FYC. Shape memory in un-cross-linked biodegradable polymers. Journal of Biomaterials Science, Polymer Edition. 2008;19:175-91.

[25] Wang X, Venkatraman SS, Boey FY, Loo JS, Tan LP. Controlled release of sirolimus from a multilayered PLGA stent matrix. Biomaterials. 2006;27:5588-95.

[26] Ponnusamy T, Lawson LB, Freytag LC, Blake DA, Ayyala RS, John VT. In vitro degradation and release characteristics of spin coated thin films of PLGA with a “breath figure” morphology. Biomatter. 2012;2:77-86.

[27] Suyatma NE, Tighzert L, Copinet A, Coma V. Effects of hydrophilic plasticizers on mechanical, thermal, and surface properties of chitosan films. J Agric Food Chem. 2005;53:3950-7.

[28] Gentile P, Chiono V, Carmagnola I, Hatton PV. An Overview of Poly(lactic-co-glycolic) Acid (PLGA)-Based Biomaterials for Bone Tissue Engineering. International Journal of Molecular Sciences. 2014;15:3640-59.

[29] Jung YC, Bhushan B. Contact angle, adhesion and friction properties of micro-and nanopatterned polymers for superhydrophobicity. Nanotechnology. 2006;17:4970.

[30] Semakina OK, Phomenko A, Leonteva A, Rymanova IE. Research of surface properties of fillers for polymers. Procedia Chemistry. 2015;15:79-83.

[31] Friedrich J. The plasma chemistry of polymer surfaces: advanced techniques for surface design: Wiley Online Library; 2012.

[32] Wan Y, Qu X, Lu J, Zhu C, Wan L, Yang J, et al. Characterization of surface property of poly (lactide-co-glycolide) after oxygen plasma treatment. Biomaterials. 2004;25:4777-83.

[33] Maenz S, Hennig M, Mühlstädt M, Kunisch E, Bungartz M, Brinkmann O, et al. Effects of oxygen plasma treatment on interfacial shear strength and post-peak residual strength of a PLGA fiber-reinforced brushite cement. Journal of the mechanical behavior of biomedical materials. 2016;57:347-58.

[34] Kizilay MY, Okay O. Effect of initial monomer concentration on spatial inhomogeneity in poly (acrylamide) gels. Macromolecules. 2003;36:6856-62.

[35] Lin H, Kai T, Freeman BD, Kalakkunnath S, Kalika DS. The Effect of Cross-Linking on Gas Permeability in Cross-Linked Poly(Ethylene Glycol Diacrylate). Macromolecules. 2005;38:8381-93.

[36] Kabiri K, Omidian H, Hashemi SA, Zohuriaan-Mehr MJ. Synthesis of fast-swelling superabsorbent hydrogels: effect of crosslinker type and concentration on porosity and absorption rate. Eur Polym J. 2003;39:1341-8.

[37] Zohuriaan ‐ Mehr MJ, Motazedi Z, Kabiri K, Ershad ‐ Langroudi A. New Super ‐ Absorbing Hydrogel Hybrids from Gum Arabic and Acrylic Monomers. Journal of Macromolecular Science, Part A. 2005;42:1655-66.

[38] Borzacchiello A, Ambrosio L. Structure-Property Relationships in Hydrogels. Hydrogels: Springer Milan; 2009. p. 9-20.

[39] Lin H, Freeman BD. Gas solubility, diffusivity and permeability in poly(ethylene oxide). Journal of Membrane Science. 2004;239:105-17.

[40] Simon FT, Rutherford JM. Crystallization and Melting Behavior of Polyethylene Oxide Copolymers. J Appl Phys. 1964;35:82-6.

[41] Nadkarni V, Jog J. Crystallization of polymers in thermoplastic blends and alloys. Handbook of Polymer Science and Technology. 1989;4:81-120.

[42] Swartjes FHM, Peters GWM, Rastogi S, Meijer HEH. Stress Induced Crystallization in Elongational Flow. Int Polym Proc. 2003;18:53-66.

[43] Rao IJ, Rajagopal KR. A study of strain-induced crystallization of polymers. Int J Solids Struct. 2001;38:1149-67.

[44] Ikeda Y, Yasuda Y, Makino S, Yamamoto S, Tosaka M, Senoo K, et al. Strain-induced crystallization of peroxide-crosslinked natural rubber. Polymer. 2007;48:1171-5.

[45] Tosaka M. Strain-Induced Crystallization of Crosslinked Natural Rubber As Revealed by X-ray Diffraction Using Synchrotron Radiation. Polym J. 2007;39:1207-20.

[46] Zhao Y, Chun Wang C, Min Huang W, Purnawali H. Buckling of poly(methyl methacrylate) in stimulus-responsive shape recovery. Appl Phys Lett. 2011;99:131911.

[47] More AP, Donald AM, Henderson A. Stress modified Case II diffusion in poly(methyl methacrylate). Polymer. 1992;33:3759-61.

[48] Fukumori K, Kurauchi T, Kamigaito O. Swelling behaviour of rubber vulcanizates: 2. Effects of tensile strain on swelling. Polymer. 1990;31:2361-7.

[49] Treloar LRG. The swelling of cross-linked amorphous polymers under strain. Transactions of the Faraday Society. 1950;46:783-9.

[50] Móczó J, Pukánszky B. Particulate Fillers in Thermoplastics. Fillers for Polymer Applications: Springer; 2017. p. 51-93.

[51] Cui J, Kratz K, Lendlein A. Adjusting shape-memory properties of amorphous polyether urethanes and radio-opaque composites thereof by variation of physical parameters during programming. Smart Mater Struct. 2010;19:065019.

[52] Seow JHS, Phillips M, Taylor D. Sonographic visibility of breast tissue markers: a tissue phantom comparison study. Australasian journal of ultrasound in medicine. 2012;15:149-57.

[53] Gu X, Mather PT. Water-triggered shape memory of multiblock thermoplastic polyurethanes (TPUs). RSC Advances. 2013;3:15783-91.

Chapter 5 Modulating Water-responsive shape recovery induced buckling in PEG Hydrogel

5.1 Introduction

Since water is one of the major components in living biological systems, water-responsive SMM holds great potential for various implantable applications, including wound healing, intravascular devices, soft tissue reconstruction, and controlled drug delivery etc. This provides motivation to combine water-activated SME and swelling in hydrogels together to enhance the performance. In many applications, such as vascular occlusion via minimally invasive surgery for liver cancer treatment, the operation time (for both start and finish) is required to be well controlled. Due to gradual and/or slow manner in water absorption for water-activated SME and swelling in hydrogels, even a combination of both effects encounters many difficulties to meet the time-requirements in real procedure of vascular occlusion

In this chapter, we experimentally and analytically investigate the water-activated shape recovery induced buckling in this biodegradable PEG hydrogel to understand the fundamentals in precisely controlling the buckling time.

Thermo-mechanical properties of PEG hydrogel in dry and wet state were extensively studied to discern the effect of various factors such as dimension, deformation strain, recovery stress, temperature.

The molecular mechanism responsible for the water-induced SME in PEG hydrogel is also elucidated. The original diameter and amount of pre-stretching are identified as two influential parameters to tailor the buckling time between one to four minutes as confirmed by both experiments and simulation.

Polyethylene Glycol hydrogel is featured by high capability to absorb a large amount of water (from 10–20% up to thousands of times their dry weight), which results in significant swelling; whereas, in its dry form it displays characteristics of crosslinked polymers. This allows to exploit various shape memory programming and actuation methods for PEG hydrogel. This generic phenomenon can be pertinent to various other similar materials and can open door to new material design approach for various applications in sensing, biomedical etc.

5.2 Swelling of PEG hydrogel.

The large amount absorbed water results in swelling, i.e., significant volume expansion. Such a large volume change in the process of wetting/drying may result in remarkable change in surface morphology and/or overall configuration. Figure 5.1 shows the evolution of PEG hydrogel from dry to completely swollen state. During swelling upon wetting in water, wrinkles appear on the surface of a piece of polyethylene glycol (PEG) hydrogel. Formation of wrinkles is caused by localised swelling which is characterized by symmetrical pattern due to differential swelling forces. The surface becomes smooth by coalescence of different swelling fronts only after a prolonged period of wetting, when the hydrogel almost reaches its maximum swelling[1, 2]. Upon keeping the piece of wrinkled hydrogel in air for a while, the water distribution becomes uniform within the hydrogel eliminating the wrinkles [3-5].

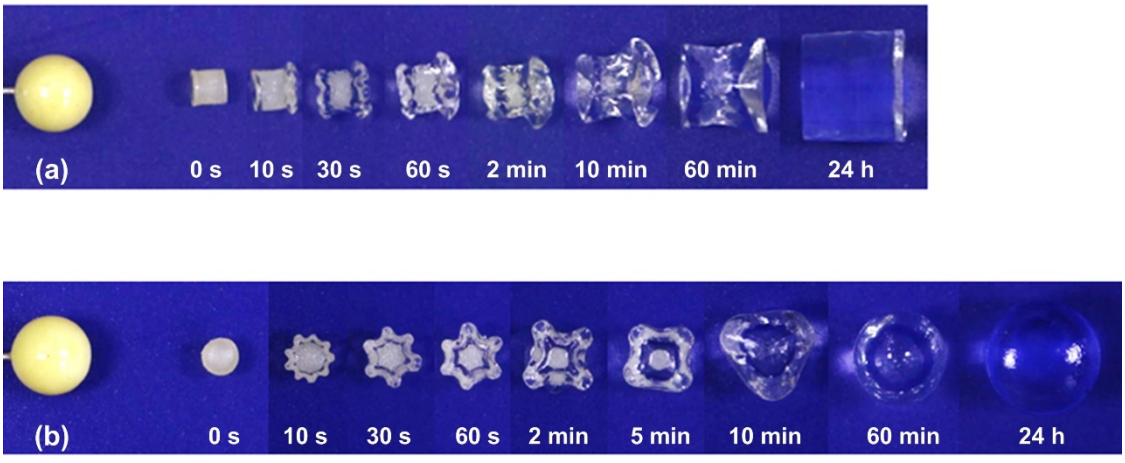

Figure 5.1 Swelling of PEG hydrogel in 37°C water. (a) Side view; (b) Top view. Yellow sphere (6 mm diameter) for benchmark.

5.3 Drying induced shape configuration in PEG hydrogel composite

Formation of hydrogel from precursor solution via photo-crosslinking in mould will result into a hydrogel of dimension limited by the mould, but this intermediate shape can further swell when hydrated in water until it reaches equilibrium swelling. During drying process of hydrogel as dehydration takes place molecules form compact shape which is driven by entropic change, and crystallization of PEG molecules takes place[6, 7]. An experiment was carried out where a flexible polyester filament was embedded in different configurations (as show in Figure 5.2 top) during photo-crosslinking of the PEG hydrogel, it was observed that depending on the placement of the core filament different shapes are formed upon complete drying. When the dried samples hydrated again they regained their original straight shape in wet form. The dry shapes in S-and/or coil-configuration can be heated above the melting temperature of PEG hydrogel (to 70 °C), and can be straightened and cooled down to room temperature to fix the shape. Thermal induced shape memory effect upon reheating the sample to 70°C transformed shape back to S-and/or coil-configuration.

This phenomenon can be explained on the basis differential swelling/shrinking of two layers triggered by water and temperature in a bilayer polymeric system [8-10]. While drying of hydrogel the flexible filament limits the contraction which results isotropic volume contraction into an anisotropic deformation or bending. While in case of co-axial concentric placement of the filament, the filament follows the same contraction path as the gel and the contraction forces are distributed uniformly around it.

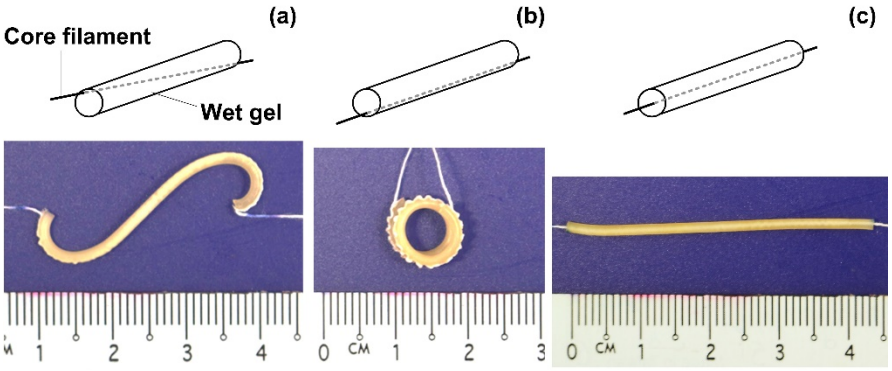

Figure 5.2 Typical shapes after drying of hydrogel composites. (a) S shape (cross-placement of core filament); (b) coil (eccentric/tangential placement of core filament); (c) straight line (co-axial concentric placement of core filament). Top: illustration of the initial position of the core filament; bottom: configuration after drying

Orientation and conformational changes of molecular chains upon cooling (crystallization) and heating (melting) is a novel way utilized in polymers to reversibly switch between two shapes [11, 12]. Likewise swelling of a hydrogel and/or the difference in swelling ratio of a hydrogel composite provide an easy yet effective approach for water induced reversible shape switching and folding/ unfolding [13-15]. Essentially, the same approach is applicable to other gels activated by non-water solvent. However, the reversible nature implies that the associated shape switching is always between two shapes, one is corresponding to the dry state and the other is corresponding to the wet state.

5.4 Water-responsive shape recovery induced buckling in PEG hydrogel

Water responsive reversible shape switching between two shapes in hydrogels (dry and wet), upon wetting/drying is termed as the shape change effect (SCE)[16, 17]. This process of SCE progresses in a gradual manner and take a longer than the time practically allowed in the medical procedure of vascular occlusion (normally around two minutes). Which is limiting factor of using swelling alone as driving force for the actuation of the device in this research work. Another limiting factor is that the higher (than allowable of catheter embolization) starting dimension is needed to achieve occlusion of target blood vessel of 4-7 mm diameter.

A combination of water-induced SME (shape recovery) and SCE (swelling) in programmed dry hydrogel could essentially overcome the limitations (e.g., limited re-configurability) with either of them applied, hence facilitating the reshaping of design in various ways [18, 19].

In following section, we experimentally and analytically investigate the water-activated shape recovery induced buckling in this biodegradable PEG hydrogel to understand the fundamentals in precisely controlling the buckling time.

5.4.1 Effect of programming strain on the mechanical properties of dry hydrogel

Figure 5.3 shows the stress vs. strain results of dry stretched PEG samples with initial diameter before stretching 2.45 mm with stretched to different programming strains at 70°C as described in section 3.10.3.

As it can be seen, the yield stress increased significantly with the increase of programming strain, whilst the stress vs. strain curves in the early liner region showed same progression. The Young's modulus of the dry stretched PEG can be obtained by measuring the slope in the early loading part of the stress vs. strain curve and it was found to be 696 ± 50 MPa.

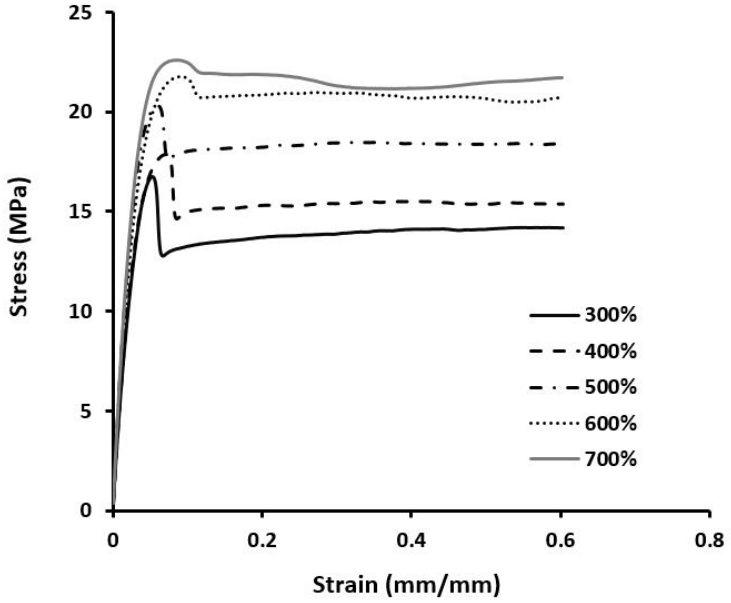

Figure 5.3 Effects of programming strain on the stress vs. strain relationship of dry PEG hydrogel.

5.4.2 Cyclic tensile testing of dry hydrogel at 70 °C

Cyclic tensile test at 70 °C was performed on dry PEG hydrogel sample with initial diameter of 2.45 mm, as described in section 3.10.5.

The cyclic stress vs. strain curves plotted in Figure 5.4 depict the viscoelastic behaviour and hysteresis of PEG hydrogel above its melting temperature, T_m with higher recovery strains. Redistribution of molecular arrangement, relative unstrained motion between crosslinks and/or slippage of chains may cause permanent deformation in the observed residual strain.[20].

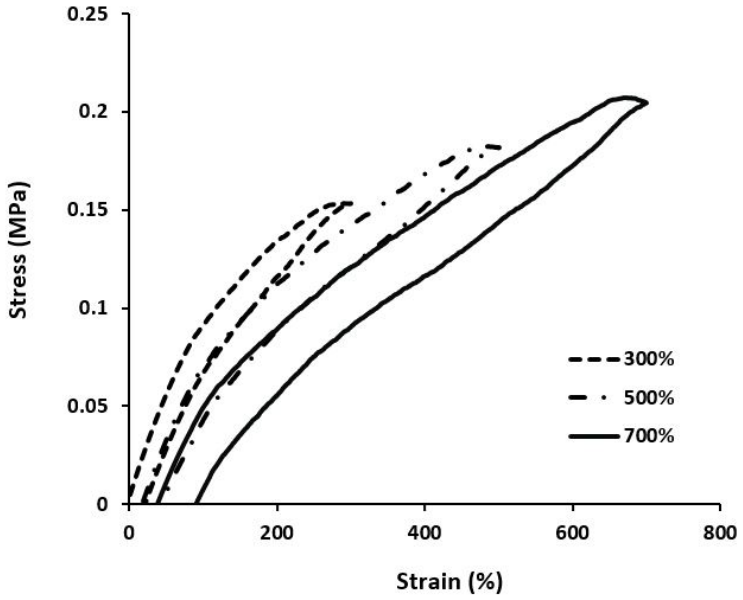

Figure 5.4 Cyclic tensile test of dry PEG hydrogel at 70 °C.

5.4.3 Mechanical properties of wet hydrogels

Mechanical properties of wet hydrogel were investigated as described in section Figure 5.5 presents typical stress vs. strain relationships till fracture. As we can see, for a sample with a larger original diameter, the corresponding slope in the earlier region of stress vs. strain curve is higher, which indicates less solvated or far from equilibrium swelling in larger sized sample upon immersing in water for 15 minutes. Another important feature observed here is limited capability in stretching in all samples. Hence, an alternative programming approach [4] is not applicable to this hydrogel to achieve a high amount of stretching. As reported in [4], where wet hydrogel is stretched to designated deformation strain and dried under same constraints to result into dry hydrogel with in-built stresses. The stresses can be relieved upon hydration of the dry hydrogel thus actuating water responsive shape memory effect.

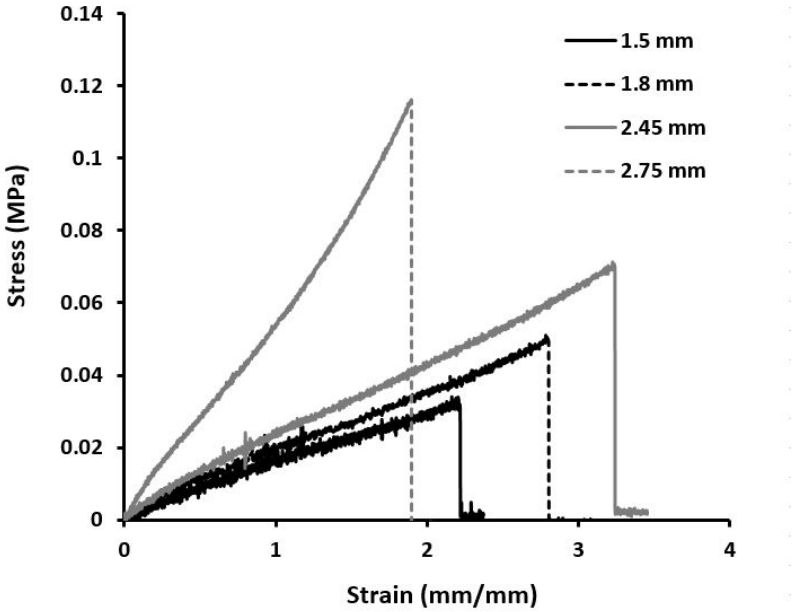

Figure 5.5 stress vs. strain relationships in uni-axial tension to fracture after wetting the PEG hydrogels in 37 ^{o}C DI water for 15 minuts for samples of different original diameters.

5.4.4 Determination of recovery force generated in hydrogel during water induced buckling of hydrogel

Dry hydrogel samples were programmed to different deformation strain as described in section 3.10.2. The recovery force generated (and responsible for shape memory activation) when the samples are subjected to immersion in 37 ^{0}C DI water was evaluated by iso-strain tests on MTS Criterion C42 Machine with MTS Bionix® EnviroBath setup as described in section 3.10.6.

Error! Reference source not found.(a) shows the recovery force vs. time curves of dry PEG hydrogel with starting 2.45 mm diameter and deformed to different programming strains. Gage length of 30 mm was used of preprogramed sample. The plot in Figure 5.6 b) report the stress as a function of immersing time to reveal the fundamentals in a dimensionless manner.

As shown in Figure 5.6 b) the evolution of recovery stress in all samples with the same original dry diameter of 2.45 mm follows more or less the same increasing path in the early wetting stage. According to Figure 5.1 the gel should swell continuously upon wetting in water, so that the effect of swelling should result in compressive stress within

the time frame of our experiments. Hence, the observed gradual increase in tensile stress should be the result of water induced shape recovery [3, 4, 21]. Upon continued immersion, a sudden upsurge in recovery stress (as marked by arrow) in all samples is observed. Given the instant nature of such upsurge in recovery stage, the only possible cause is buckling as previously reported [22, 23]. However, after the maximum stress is reached, the swelling effect becomes relatively more influential, so that the observed stress starts to gradually decrease. While the final stress (within the time frame of our experiments) increases with the increase in programming strain, a higher programming strain induces earlier buckling.

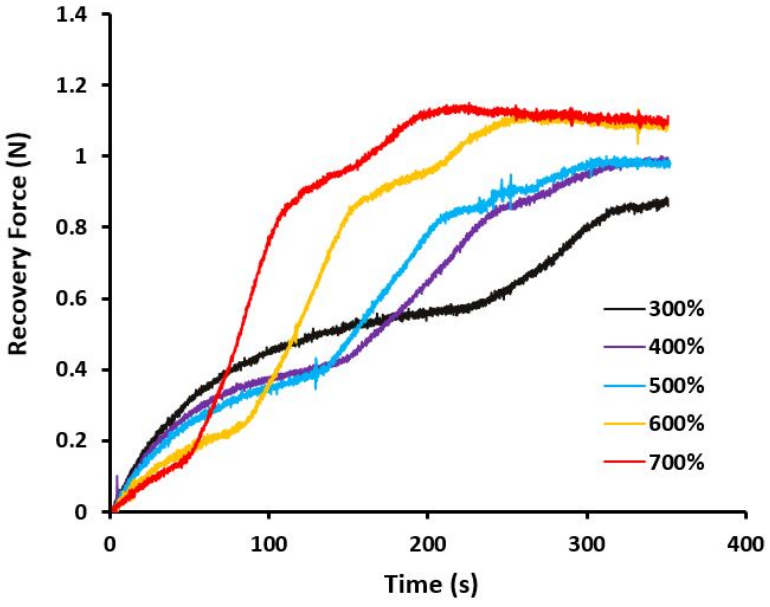

(a)

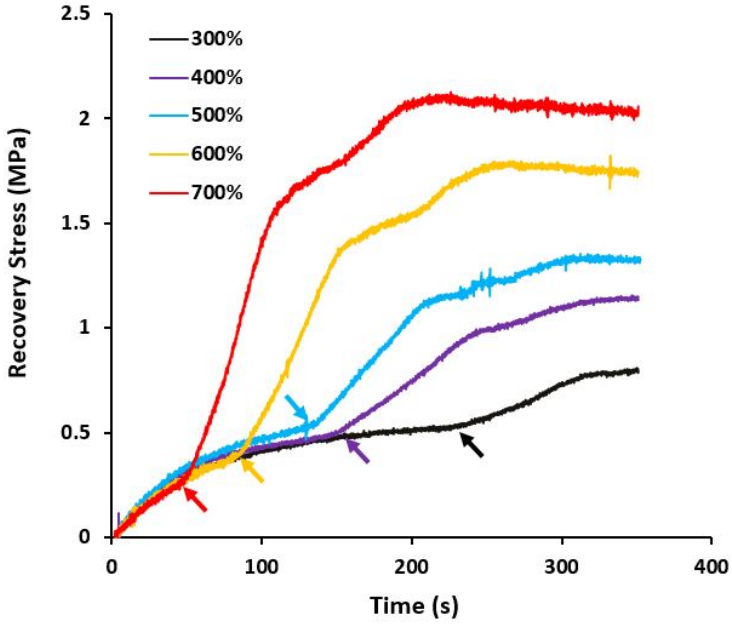

(b)

Figure 5.6 Evolution of recovery force (a)[stress (b)] upon wetting in original 2.45 mm diameter PEG samples with different programming strains.

In another investigation, where deformation strain during programming step is constant to 500%, while the original sample diameter is a variable, similar trend is still observed in the stress vs. time relationship as shown in Figure 5.7. However, the stress increases faster in the sample with a larger original diameter, while the upsurge in stress occurs earlier in the sample with a smaller original diameter.

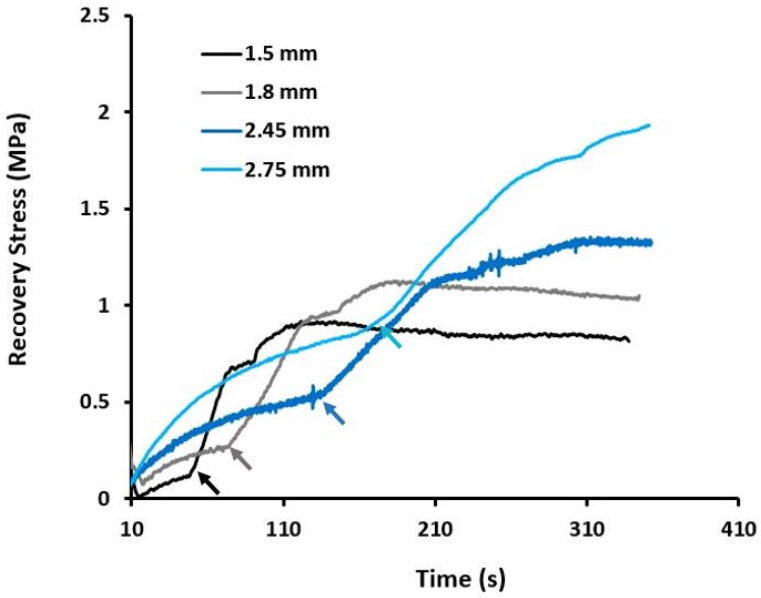

Figure 5.7 Evolution of recovery stress upon wetting in 500% pre-stretched PEG samples with 30 mm gage length and different original diameters.

In similar experimental setup with sample fixed in in top grip and free at the bottom end, upon wetting the pre-programmed samples in 37 °C DI water, shape recovery and/or change were recorded by a video camera. Figure 5.8 depicts the snapshots of one typical test, for the 30 mm free length of sample with original diameter 2.45 mm and programming strain of 400%. The same tests were performed on samples with different programming strain and original diameter and the corresponding bulking time was recorded.

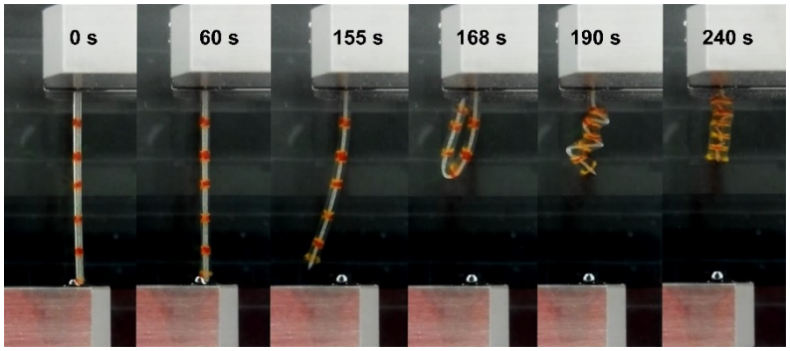

Figure 5.8 Water-induced shape recovery (buckling and swelling) of crosslinked PEG hydrogel filament stretched to 400% deformation strain, in water at 37 °C.

5.5 Feasibility of PEG hydrogel alone as embolic device.

Dry PEG hydrogel filament with initial diameter of 2.35 mm and preprogramed to 600% deformation strain with new diameter of 0.87 mm was deployed in 4 mm tube of dynamic flow set up as described in section 3.9. As shown in Figure 5.9, 4F catheter used to deliver and deploy the PEG filament to the target location in a tube with 37°C DI water flowing at the rate of 120 ml/min.

Combination of water induced shape memory effect and shape change effect due to swelling resulted into buckling of a device in constrained space achieving successful occlusion of the tube (Figure 5.10).

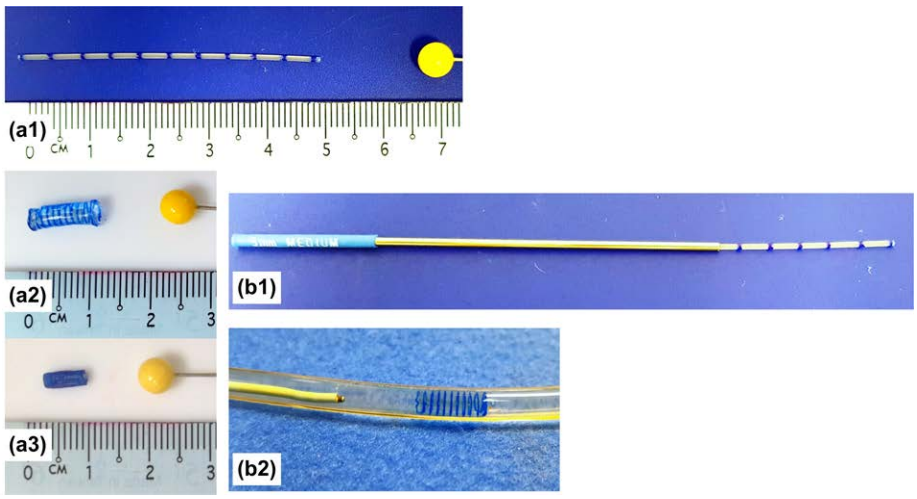

Figure 5.9 Shape change of PEG sample (with blue mark for better visualization). (a1) After 600% pre-stretching; (a2) after wetting in 4 mm diameter tube; (a3) after drying. (b1) Pre-stretched PEG in the catheter loader for delivery; (b2) 4 mm diameter tube is fully blocked. Yellow sphere (6 mm diameter) for benchmark.

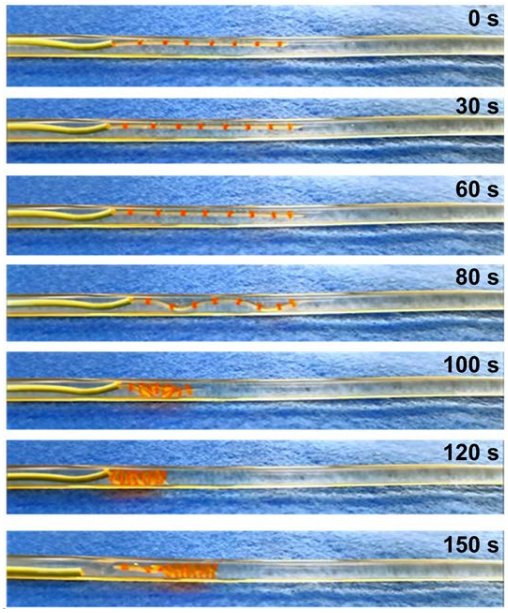

Figure 5.10 Images showing the process of buckling induced occlusion with time (PEG sample marked in red for illustration).

The application of vascular embolization demands visibility under X-ray fluoroscopy, without chemical modification it is difficult to impart radiopacity to the PEG hydrogel. So, having radiopaque PLGA as core filament not only impart radiopacity to device but also assist in shape recovery of the plug due to water- and/or thermo-responsive SME as seen in chapter.

Nonetheless combination of SME and SCE in PEG hydrogel alone can be useful in other applications, or can be extended to other materials.

5.6 Mechanism of water-responsive shape recovery induced buckling in biodegradable PEG hydrogel

The mechanism of above water-responsive process in PEG hydrogel is illustrated in Figure 5.11 and is explained as following. In cross-linked PEG hydrogel, chemical covalent crosslinks serve as the permanent netpoints responsible for holding the permanent shape. Upon wetting in water, the material swells continuously until the maximum is reached (Figure 5.11e). During the process of programming (e.g., uni-axial stretching) at 70 °C, which is above the T_m of PEG crystalline phase, amorphous molecular chains get oriented along the direction of deformation with loss of entropy

and gain of elastic energy (Figure 5.11b). The temporary deformed shape is fixed by the PEG recrystallization as the temperature is lowered to room temperature (Figure 5.11c). PEG crystallites act as the reversible switch points. Upon immersion in water at 37 °C, water molecules diffuse into the system and as the PEG crystalline phase "dissolves", the network becomes fully amorphous [24], actuating the shape recovery of PEG in conjunction with swelling (Figure 5.11d). After a prolonged period of immersing in water, the final shape of the hydrogel (Figure 5.11e) is essentially the same as that of without programming.

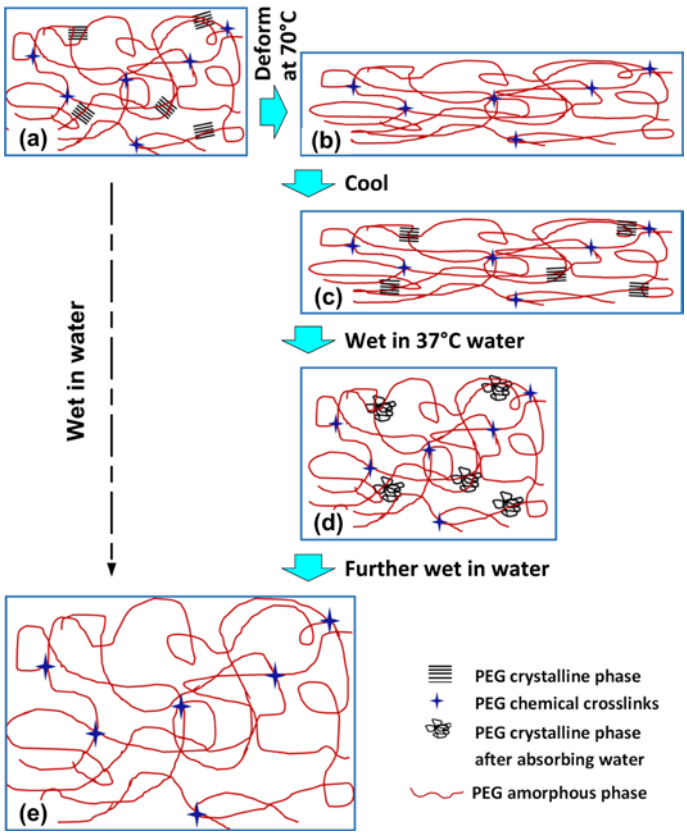

Figure 5.11 Illustration of mechanism of water induced SME and swelling in PEG hydrogel.

5.7 Modelling of shape recovery induced buckling in pre-stretched PEG hydrogel filament

Zhao, Y.et al., (2011) [22] have studied buckling of poly(methyl methacrylate) (PMMA) in stimulus-responsive shape recovery.

(referring to Figure 2.6), If the Young's modulus of the dry sample is much higher than that of the wet one, according to [22], for buckling to happen, the critical value (r^c) of radius r of hard dry core may be estimated by

$$\boldsymbol{r^c = \frac{2\sqrt{2}L}{\pi\sqrt{E_r}}\left[\sqrt{\sigma^2 + \frac{\pi^2}{4L^2}E_r R^2\sigma} - \sigma\right]^{1/2}} \quad 5.1$$

where R is the radius of the sample after pre-stretching; L is the length of the sample; E_r is the Young's modulus of hard core; σ is the compressive stress acting on the softened part.

We assume $\sigma=\varepsilon E_R$ and $L=L_0(1+\varepsilon)$, where E_R is the modulus of the outer soft layer, ε is the programming strain, and L_0 is the original length of the sample before programming. We may further assume that the volume is conserved when a piece of sample is stretched in its dry state. Thus, the radius after stretching can be approximated as $R=R_0(1+\varepsilon)^{-1/2}$, where R_0 is the original diameter of the dry sample.

Instead of using the case II theory for diffusion of ethanol in PMMA in [22], for PEG hydrogel, the diffusion of water should follow the Fick's law, which gives

$$\boldsymbol{R - r^c = v_p t_c^{\,2}} \quad 5.2$$

where v_p is a constant to characterize the diffusion rate and t_c is the critical bulking time.

Thus, Eqn. (5.1) can be rewritten as,

$$v_p t_c^{\,2} = R_0(1+\varepsilon)^{-1/2} - \frac{2\sqrt{2}\,L_0(1+\varepsilon)}{\pi}\left[\sqrt{\frac{E_R^2\varepsilon^2}{E_r^2} + \frac{\pi^2 R_0^2 E_R \varepsilon}{4L_0^2\,(1+\varepsilon)^3 E_r}} - \frac{E_R\varepsilon}{E_r}\right]^{1/2} \quad 5.3$$

A close examination of Eqn. (5.3) reveals that the critical bulking time is mainly determined by not only the original diameter of the sample, but also the programming strain.

Following parameters are used in Eqn. (5.3) for numerical analysis of the buckling time of PEG hydrogel upon wetting in water. E_R= 0.0216 MPa and E_r= 696 MPa, which are calculated from the stress vs. strain curves of fully swollen and dry specimens as shown in **Error! Reference source not found.** and **Error! Reference source not found.**, respectively. v_p is set as 2.6×10^{-6} mm/s^2, which is obtained through data-fitting of the critical buckling time in samples programmed with 500% strain and original diameter of 2.45 mm.

In Figure 5.12, the calculated buckling time as a function of programming strain in original 2.45 mm diameter PEG hydrogel is plotted and compared with the experimental results obtained for both one-end free recovery (by observing the shape change in, e.g., **Error! Reference source not found.**) and constrained samples (by monitoring the recovery stress in **Error! Reference source not found.**). Good agreement is observed in all of them. With the increase of programming strain from 300% to 700%, the buckling time is reduced from about 275 s to less than 100 s.

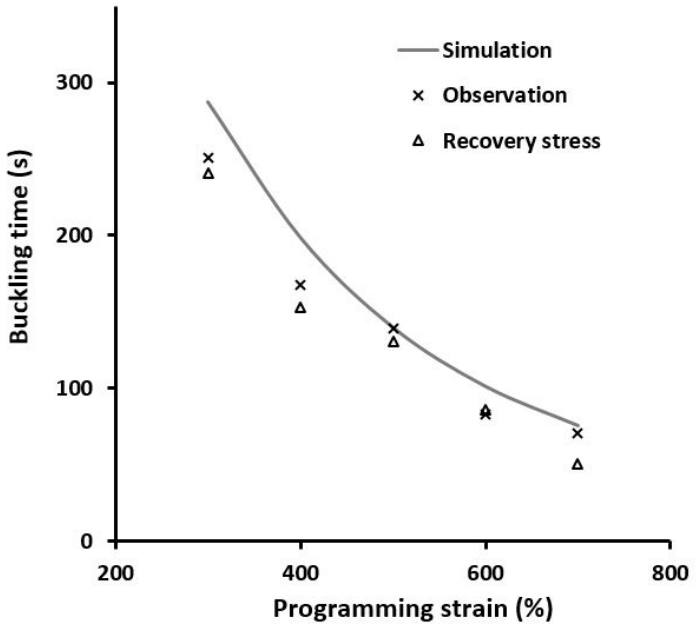

Figure 5.12 Buckling time as a function of programming strain (original diameter: 2.45 mm).

Using the same set of parameters, simulation of buckling time as a function of original diameter is compared with the experimental data of both one-end free and constrained samples in Figure 5.13, in which a constant programming strain of 500% is applied. It is confirmed that same as that in the buckling time vs. programming strain relationship, given a fixed programming strain, the buckling time observed in one-end free test is very close to that spotted by the start of sharp stress increase in the constrained test. With the increase of the original diameter from 1.5 mm to 2.75 mm, the buckling time is extended from about 60 s to around 160 s.

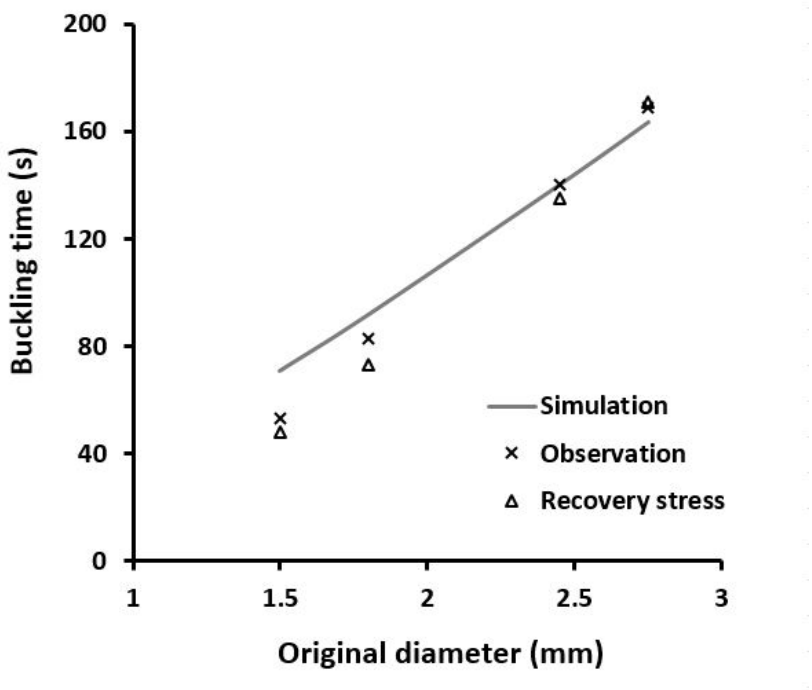

Figure 5.13 Buckling time as a function of original diameter at a fixed programming strain of 500%.

At this point, we may conclude that buckling time in water induced shape recovery of pre-stretched PEG hydrogel can be well controlled by tailoring the original diameter and/or programming strain. The actual buckling time can be estimated based on one set of parameters. Buckling does not require full wetting of the whole hydrogel, so that it occurs within a much shorter period of wetting time.

5.7.1 Shape recovery induced buckling in PLGA-PEG hydrogel composite

Buckling time for PLGA-PEG hydrogel composite can be compared to the only PEG hydrogel composite by considering the flexural rigidity for both the structures. flexural rigidity is represented by the product of area moment of inertia (I) around the lateral axis and the modulus of the material (E).

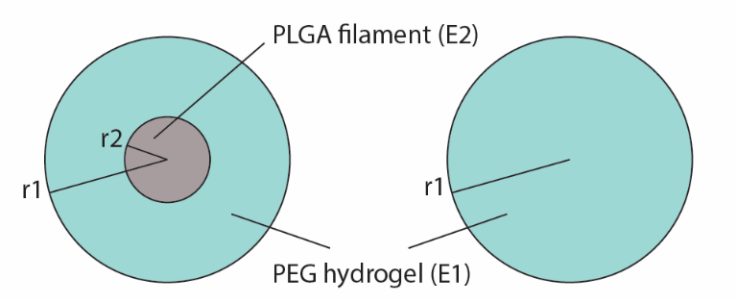

Figure 5.14 Schematic diagram of sectional view of PLGA-PEG hydrogel composite

For composite structure (Figure 5.14),

$$EI_c = E_2 I_{PLGA} + E_1\, I_{hollow\ PEG}$$

$$\boldsymbol{EI_{composite} = E_2\left(\frac{\pi {r_2}^4}{4}\right) + E_1\left[\frac{\pi}{4}({r_1}^4 - {r_2}^4)\right]} \qquad \textbf{5.4}$$

For only hydrogel,

$$EI_{hydrogel} = E_1\left(\frac{\pi {r_1}^4}{4}\right) \qquad 5.5$$

Where, r_1 is the outer radius of hydrogel/composite

r_2 is the radius for PLGA filament

E_1 is the modulus of the dry PEG hydrogel

E_2 is the modulus of the PLGA (37 ^{0}C)

Considering the values of E1 and E2 as 696 MPa and 57.33 MPa respectively, as obtained from the experiments.

For the polymer-hydrogel composite with initial diameter 2.54 mm and stretched to 700% at 70^{o}C, r_1 and r_2 were 0.43 and 0.15 mm respectively, as calculated from the SEM imaging of the cross section as shown in Figure 4.1.

Using equation (5.4 & 5.5) the ratio of flexural rigidity (D) was calculated as

$$D = \frac{EI_{composite}}{EI_{hydrogel}}$$

The flexural rigidity ratio D was found to be 0.98 which implies that addition of PLGA core does not change the flexural rigidity of the polymer-hydrogel composite significantly. Hence force required for buckling to occur in PLGA-hydrogel composite is same as that of PEG hydrogel. Considering the same diffusion rate and swelling kinetics, the buckling time should be approximately same for both PLGA hydrogel composite and PEG hydrogel.

Experimental buckling time, observed for the polymer-hydrogel composite stretched to 700% was found to be 64 ± 3 s which was approximately same (71 ± 4 s) as observed for PEG hydrogel of same dimension.
The results imply that the model developed to determine buckling time in PEG hydrogel can be extended to PLGA-hydrogel composite as a good estimation.

Conclusion

Experimental and simulation results confirmed that buckling induced by water-responsive SME and swelling in hydrogel can not only overcome the limitation with either of them being applied, but also achieve time-controlled activation. Original diameter and programming strain are identified as two key parameters for tailoring the actual buckling (actuation) time within a wide range. Since buckling does not require full wetting of the whole hydrogel, it occurs within a much shorter period of wetting time. Although demonstrated here is targeted for a particular application of vascular occlusion via minimally invasive surgery for liver cancer treatment using a biodegradable PEG hydrogel, the phenomenon reported here, i.e., chemically-induced buckling via a combination of the SME and swelling, is generic and it can be extended to various other hydrogel materials and applications thereof.

References

[1] Breid D. Controlling morphology in swelling-induced wrinkled surfaces. 2012.
[2] Guvendiren M, Yang S, Burdick JA. Swelling‐Induced Surface Patterns in Hydrogels with Gradient Crosslinking Density. Adv Funct Mater. 2009;19:3038-45.

[3] Zhang JL, Huang WM, Lu HB, Sun L. Thermo-/chemo-responsive shape memory/change effect in a hydrogel and its composites. Mater Des. 2014;53:1077-88.
[4] Zhang JL, Huang WM, Gao G, Fu J, Zhou Y, Salvekar AV, et al. Shape memory/change effect in a double network nanocomposite tough hydrogel. Eur Polym J. 2014;58:41-51.
[5] Huang WM, Lu HB, Zhao Y, Ding Z, Wang CC, Zhang JL, et al. Instability / collapse of polymeric materials and their structures in stimulus-induced shape / surface morphology switching. Mater Des. 2014;59:176-92.
[6] Yang T. Mechanical and swelling properties of hydrogels: KTH Royal Institute of Technology; 2012.
[7] Parlato M, Reichert S, Barney N, Murphy WL. Poly (ethylene glycol) hydrogels with adaptable mechanical and degradation properties for use in biomedical applications. Macromolecular bioscience. 2014;14:687-98.
[8] Zhang E, Wang T, Hong W, Sun W, Liu X, Tong Z. Infrared-driving actuation based on bilayer graphene oxide-poly (N-isopropylacrylamide) nanocomposite hydrogels. J Mater Chem A. 2014;2:15633-9.
[9] Liu L, Jiang S, Sun Y, Agarwal S. Giving direction to motion and surface with ultra‐fast speed using oriented hydrogel fibers. Adv Funct Mater. 2016;26:1021-7.
[10] Hu Z, Zhang X, Li Y. Synthesis and application of modulated polymer gels. Science. 1995;269:525.
[11] Bothe M, Pretsch T. Two-Way Shape Changes of a Shape-Memory Poly(ester urethane). Macromol Chem Phys. 2012;213:2378-85.
[12] Bothe M, Pretsch T. Bidirectional actuation of a thermoplastic polyurethane elastomer. J Mater Chem A. 2013;1:14491-7.
[13] Shim TS, Kim SH, Heo CJ, Jeon HC, Yang SM. Controlled origami folding of hydrogel bilayers with sustained reversibility for robust microcarriers. Angew Chem Int Ed. 2012;51:1420-3.
[14] Zhang Y, Ionov L. Reversibly cross-linkable thermoresponsive self-folding hydrogel films. Langmuir. 2015;31:4552-7.
[15] Huang WM, Zhao Y, Wang CC, Ding Z, Purnawali H, Tang C, et al. Thermo/chemo-responsive shape memory effect in polymers: a sketch of working mechanisms, fundamentals and optimization. J Polym Res. 2012;19:9952.

[16] Lendlein A, Kelch S. Shape-Memory Polymers. Angew Chem Int Ed. 2002;41:2034-57.

[17] Sun L, Huang WM, Ding Z, Zhao Y, Wang CC, Purnawali H, et al. Stimulus-responsive shape memory materials: A review. Mater Des. 2012;33:577-640.

[18] Yue JJ, Morgenstern R, Morgenstern C, Lauryssen C. Shape Memory Hydrogels–A Novel Material for Treating Age-related Degenerative Conditions of the Spine. Eur Musculoskeletal Rev. 2011;6:184-8.

[19] Lauryssen C, Yue JJ, Jaramillo-de la Torre JJ, Chen A, Prewett A. Novel application of biomedical hydrogels for treating degenerative conditions of the spine. Eur Musculoskeletal Rev. 2010;5:36-8.

[20] Cantournet S, Desmorat R, Besson J. Mullins effect and cyclic stress softening of filled elastomers by internal sliding and friction thermodynamics model. Int J Solids Struct. 2009;46:2255-64.

[21] Huang WM, Yang B, An L, Li C, Chan YS. Water-driven programmable polyurethane shape memory polymer: Demonstration and mechanism. Appl Phys Lett. 2005;86:114105.

[22] Zhao Y, Wang CC, Huang WM, Purnawali H. Buckling of poly(methyl methacrylate) in stimulus-responsive shape recovery. Appl Phys Lett. 2011;99:131911.

[23] Wang CC, Zhao Y, Purnawali H, Huang WM, Sun L. Chemically induced morphing in polyurethane shape memory polymer micro fibers/springs. React Funct Polym. 2012;72:757-64.

[24] Gu X, Mather PT. Water-triggered shape memory of multiblock thermoplastic polyurethanes (TPUs). RSC Adv. 2013;3:15783-91.

Chapter 6 Embolic device feasibility and safety studies

6.1 Introduction

In this chapter, the embolic device is characterized for properties concerning the safety of the device in biological environment, stability of the device and its ability to retain the functionality through the storage period, safety regarding the migration of the device upon deployment and the degradation of the device.

6.2 Shelf-life study for the embolic plug

The shelf life of the device as whole with respect to its intended functionality, material and mechanical stability at different time points is reported and discussed in the following section. ETO sterilized samples packets were stored in desiccator at 25 ^{0}C and 35% relative humidity (RH) for the period of 180 days. The different characterizations were carried out at four time points as day 0, day 30, day 90 and day 180.

6.2.1 Mechanical Properties:

Physical or chemical changes in the materials have effect on their bulk mechanical properties. Evaluation of the mechanical properties at different time point period can infer the changes at molecular level such as molecular scission, change in crystallinity etc[1]. So, the stability of the material at storing condition and period can be assessed.

The mechanical property (Figure 6.1.) results show the tensile modulus and yield strength of the embolic plug stored at 25^{0}C and 35% relative humidity (RH) at different timepoints over a period of 180 days. Tensile modulus dropped from 744 ± 52 MPa at day 0 to 643 ± 34 MPa at day 30 and no further significant change is observed through the period Day 30 to Day180 ($p > 0.05$). Yield tensile strength followed the same trend with initial drop from 19.2 ± 0.4 MPa to 16.8 ± 0.7 MPa, followed by insignificant change over a period of 180 days.

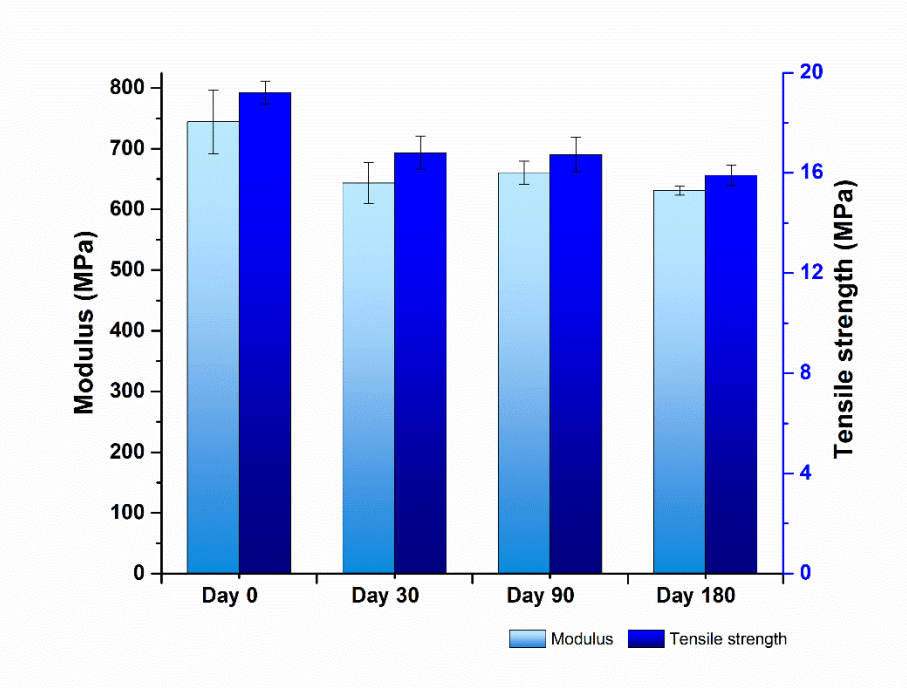

Figure 6.1 Shelf life study of embolic device – effect of storage condition and time on the mechanical properties of embolic device

The decrease in mechanical properties at beginning can be associated with the fact that the Day 0 samples were tested immediately after the ETO sterilization process, so the residual moisture in the sterilized packets did not affect the Day 0 results. Stable mechanical properties from day 30 to day 180 suggests that there are no physical or chemical changes taking place at experimental storing conditions[2-4].

6.2.2 Water induced shape recovery:

The functional property of the embolic device is to transform from the temporary compact shape to expanded shape to occlude the target blood vessel. This transformation progresses via intermediate step of water induced buckling and it is supposed to start actuation and complete it within certain timeframe, which can be tailored as discussed in chapter 5.

To determine if there is any effect (positive or adverse) on the functional property of the embolic device test is carried out as described in 3.10.7. The time taken by the embolic plug for water induced shape memory actuation in 37^0 C DI water, is presented in the Figure 6.2, for different storage timepoints. There is no significant change is observed in

the shape recovery time for the samples stored for different timepoints, the value remains close to 72 ± 6 seconds. This is fundamental requirement of the device.

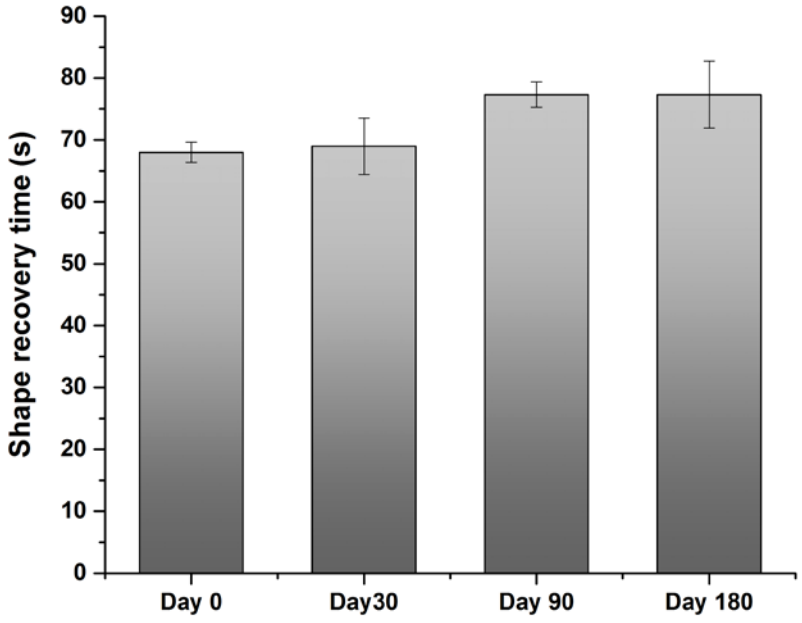

Figure 6.2 Shelf life study of embolic device – effect of storage condition and time on the shape memory effect of embolic device

6.2.3 Swelling ratio for hydrogel and Molecular weight for PLGA

Individual constituents of the device i.e. PEG hydrogel and Radiopaque PLGA filament were examined over a storage time to investigate the degradation possibility at storage condition.

For the PEG hydrogel the swelling ratio was chosen as the parameter to depict the degradation since hydrolysis of the end-group acrylate esters causes breakage of crosslinks resulting into higher swelling ratio. Figure 6.3 represent the swelling ratio in DI water. The swelling ratio did not show any significant change when tested at different time points. The value of swelling ratio was found to be 33 ± 0.4. This confirms that there is no degradation taking place in the PEG hydrogel in dry state when stored at 25^0C and 35% relative humidity (RH) over a period of 180 days.

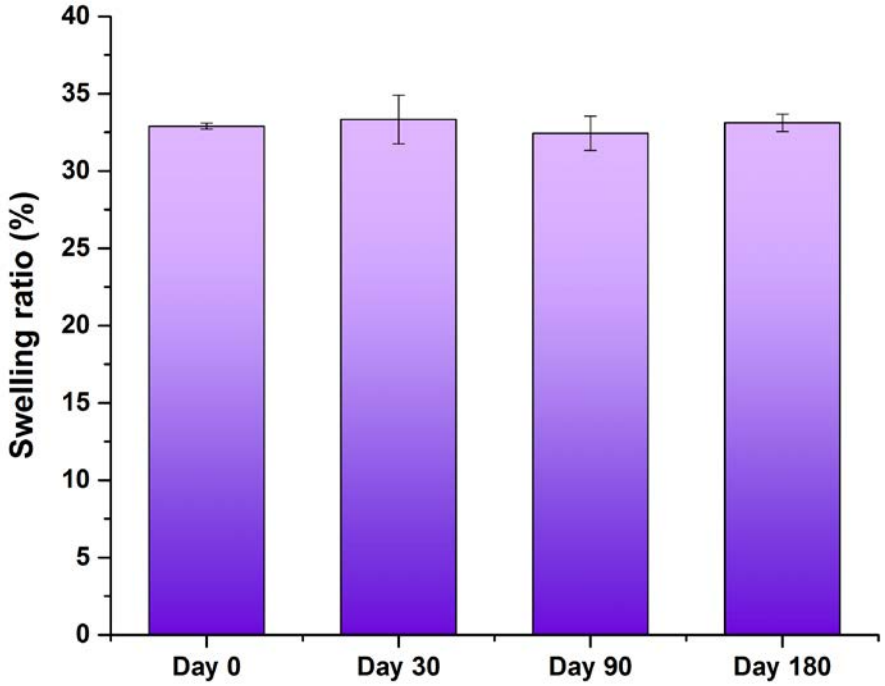

Figure 6.3 Shelf life study of embolic device – effect of storage condition and time on the PEG swelling ratio (degradation)

Molecular weight of PLGA obtained by GPC is plotted against the storage period as shown in Figure 6.4 The molecular weight at day 0 was found to be 60 ± 3 kDa , followed by 56 ± 2 kDa, 56 ± 1.5 kDa, and 52 ± 3 kDa for day 30, day 90 and day 180 respectively. Statistical analysis (ANOVA and two tailed t-test) showed change is insignificant ($p > 0.05$). The small drop in molecular weight might be the result of moisture in the packet or bound water in plasticized PLGA causing hydrolytic degradation, but it is limited. Moisture sensitivity and plasticizing effect of water on PLGA is well known[2-6], so to eliminate possibility of degradation moisture proof packaging is recommended.

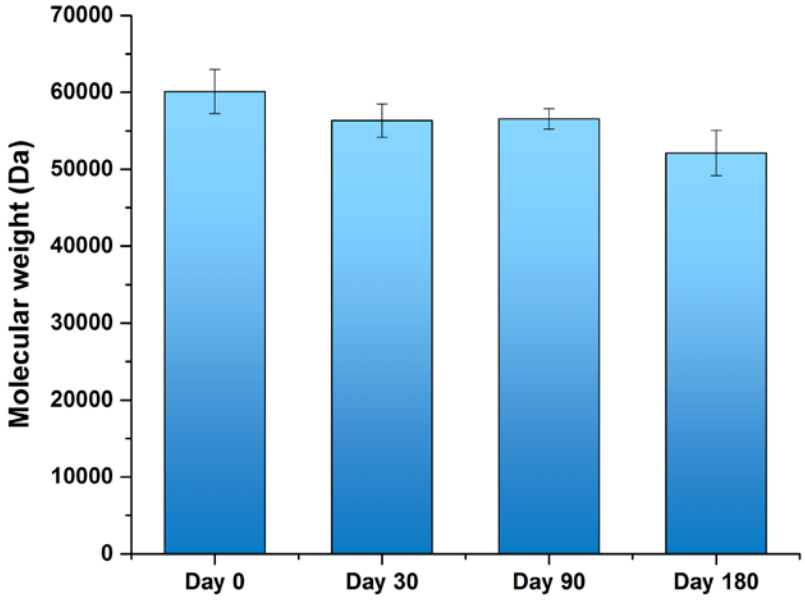

Figure 6.4 Shelf life study of embolic device – effect of storage condition and time on the PLGA composite molecular weight

All the above results concluded that the embolic plug retain its integrity/stability without any loss in functional properties when stored in ETO sterilized seal packets in desiccator at 25 ^{0}C and 35% relative humidity (RH) for the period of 180 days.

6.3 *In-vitro* degradation of the device and individual components

A temporary embolic plug should degrade within a few weeks so that patency of the vessel embolized is restored. PLGA and PEG hydrogel have been selected as the starting materials partly because their degradation timeframes meet this requirement. As shown in Figure 6.5a, *in vitro* degradation of PLGA was monitored by change of molar mass and overall mass loss. It can be seen that there was dramatic decrease in M_w in the PLGA sample with ~ 90% decrease in day 25. In addition, the mass loss data showed minimal mass loss in the first month, followed by rapid mass loss to 75% at day 70. It is due to the fact that the molar mass of the polyesters has to be reduced substantially to permit mass loss through solubilization of the oligomers [7].

Furthermore, the *in vitro* degradation of PEG hydrogel was monitored by mass loss and there was ~70% mass loss at week 10 (Figure 6.5b). Degradation of PEG hydrogel is primarily due to the hydrolysis of the acrylate esters [8-10].

There is concern that as the plug degrades, plug fragments may flow downstream and result in undesired occlusion of downstream vessels. Therefore, the *in vitro* degradation of the embolic device was studied. As shown in Figure 6.5c, the overall mass loss profile of the embolic device mirrored that of the PEG hydrogel. It is worth noting that the degradation timeframe for PLGA core is shorter compared to that of PEG hydrogel and PEG hydrogel also functions as a barrier to contain faster degraded PLGA fragments, and helps absorbing water to impart plasticizing effect to PLGA. As the PLGA degrades inside the embolic device, it can be seen that the degraded PLGA polymer was contained or encapsulated within the degrading PEG hydrogel matrix even as the whole device disintegrated at 2 months (Figure 6.6).

This is desirable for the application since it translates to much reduced chances of migration of the degraded PLGA fragments. Another positive aspect of this encapsulation effect is the retained radio-opacity of the device over the degradation period.

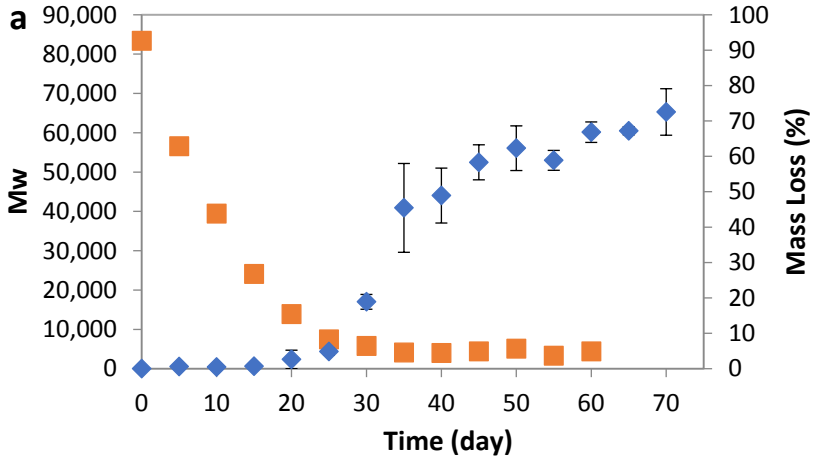

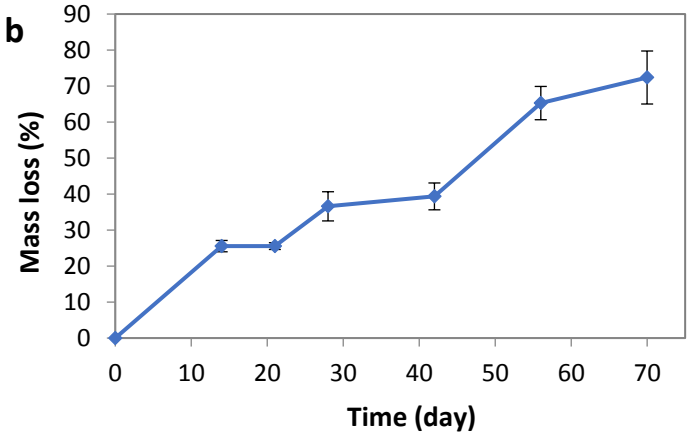

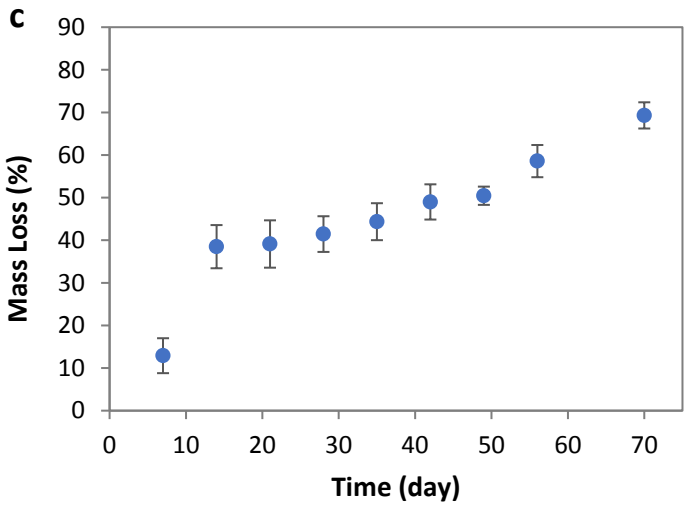

Figure 6.5 *In vitro* degradation behaviour of (a) PLGA-BO504 [red square = Mw and blue diamond = mass loss]; (b) PEGDA hydrogel and (c) embolic device.

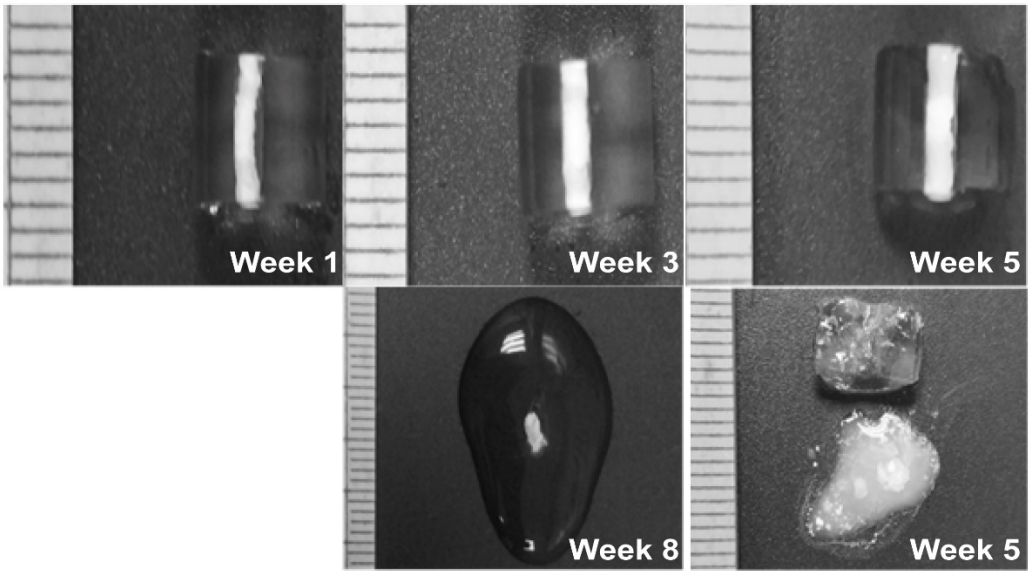

Figure 6.6 Photos of embolic device undergone *in vitro* degradation. (e) Cross section of the embolic device after 5 weeks of *in vitro* degradation.

6.4 Cytotoxicity

As a prerequisite to any potential medical application, the cytotoxicity of the device has to be assessed. Each component of the developed embolic plug, PLGA, PEG and bismuth oxychloride, has shown good biocompatibility and has been used in clinical trials involving implanted devices, as reported in the literature [11, 12]. From Figure 6.7, it can be observed that there was no significant difference in the cell numbers between the cells co-cultured with the device and the monolayer control, suggesting that the developed

prototype had good cytocompatibility. Certainly, more detailed biocompatibility tests according to ISO standard are to be performed for the full assessment of the developed plug.

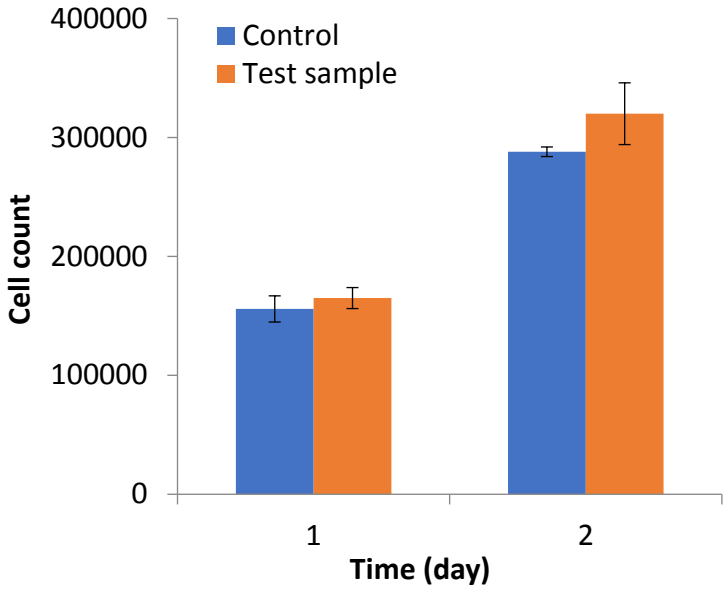

Figure 6.7 Cytotoxicity study of the developed embolic plug (test sample).

6.5 In-vitro hemocompatibility studies of the embolic plug

For biomedical applications it is important that the material should have no or minimal unintended side effects at the local or systemic site in the body while performing its intended function [13-15].

.

6.5.1 Hemolytic activity of embolic plug

For the medical devices intended for use under direct exposure to blood, hemocompatibility testing is necessary. One measure of hemocompatibility is the hemolysis of red blood cells (RBCs), which assesses the amount of damage or lysis of the erythrocyte membrane due to contact with the material. This is calculated indirectly from the amount of hemoglobin released from RBCs. [16, 17].

6.5.2 Isolation of blood components

Citrated whole blood (in 3.8% w/v sodium citrate at a volume ratio of 1:9) from a single healthy human volunteer was collected in a 15 ml falcon (clear polystyrene) tube and centrifuged at 400 g for 30 min at 20 °C. The blood was first separated into platelet-rich plasma (PRP), mononuclear leukocyte 'buffy coat' and red blood cell fractions. The PRP was carefully collected, while the 'buffy coat' was removed and discarded, leaving behind the packed RBC layer in the tube. To obtain platelet-poor plasma (PPP), PRP was centrifuged at 2,000 g for 15 min and the supernatant was collected. All human blood collection procedures were performed under protocols approved by the NTU Institutional Review Board (IRB-2017–10-032, 24th November 2017).

Hemolytic activity of the embolic plug and control (gelfoam) was measured by absorbance of free hemoglobin (Hb) at 450 nm as described in [17, 18]. In brief, the packed red blood cell (RBC) fraction isolated from whole human blood was resuspended in 1 × PBS to the original volume and further diluted with 1 × PBS (50 volumes) to obtain the RBC suspension for use in the hemolysis assay. Both embolic plug (30 mm length and 0.8 mm diameter) and gelfoam (10 mm × 7 mm × 5 mm) were placed in each well of a polystyrene well plate and incubated with 2 mL RBC suspension at 37 °C for 3 h. Triton-X100 added to the RBC suspension (1% w/v) for complete lysis (100%) and release of hemoglobin was used as the positive control. The negative control, which accounted for background hemolysis of the RBCs in PBS, was the diluted RBC suspension in the 12-well plate with no material sample. After 3 h incubation, 1 ml of the RBC suspension was removed and centrifuged at 4,000 rpm for 15 min, and the supernatant was collected. The absorbance of the hemoglobin in the supernatant was measured at 380 nm, 415 nm and 450 nm Infinite 200 microplate reader (Tecan Inc). The reading for the blank control was subtracted and the corrected absorbance (Ab) was calculated as follows:

$$\boldsymbol{Ab_{free\ hemoglobin} = 2 \times A_{415} - (A_{380} + A_{450})} \quad 6.1$$

where A415, A380 and A450 are the corrected absorbance readings of the sample at 415 nm, 380 nm and 450 nm, respectively, after normalization with absorbance readings of the PBS blank control. The hemolysis percentage was calculated by dividing the free hemoglobin of the test sample by the total amount of free hemoglobin released in the positive control sample (100% lysis):

$$\%\ Hemolysis = \frac{Ab_{free\ hemoglobin}\ for\ test\ sample}{Ab_{free\ hemoglobin}\ of\ positive\ control} \times 100\% \qquad 6.2$$

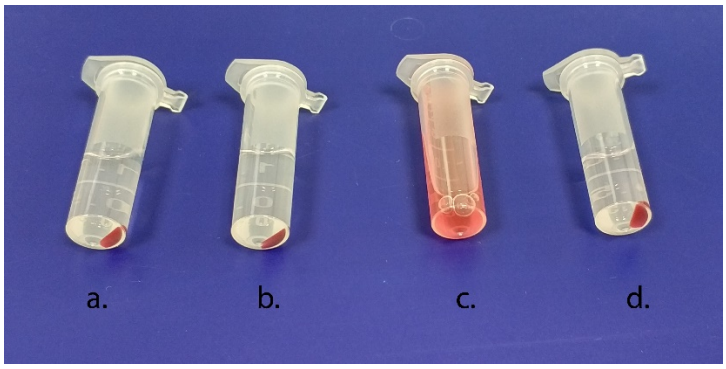

Figure 6.8 RBC suspension supernatant for hemolysis study a.) Gel foam; b.) Embolic device; c.) 1% Triton-X100 (positive control) and; d.) RBC alone (negative control)

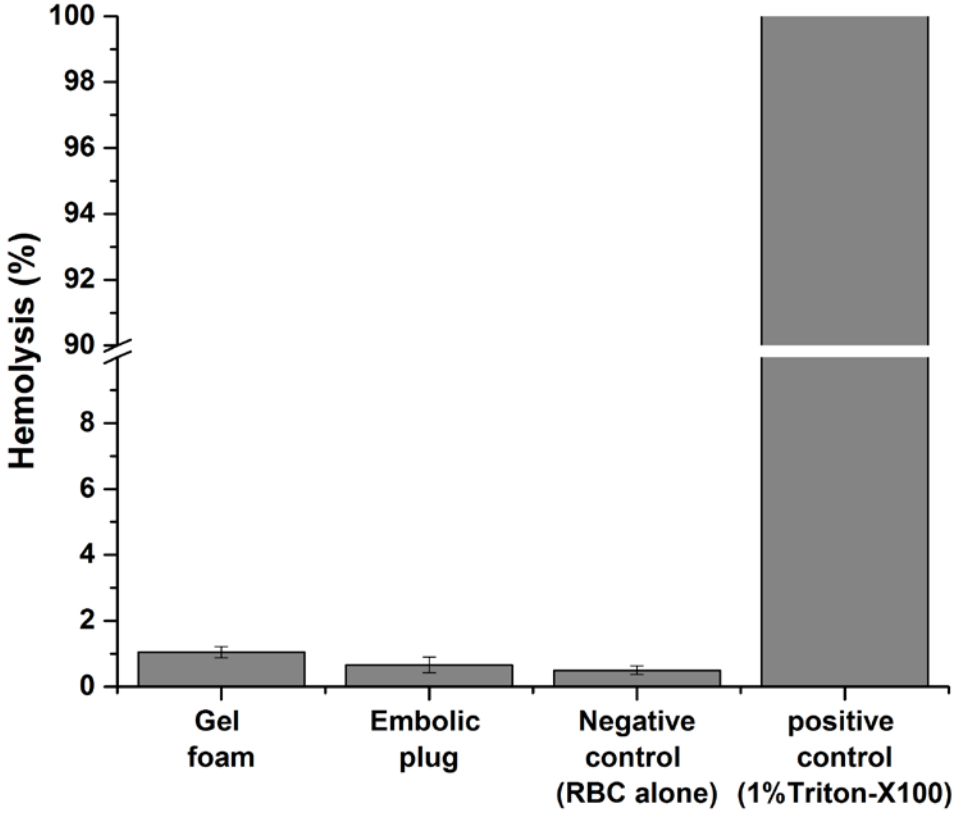

Figure 6.9 Hemocompatibility of embolic plug and gel foam (control) - Percentage of red blood cell (RBC) hemolysis after incubation of diluted RBC fractions of whole human blood,

According to in vitro hemolysis test, embolic device in contact with blood showed a mean hemolysis value <1.0 % (0.66 ± 0.23 %) in the direct contact assay which is intermediate between existing embolic material Gelfoam (1.04 ± 0.17 %) and negative control (0.49 ± 0.13 %). According to results obtained, the device exerts almost negligible hemolytic activity.

6.5.3 Thrombogenicity of embolic device:

Qualitative assessment of thrombogenicity of the embolic device and Gelfoam (control) were performed. These samples were immersed in freshly drawn recalcified citrated blood and surface initiated clot formation was assessed[17, 19].

Assessment of thrombogenicity of the embolic device and Gelfoam (control) was performed by measuring the plasma recalcification times (PRT) for clot formation of calcium-sequestered (citrated) whole blood upon contact with the materials. Specifically, this is widely used in studies to investigate the rate of contact phase activation via Factor XII on the surface of materials[20] These samples were immersed in 2 ml of freshly drawn recalcified citrated blood in a polystyrene tube and surface initiated clot formation was timed after the addition of 2 ml of 0.025M calcium chloride at 37 °C [17, 19].
As it can be seen in Figure 6.10, the dense thrombus formation is observed for Gelfoam sample. Gelfoam has expected thrombogenicity, since its main mode of occlusion is achieved by a combination of mechanical blockage and thrombus formation. Gelatin acts as a physical matrix to promote clot formation, this is also the reason in some cases for unpredictable degradation of gelfoam or permanent occlusion of vessel [21]. Clots formed in contact with Gelfoam are trapped within the gelatin fiber matrices (Figure 6.10 right). This property is favourable for embolic materials where permeant occlusion is desirable[21]. The average clot formation time of whole blood for Gelfoam was 413 s, 14% faster than the whole blood alone in the polystyrene tube (acting as the reference clotting time). The embolic plug showed a clot formation of 566 s, 17.9% prolonged over the reference time. This indicates that the embolic device has a lower thrombogenicity than the Gelfoam. While the embolic device consisted of the PLGA filament and PEG hydrogel, some thrombus formation was observed on the PEG hydrogel surface, and to some degree at the interphase between filament and the hydrogel. After rinsing, it was

observed that, unlike the Gelfoam, the PEG hydrogel remains largely free of clots (Figure 6.8 left).

The data obtained suggested that the embolic plug has a reduced thrombogenic potential as compared to the Gelfoam. In addition, the use of PEG in blood interfacing applications is promising due to its known reduced thrombin adsorption, intrinsic resistance to protein adsorption and cell adhesion, as evident in the literature [22-24].

Table 6.1 Thrombogenicity of embolic device

Samples	Whole blood clotting time	
	Actual time, s	Relative to reference (PS well plate), %
Gelfoam	413 ± 12	- 14.0
Embolic plug	566 ± 25	+ 17.9

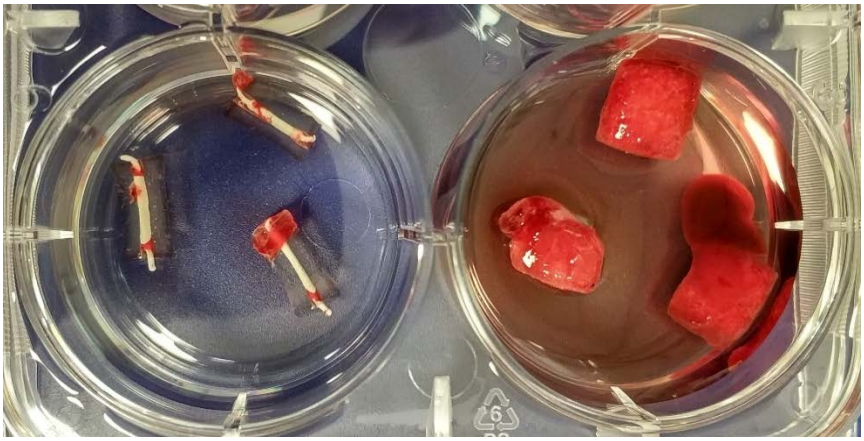

Figure 6.10 Qualitative assessment of thrombogenicity Embolic device (left) and Gelfoam (right)

6.6 Stability of the embolic device in dynamic flow model

One of the major concerns with the embolic devices specifically with coils is the system migration during deployment [25, 26]. A too small coil can result in distal migration, whereas, oversized coil can push the catheter back during deployment causing non-intended proximal embolization, or migration into a critical vessel. It is important to evaluate the maximum pressure that device can withstand, since hepatic arterial pressure, device has to withstand is in the range of 90-100 mmHg [26].

Using a dynamic flow setup (Figure 6.11), an experiment was carried out, where the device was deployed in one of the two tube branches of diameter 3.175 mm using 4F catheter. Peristaltic pump was used to deliver a 37 ^{0}C DI water at the flow rate of 120 ml/min. As embolic device recovers the flow rate drops from that particular branch and the flow is diverted to another branch as we have seen in section. Using a locking plier on second branch, pressures is gradually generated, which is monitored using a pressure gauge with the range 0 to 2.5 bar (WIKA Instrumentation, Germany). The maximum pressure required force the embolic device out of the tube was recorded.

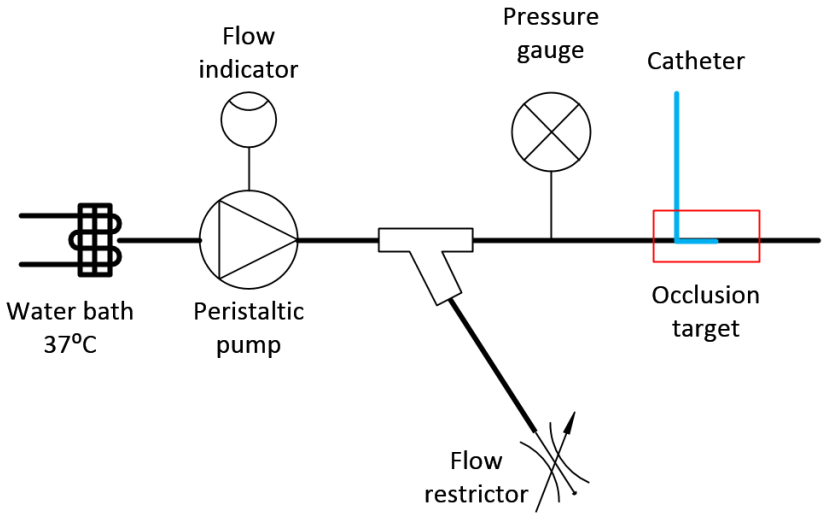

Figure 6.11 Schematic of the dynamic flow model for pressure evaluation

The maximum pressure that device could withstand was found to be 544 ± 42 mmHg. This pressure is much higher than the arterial flow pressure i.e. 90-100 mmHg. This suggests that the normal arterial pressure will not cause the embolic device to migrate once it has blocked the vessel.

6.7 Measurement of radial force for embolic device

In metallic embolization coils and vascular stents applications the radial outward force is important criteria for device safety. Both excessive or inadequate force can pose hazards such as vascular trauma and migration of the device respectively[27].

In case of PLGA-PEG hydrogel embolic device as the hydrogel expands, it exerts outward radial force on the vessel. To determine radial force exerted by the device on blood vessels

of different diameter compression test using parallel plates based on “ISO 25539-2 - Cardiovascular implants —Endovascular devices” was carried out[27-29]. In brief, a fully expanded device was placed between two parallel plates and compression test was performed using MTS Criterion C42 Machine (MTS Systems, USA) with 50N load cell, pre-load force of 0.01N and extension rate of 5mm/min. The device is then cyclically deformed to 50% of diameter with 10% increment in each cycle.

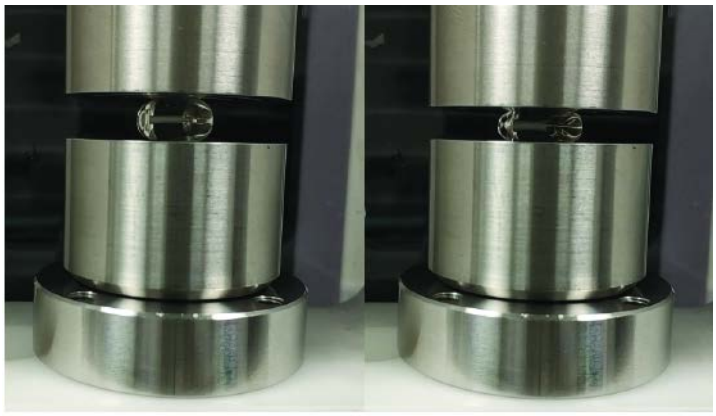

Figure 6.12 Parallel plate compression test setup for embolic device

Figure 6.13 depict the compression force values for an embolic device with fully swollen state diameter 6.9 mm and length 11mm at different compressive strain. When the deformation is converted to equivalent diameters, it tells the force exerted by the device on blood vessels of different diameters. According to previous studies, parallel plate evaluations of the radial force of stents are approximately 10–14% of the total radial force[30, 31]. With this knowledge the radial force can be estimated as shown in Table 6.2.

Table 6.2 Deformation and corresponding radial force for the fully expanded embolic plug

Deformation %	Equivalent Diameter mm	Compressive force N	Radial force N
10	6.2	0.05	0.5
20	5.5	0.12	1.2
30	4.8	0.24	2.4
40	4.1	0.43	4.3
50	3.4	0.77	7.7

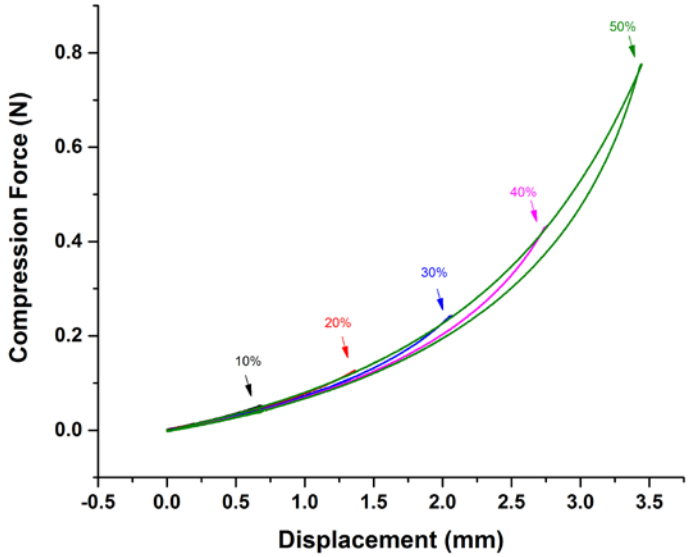

Figure 6.13 Cyclic compression test of PLGA-PEG hydrogel embolic plug at different strain points.

The maximum value of 7.7 N for the diameter of 3.4 mm is observed. The value is around 20% of the radial force exerted by common vascular stent[30, 31]. The force-displacement curve shown in figure also indicate highly elastic deformation nature of the hydrogel confirmed by minimal hysteresis between loading and unloading[32, 33]. This is favorable to provide good apposition to vessel wall.

6.8 Feasibility study of embolic plug in vivo

The prototypes were deployed in the following arteries – left and right carotid, left subclavian, hepatic, superior mesenteric, left and right renal. The 0.035” prototypes were delivered via the 4F Berenstein catheter while the 0.018” prototypes were delivered via a 2.7F Progreat microcatheter (Terumo, Tokyo, Japan) introduced coaxially via the 4F catheter. Table 5 shows the prototype length and diameter, the name of artery embolized, time to complete vessel occlusion and whether there was distal migration of the prototype. There was significant distal migration (>2cm) of 1 prototype (subject 7 in Table 6.3). Complete vascular occlusion occurred in all cases under 2 minutes (Figure 6.14). No vessel rupture was seen in the explanted specimens, but the vessels appeared rather distended at the embolized site (Figure 6.14f).

Table 6.3 *In vivo* procedural results

Subject	Device diameter (mm)	Device length (cm)	Name of artery embolized	Time to complete vessel occlusion (sec)	Distal migration of the device
1	0.80	4	Carotid artery	120	No
2	0.80	2	Carotid artery	108	No
3	0.80	3	Celiac axis	90	No
4	0.80	3	Superior mesenteric artery	87	No
5	0.80	3	Superior mesenteric artery	80	No
6	0.80	3	Renal artery	96	No
7	0.55	2	Carotid artery	80	Yes
8	0.55	3	Carotid artery	82	No
9	0.55	2	Celiac axis branch	40	No
10	0.55	3	Superior mesenteric artery branch	30	No
11	0.55	2	Superior mesenteric artery branch	56	No
12	0.55	2	Superior mesenteric artery branch	40	No
13	0.55	2	Superior mesenteric artery	38	No

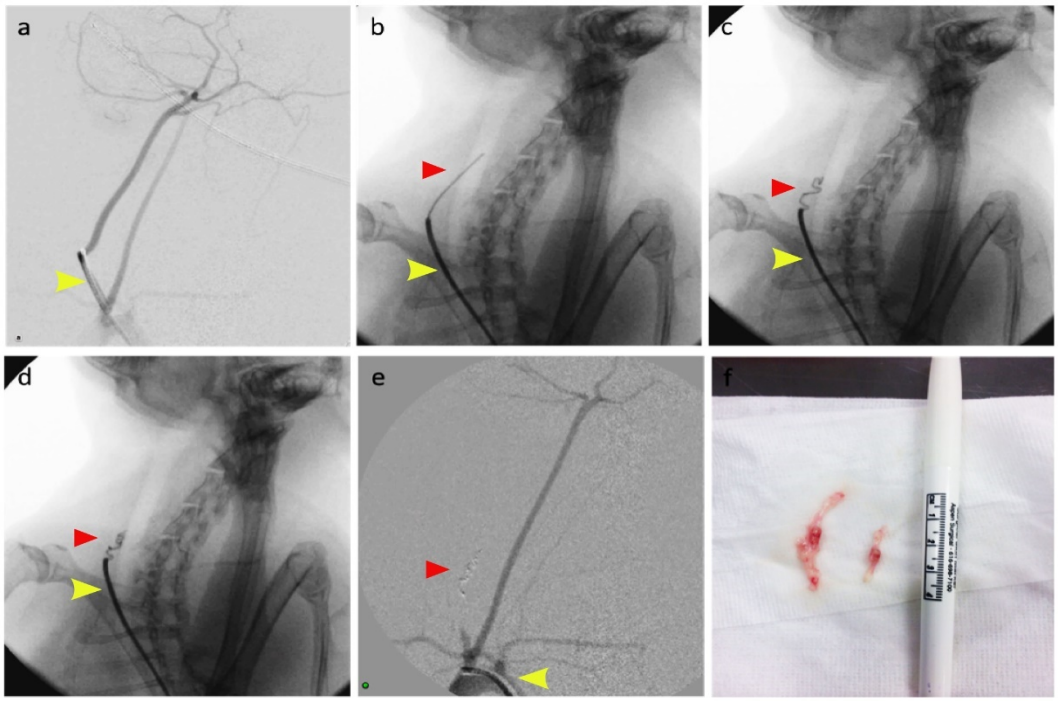

Figure 6.14 Angiogram and appearance of the carotid artery: (a) digital subtraction angiogram (DSA) taken with catheter (yellow arrow) in the right carotid artery. The left carotid artery was also opacified due to contrast reflux; (b) fluoroscopic image showed deployment of prototype (red arrow); (c) & (d) continued fluoroscopy showed recovery and buckling of the prototype; (e) completion DSA showed complete occlusion of flow in the embolized right carotid artery with no migration of prototype. The left carotid artery remained patent; (f) appearance of the explanted vessel.

Conclusion

Overall, *in-vitro* results of the studies have discerned the embolic device based on PLGA-PEG hydrogel composite as safe and feasible biodegradable device. Shelf life studies have confirmed the integrity and mechanical stability of the device without loss of shape memory functionality when stored at 25 °C and 35% relative humidity over a period of six months. This implies favorable time duration for a medical device product. Long term-term shelf life assessment need to be conducted for a period of 12 months.

In-vitro biological studies have confirmed the device as biocompatible and non-hemolytic, further assessment is needed to confirm the safety of the device and its degradation products *in-vivo.*

In vivo evaluation of the embolic plugs in a rabbit embolization model revealed that the prototypes can be deployed at the specific target location in a branch of a blood vessel with both 4F and micro-catheter. The embolic plugs were visible under fluoroscopy and complete vascular occlusion by blood induced shape memory effect, was occurred in all cases less than 2 minutes. All these results indicated that the developed embolic plug can be used as biocompatible and biodegradable embolic agent for temporary embolization. More time points would be desired for a full evaluation of the *in vivo* degradation, recanalization rate of embolized artery and tissue response to temporary occlusion with the embolic plug in the future.

References

[1] Chu C. Hydrolytic degradation of polyglycolic acid: tensile strength and crystallinity study. J Appl Polym Sci. 1981;26:1727-34.

[2] Jamshidian M, Tehrany EA, Imran M, Jacquot M, Desobry S. Poly‐Lactic Acid: production, applications, nanocomposites, and release studies. Comprehensive Reviews in Food Science and Food Safety. 2010;9:552-71.

[3] Blasi P, D'souza SS, Selmin F, DeLuca PP. Plasticizing effect of water on poly (lactide-co-glycolide). J Controlled Release. 2005;108:1-9.

[4] Passerini N, Craig D. An investigation into the effects of residual water on the glass transition temperature of polylactide microspheres using modulated temperature DSC. J Controlled Release. 2001;73:111-5.

[5] Houchin M, Topp E. Physical properties of PLGA films during polymer degradation. J Appl Polym Sci. 2009;114:2848-54.

[6] Liu Y, Bai X, Liang A. Synthesis, Properties, and In Vitro Hydrolytic Degradation of Poly (d, l-lactide-co-glycolide-co-ε-caprolactone). International Journal of Polymer Science. 2016;2016.

[7] Huang Y, Wong YS, Wu J, Kong JF, Chan JN, Khanolkar L, et al. The mechanical behavior and biocompatibility of polymer blends for Patent Ductus Arteriosus (PDA) occlusion device. Journal of the Mechanical Behavior of Biomedical Materials. 2014;36:143-60.

[8] Browning M, Cereceres S, Luong P, E CH. Determination of the in vivo degradation mechanism of PEGDA hydrogels. Journal of Biomedical Materials Research Part A. 2014;102:4244-51.

[9] Browning MB, E C-H. Development of a biostable replacement for PEGDA hydrogels. Biomacromolecules. 2012;13:779-86.

[10] Knop K, Hoogenboom R, Fischer D, US S. Poly (ethylene glycol) in drug delivery: pros and cons as well as potential alternatives. Angewandte Chemie International Edition. 2010;49:6288-308.

[11] Owen RJ, Nation PN, Polakowski R, Biliske JA, Tiege PB, Griffith IJ. A preclinical study of the safety and efficacy of Occlusin 500 artificial embolization device in sheep. Cardiovascular and Interventional Radiology. 2012;35:636-44.

[12] Calo E, Khutoryanskiy VV. Biomedical applications of hydrogels: A review of patents and commercial products. European Polymer Journal. 2015;65:252-67.

[13] Bruck S. Problems and artefacts in the evaluation of polymeric materials for medical uses. Biomaterials. 1980;1:103-7.

[14] Park JB, Lakes RS. Tissue response to implants. Biomaterials. 2007:265-90.

[15] Pizoferrato A, Vespucci A, Ciapetti G, Stea S. Biocompatibility testing of prosthetic implant materials by cell cultures. Biomaterials. 1985;6:346-51.

[16] Tomić SL, Jovašević JS, Filipović JM. Hemocompatibility, swelling and thermal properties of hydrogels based on 2-hydroxyethyl acrylate, itaconic acid and poly (ethylene glycol) dimethacrylate. Polym Bull. 2013;70:2895-909.

[17] Xiong GM, Yuan S, Wang JK, Do AT, Tan NS, Yeo KS, et al. Imparting electroactivity to polycaprolactone fibers with heparin-doped polypyrrole: Modulation of hemocompatibility and inflammatory responses. Acta Biomater. 2015;23:240-9.

[18] Henkelman S, Rakhorst G, Blanton J, van Oeveren W. Standardization of incubation conditions for hemolysis testing of biomaterials. Materials Science and Engineering: C. 2009;29:1650-4.

[19] Kim SW, Jacobs H. Design of nonthrombogenic polymer surfaces for blood-contacting medical devices. Blood purification. 1996;14:357-72.

[20] Rhodes N, Williams D. Plasma recalcification as a measure of contact phase activation and heparinization efficacy after contact with biomaterials. Biomaterials. 1994;15:35-7.

[21] Poursaid A, Jensen MM, Huo E, Ghandehari H. Polymeric materials for embolic and chemoembolic applications. J Controlled Release. 2016;240:414-33.

[22] Szycher M, Sharma CP. Blood compatible materials and devices: perspectives towards the 21st century: CRC Press; 1990.

[23] Deible CR, Petrosko P, Johnson PC, Beckman EJ, Russell AJ, Wagner WR. Molecular barriers to biomaterial thrombosis by modification of surface proteins with polyethylene glycol. Biomaterials. 1998;19:1885-93.

[24] Gombotz WR, Guanghui W, Horbett TA, Hoffman AS. Protein adsorption to poly (ethylene oxide) surfaces. Journal of biomedical materials research. 1991;25:1547-62.

[25] Bilbao JI, Martínez-Cuesta A, Urtasun F, Cosín O. Complications of embolization. Seminars in interventional radiology: Copyright© 2006 by Thieme Medical Publishers, Inc., 333 Seventh Avenue, New York, NY 10001, USA.; 2006. p. 126-42.

[26] Lopera JE. Embolization in trauma: principles and techniques. Seminars in interventional radiology: © Thieme Medical Publishers; 2010. p. 014-28.

[27] BS EN ISO 25539-2:2012 Cardiovascular implants —Endovascular devices Part 2: Vascular stents. BSI Standards Publication.

[28] Kim BM, Kim DJ, Kim DI. Stent application for the treatment of cerebral aneurysms. Neurointervention. 2011;6:53-70.

[29] Krischek Ö, Miloslavski E, Fischer S, Shrivastava S, Henkes H. A comparison of functional and physical properties of self-expanding intracranial stents [Neuroform3, Wingspan, Solitaire, Leo (+), Enterprise]. min-Minimally Invasive Neurosurgery. 2011;54:21-8.

[30] Kim DB, Choi H, Joo SM, Kim HK, Shin JH, Hwang MH, et al. A comparative reliability and performance study of different stent designs in terms of mechanical properties: foreshortening, recoil, radial force, and flexibility. Artificial organs. 2013;37:368-79.

[31] Landsman T, Touchet T, Hasan S, Smith C, Russell B, Rivera J, et al. A shape memory foam composite with enhanced fluid uptake and bactericidal properties as a hemostatic agent. Acta Biomater. 2017;47:91-9.

[32] Nemir S, Hayenga HN, West JL. PEGDA hydrogels with patterned elasticity: Novel tools for the study of cell response to substrate rigidity. Biotechnol Bioeng. 2010;105:636-44.

[33] Visentin AF, Dong T, Poli J, Panzer MJ. Rapid, microwave-assisted thermal polymerization of poly (ethylene glycol) diacrylate-supported ionogels. J Mater Chem A. 2014;2:7723-6.

Chapter 7 Conclusion

In this work mechanical, shape memory and radiopacity properties of individual polymers: PEG hydrogel and PLGA filaments are studied. Water induced buckling of PEG hydrogel is the key to design embolic device using the polymer-hydrogel composite, which will actuate on contact with blood at body temperature.

The PLGA was modified with PEG plasticizer and radiopaque fillers to bring down the glass transition temperature to near body temperature and improve radiopacity. The effect of plasticizer and radiopacifier on mechanical, shape memory and radiopacity was studied. PLGA filament with 2% PEG plasticizer and 50% bismuth oxychloride exhibited best radiopacity and shape memory properties at 37°C. Molecular entanglements as net-points and vitrification at glass transition was responsible for the thermo-responsive shape memory effect. PEG hydrogel was successfully synthesized using photo-crosslinking method. The formulation of PEG hydrogel was optimized using swelling and rheological studies of the hydrogel. The hydrogel photo-synthesized using 7.5% PEGDA (w/v) and 2%(w/w) Irgacure 2959 initiator exhibited optimum mechanical stability and swelling properties. For hydrogel composition with radiopaque fillers, no significant improvement in radiopacity is observed in dry of wet state except for the omnipaque 300 liquid contrast agent. With omnipaque 300 liquid contrast agent (10% w/v) radiopacity in both dry and wet state increased substantially, but it significantly reduced swelling properties. Effect of different deformation strains on the water induced shape recovery and buckling were studied and maximum amount of permissible strain that fast recovery speed without breaking of gel was found to be (600-650%) at 70°C. The device was fabricated by coating hydrogel on the PLGA filament followed by programming it for water induced shape memory by stretching it to different deformation strains at 70°C. The bonding between hydrophobic PLGA and PEG hydrogel were improved by using plasma treatment. Contact angle experiments showed the enhanced surface wettability of PLGA and so the adhesive interfacial strength. The device was tested in *in-vitro* flow model inside tubing's with series of diameters, using a peristaltic pump to generate different flow rates. The deployment of device under guidance of X-ray fluoroscopy was carried out, which discerned the need of flushing of catheter with lipidol, an oil based contrast agent, to overcome premature swelling. The *in-vitro* flow test results 100% occlusion was observed within 3 minutes of deployment for the optimized formulation.

The buckling is complex process, which depends on various parameters such as dimensions of sample, swelling kinetics, modulus of the material, pre-deformation strain, and temperature etc. PEG hydrogel unveils shape change effect (SCE)/swelling, water- and thermos-responsive shape memory effect (SME). Melting transition of the PEG hydrogel was used fix the temporary shape by formation of crystallites upon cooling in deformed state. This method allows to fix higher deformation strain in temporary shape. Actuation of shape memory in PEG hydrogel is effected by dissolution of crystals either by thermal means or by hydration, imparting both thermo-and water responsive SME in PEG hydrogel. Experimental and simulation results proved that buckling induced by water-responsive SME and swelling in hydrogel can not only overcome the limitation with either of them being applied, but also achieve time-controlled activation. Original diameter and programming strain are identified as two key parameters for tailoring the actual buckling (actuation) time within a wide range. This generic phenomenon can be pertinent to various other similar materials and can open door to new material design approach for various applications in sensing, biomedical etc.

In-vitro degradation studies of the device and individual components showed that as PLGA degrades within the embolic device, degraded PLGA polymer is seen to confined or encapsulated, within the degrading PEG hydrogel matrix, even as the device progresses towards its complete degradation at two months. This ensures the radio-opacity of the device over the degradation period, thus allowing subsequent monitoring of its location in-vivo. The embolic device showed sterilization feasibility with ETO sterilization method. The sealed packages after ETO sterilization stored at 25 °C and 35 % relative humidity confirmed safe shelf life for six months observation period. This was confirmed by unaltered mechanical stability and shape memory functionality of the device. The cytotoxicity and hemocompatibility studies substantiated the embolic device to be biocompatible, non-hemolytic and non-thrombogenic as blood contacting device. *In vivo* evaluation of the embolic plugs in a rabbit embolization model revealed that the prototypes were visible under fluoroscopy and complete vascular occlusion occurred in all cases less than 2 minutes. A future animal study is needed to assess the prototype's biodegradation profile, prototype migration over time as the prototype undergoes hydrolysis, recanalization rate of embolized artery and histological tissue response of the embolized artery. Overall this work has demonstrated feasibility of having fully

bioabsorbable shape memory polymer for embolization in liver cancer treatment using water induced buckling of polymer-hydrogel composite at physiological environment.

To date, there is no existing biodegradable solid embolic plug which occludes the blood vessel at specific targeted site in shortest period and with ease of delivery by existing methods. This device presents significant market potential in other embolization applications as well, as a more affordable compared to microspheres and coil but more predictable than gelfoam and collagen sponge.

Chapter 8 Future work and recommendations

1. *In vivo* degradation study of prototypes in rabbit model.

In this study of vascular embolization in rabbits, the safety, efficacy and biodegradation of the developed prototype is evaluated for 6 months in comparison to metallic coil. This study also examines other important device-related issues, including ease of administration, extent of target vessel occlusion, rate of degradation, device migration, vessel recanalization and local tissue reaction.

New Zealand white rabbits weighting 3-3.5 kg will be used. An initial pilot study with 1 rabbit will be performed followed by the actual animal study utilizing 24 rabbits (7 time points and 2 rabbits per time point; total = 14 treated with the prototypes and 7 treated with metallic coils). Briefly, general anaesthesia is administrated intramuscularly to each rabbit. The right femoral artery is surgically exposed, and a 4-Fr sheath is inserted under fluoroscopy. Using fluoroscopic guidance, a 4-Fr catheter is manipulated into the carotid artery. A 3-Fr microcatheter loaded with the developed prototype is advanced coaxially through the 4-Fr catheter within the carotid artery. The prototype is then deployed under fluoroscopy using a guide wire to slowly advance the prototype out of the catheter, allowing it to expand and occlude the artery. After embolization, angiography is performed to ensure proper device deployment and to confirm vessel occlusion. The catheter and sheath are removed, the femoral artery ligated, the skin closed with sutures and the rabbit is recovered.

Angiographic examination:

Angiography is performed as scheduled on post op day 1, 7 and 14 and 1, 2, 4 and 6 months. The follow-up angiograms will be compared with the immediate post-embolization angiograms to assess for visibility of the device, any device migration, degree of vessel occlusion and recanalization.

Histologic analysis:

The rabbits will be euthanized using overdose injection of pentobarbital on day 1, 7, 14 and 1, 2, 4 and 6 months. One rabbit from the metallic coil group and two rabbits from the prototype group will be euthanized at each time point. The arterial segment with the implanted devices is then surgically removed. Samples are fixed in 10% buffered formalin and sent for hematoxylin & eosin (H&E) staining and histologic evaluation for inflammatory cells, thrombus and fibrotic tissues and rate of device degradation.

2. Drug delivery function of the device

Depending on the results of the long-term animal studies as described in previous section, if needed the therapeutics such as heparin (anticoagulant) or t-PA (thrombolytic agent) can be incorporated in either PLGA filament or in hydrogel coating.
Drug release studies can be carried out to study the effect of drug loading, drug carrier (PEG hydrogel or PLGA filament), and the degradation of the polymer on drug release kinetics.

3. Chemical modification of PEG hydrogel with iodinated compounds for radiopacity

One area for improvement is to modify hydrogel with the iodinated compounds such as 2,4,6-triiodophenylpenta-4-enoate, or 5-acrylamido-2,4,6-triiodo-n,n'-bis-(2,3 dihydroxypropyl)isophthalamide, to extend radiopacity to the whole device after swelling. This will enable monitoring degradation of hydrogel under x-say fluoroscopy. Constant et al., have reported the preparation of radiopaque hydrogel filament based on chemical modification with iodine based compounds[1].

4. Surface coating on dry PEG hydrogel to avoid premature swelling.

Poly (ethylene glycol-b-tetramethylene oxide) (PEGTMO)

In current practice we are using Lipidol, an oil based contrast agent to reduce the risk of device getting stuck inside the catheter because of premature swelling of the hydrogel. This method is found to be adequate, but it adds an extra step to the procedure.

PEGTMO, is an amphiphilic block co-polymer synthesized from equimolar concentration of poly(ethylene oxide) (PEO) and poly(tetramethylene oxide) (PTMO) using a catalyst, dibutyltin dilaurates. The resulting co-polymer can be dissolved in ethanol and applied as coating by simply dip and dry method.

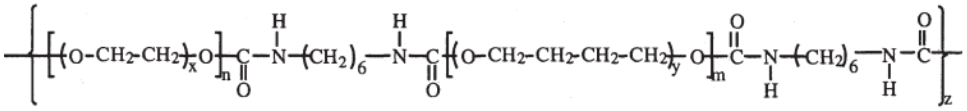

Figure 8.1 Chemical structure of Poly (ethylene glycol-b-tetramethylene oxide) PEGTMO

The previous study N. Park et al., have reported use of PEGTMO coating on the superporous hydrogels to control the swelling kinetics[2]. The results have evinced delayed swelling, controlled by the concentration of PEGTMO, without affecting equilibrium swelling ratio and mechanical properties. The mechanism of delayed swelling is by decrease in surface hydrophilicity and surface porosity. In endovascular chemoembolization applications[3], premature swelling of the embolic device can have prevented until it reaches the intended site of action in the blood vessel, thus, extending the safety of the device and improving feasibility of the procedure by avoiding lipiodol flushing. For the embolic device based on PLGA and PEG hydrogel PEGTMO solution in ethanol can be used since, PEG hydrogel is not affected by ethanol.

5. Controlled folding during buckling of the hydrogel

It would be interesting to incorporate controlled folding feature to the embolic device. PEGTMO coating (as described above) can be applied to embolic device in a pattern to impart differential swelling kinetic to coated and uncoated surface by tailoring the pattern and concentration of coating. When the such sample is exposed to DI water at 37°C, uncoated part will be hydrated faster, activating the shape memory locally while the coated part will be still dehydrated. Tuning the different parameters such as PEGTMO coating concentration, pattern and dimensions of the sample, the existing device can be conferred with elastic shape memory feature (like metal coils), wherein, the uncoated part will get hydrated in the catheter during delivery, and as it emerges out of the catheter it will be coiled or folded to programmed shape.

6. Potential applications

The proposed embolic device has the potential for applications beyond liver cancer treatment including other types of cancer which might benefit from embolic therapy such as renal tumours, uterine fibroids, cerebral aneurysm, gastrointestinal bleeding, emergent pelvic bleeding, post biopsy tract embolization and to treat arteriovenous malformation (AVM).

References

[1] Constant MJ, Keeley EM, Cruise GM. Preparation, characterization, and evaluation of radiopaque hydrogel filaments for endovascular embolization. Journal of Biomedical Materials Research Part B: Applied Biomaterials. 2009;89:306-13.

[2] Baek N, Park K, Park JH, Bae YH. Control of the swelling rate of superporous hydrogels. Journal of bioactive and compatible polymers. 2001;16:47-57.

[3] Hwang S-J, Baek N, Park H, Park K. Hydrogels in cancer drug delivery systems. Drug Delivery Systems in Cancer Therapy. 2004:97-115.

Appendix

List of Publications

Salvekar, A. V., Huang, W. M., Xiao, R., Wong, Y. S., Venkatraman, S. S., Tay, K. H., & Shen, Z. X. (2017). “Water-Responsive Shape Recovery Induced Buckling in Biodegradable Photo-Cross-Linked Poly (ethylene glycol)(PEG) Hydrogel”. ***Accounts of Chemical Research***, 50(2), 141-150.

Yee Shan Wong, **Salvekar Abhijit Vijay*** Kun Da Zhuan, Hui Liu, William Birch, Kiang Hiong Tay, Weimin Huang and Subbu S. Venkatraman. “Bioabsorbable radiopaque water-responsive shape memory embolization plug for temporary vascular occlusion.” ***Biomaterials*** 102 (2016): 98-106. (* co-first author)

Salvekar, Abhijit Vijay, Ye Zhou, Wei Min Huang, Yee Shan Wong, Subbu S. Venkatraman, Zexiang Shen, Guangming Zhu, and Hai Po Cui. "Shape/temperature memory phenomena in un-crosslinked poly-ε-caprolactone (PCL)." ***European Polymer Journal*** 72 (2015).

Zhang, Ji Liang, Wei Min Huang, Guorong Gao, Jun Fu, Ye Zhou, **Abhijit Vijay Salvekar**, Subbu S. Venkatraman, Yee Shan Wong, Kiang Hiong Tay, and William R. Birch. "Shape memory/change effect in a double network nanocomposite tough hydrogel." ***European Polymer Journal*** 58 (2014).

WS Lim, K Chen, TW Chong, GM Xiong, WR Birch, J Pan, B H Lee, PS Er, **AV Salvekar**, SS Venkatraman, YY Huang. “A bilayer swellable drug-eluting ureteric stent: Localized drug delivery to treat urothelial diseases” ***Biomaterials*** (2017)

Patent

Venkatraman, Subramanian, Weimin Huang, Yee Shan Wong, **Abhijit Vijay Salvekar**, and Kiang Hiong Tay. "Embolic device, an apparatus for embolizing a target vascular site and a method thereof." U.S. Patent Application 15/110,328, filed November 17, 2016.